NASA TECHNICAL NOTE

NASA TN D-6049

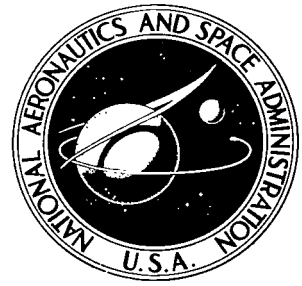

EFFECTS OF WING ELEVATION, INCIDENCE, AND CAMBER ON THE AERODYNAMIC CHARACTERISTICS OF A REPRESENTATIVE HYPERSONIC CRUISE CONFIGURATION AT MACH NUMBERS FROM 0.65 TO 10.70

by Walter P. Nelms, Jr., and John A. Axelson

Ames Research Center
Moffett Field, Calif. 94035

NATIONAL AERONAUTICS AND SPACE ADMINISTRATION • WASHINGTON, D. C. • OCTOBER 1970

1. Report No.	2. Government Accession No.	3. Recipient's
NASA TN D-6049		

4. Title and Subtitle	5. Report Date
EFFECTS OF WING ELEVATION, INCIDENCE, AND CAMBER ON THE AERODYNAMIC CHARACTERISTICS OF A REPRESENTATIVE HYPERSONIC CRUISE CONFIGURATION AT MACH NUMBERS FROM 0.65 to 10.70	October 1970
	6. Performing Organization Code
7. Author(s)	8. Performing Organization Report No.
Walter P. Nelms, Jr., and John A. Axelson	A-3701
	10. Work Unit No.
9. Performing Organization Name and Address	722-01-10-02-00-21
NASA Ames Research Center Moffett Field, Calif.. 94035	11. Contract or Grant No.
	13. Type of Report and Period Covered
12. Sponsoring Agency Name and Address	Technical Note
National Aeronautics and Space Administration Washington, D. C. 20546	14. Sponsoring Agency Code

15. Supplementary Notes

16. Abstract

A delta-wing and body configuration representative of an airbreathing, liquid-hydrogen fueled, hypersonic cruise aircraft was tested with the wing in high, mid, and low positions at zero incidence on the body, and the incidence angle was varied from -2^0 to $+2^0$ in the mid position. Wings with positive cambered, symmetrical, and negative cambered airfoil sections were studied for the mid position at zero incidence. The tests were conducted over a nominal angle-of-attack range from -4^0 to $+12^0$, and angle-of-sideslip range from -4^0 to $+10^0$.

The results indicate that variations in wing elevation on the fuselage had little effect on the lift and pitching-moment characteristics but had significant effects on the lateral and directional stability at most Mach numbers of the study. Changing wing incidence varied the pitching moment at zero lift over the entire test Mach number range with little or no reduction in the maximum lift-drag ratio at supersonic and hypersonic speeds. At transonic and supersonic Mach numbers, wing camber significantly affected the pitching moment at zero lift but only slightly affected this parameter at hypersonic speeds.

17. Key Words (Suggested by Author(s))	18. Distribution Statement
Hypersonic Aircraft Aerodynamic Configurations Aerodynamic Characteristics Aircraft Stability Lift-Drag Ratio Wind Tunnel Models	Unclassified - Unlimited

19. Security Classif. (of this report)	20. Security Classif. (of this page)	21. No. of Pages	22. Price*
Unclassified	Unclassified	73	$3.00

*For sale by the Clearinghouse for Federal Scientific and Technical Information
Springfield, Virginia 22151

SYMBOLS

The force and moment coefficients are referred to the stability axes system with the origin located on the fuselage center line at the 25-percent point of the wing mean aerodynamic chord.

a.c.	longitudinal aerodynamic center defined at $\left(\frac{L}{D}\right)_{max}$, percent $\bar{c}$
b	wing span
c	local chord length
$\bar{c}$	mean aerodynamic chord of wing
C_D	drag coefficient, $\frac{drag}{qS}$
C_{D_o}	drag coefficient at zero lift
C_L	lift coefficient, $\frac{lift}{qS}$
C_{L_o}	lift coefficient at $\alpha = 0^o$
C_{L_α}	lift-curve slope at zero lift, $\frac{\partial C_L}{\partial \alpha}$, per deg
C_l	rolling-moment coefficient, $\frac{\text{rolling moment}}{qSb}$
C_{l_β}	lateral-stability parameter, $\frac{\partial C_l}{\partial \beta}$, per deg
C_m	pitching-moment coefficient, $\frac{\text{pitching moment}}{qS\bar{c}}$
C_{m_o}	pitching-moment coefficient at zero lift
C_n	yawing-moment coefficient, $\frac{\text{yawing moment}}{qSb}$
C_{n_β}	directional-stability parameter, $\frac{\partial C_n}{\partial \beta}$, per deg
C_Y	side-force coefficient, $\frac{\text{side force}}{qS}$
C_{Y_β}	side-force parameter, $\frac{\partial C_Y}{\partial \beta}$, per deg
d	model body diameter
d_{max}	maximum body diameter
i_w	wing incidence angle relative to fuselage center line, positive in same sense as α, deg

$\frac{L}{D}$	lift-drag ratio
$\left(\frac{L}{D}\right)_{max}$	maximum lift-drag ratio
l	overall body length
M	free-stream Mach number
q	free-stream dynamic pressure
Re	Reynolds number, per ft
S	wing planform area (reference area)
$\frac{t}{c}$	airfoil thickness-to-chord ratio
TP	tangency point
x	longitudinal coordinate, measured rearward from model nose
α	angle of attack (referred to fuselage center line), deg
β	angle of sideslip, deg

The following code is used to designate the various components of the model:

B	body
N	wing-mounted nacelles
V	vertical tail
W	wing

EFFECTS OF WING ELEVATION, INCIDENCE, AND CAMBER ON THE AERODYNAMIC CHARACTERISTICS OF A REPRESENTATIVE HYPERSONIC CRUISE CONFIGURATION AT MACH NUMBERS FROM 0.65 to 10.70

Walter P. Nelms, Jr., and John A. Axelson

Ames Research Center

SUMMARY

A delta-wing and body configuration representative of an airbreathing, liquid-hydrogen fueled, hypersonic cruise aircraft was tested with the wing in high, mid, and low positions at zero incidence on the body, and the incidence angle was varied from -2° to $+2^{\circ}$ in the mid position. Wings with positive cambered, symmetrical, and negative cambered airfoil sections were studied for the mid position at zero incidence. The tests were conducted over a nominal angle-of-attack range from -4° to $+12^{\circ}$, and angle-of-sideslip range from -4° to $+10^{\circ}$.

The results indicate that variations in wing elevation on the fuselage had little effect on the lift and pitching-moment characteristics but had significant effects on the lateral and directional stability at most Mach numbers of the study. Changing wing incidence varied the pitching moment at zero lift over the entire test Mach number range with little or no reduction in the maximum lift-drag ratio at supersonic and hypersonic speeds. At transonic and supersonic Mach numbers, wing camber significantly affected the pitching moment at zero lift but only slightly affected this parameter at hypersonic speeds.

INTRODUCTION

Hypersonic cruise aircraft configurations with airbreathing propulsion systems employing liquid hydrogen fuel have shown potential for both transport and boost missions in a number of performance studies typified by references 1 through 4. In the course of these investigations, many problems requiring future research were identified. Among these was the need to define experimentally the aerodynamic characteristics of configurations having large fuselage volumes necessitated by the storage requirements of hydrogen fuel. For this reason, a research program was undertaken at Ames Research Center to provide experimental data on representative hypersonic cruise configurations over a broad Mach number range. Reference 5 presents the longitudinal aerodynamic characteristics of several configurations investigated in this program.

During the phase of the program discussed here, tests were made at hypersonic Mach numbers of a model with several geometric alterations that were known at lower speeds to be effective in varying the configuration aerodynamic efficiency and stability characteristics. Particular emphasis was

given to the wing geometry and the location of the wings on the fuselage. This report presents the effects of wing elevation, wing incidence, and wing camber on the aerodynamic characteristics of a representative hypersonic cruise configuration.

The experimental investigation was made in the Ames 6- by 6-foot supersonic, 1- by 3-foot supersonic, and 3.5-foot hypersonic wind tunnels over a Mach number range from 0.65 to 10.70. Reynolds number was held constant at 3.5×10^6 per foot for all tests except those at Mach numbers 2.0 and 10.7 where the Reynolds numbers were 2.5×10^6 and 2.0×10^6 per foot. The tests were conducted over a nominal angle-of-attack range from -4° to $+12^\circ$ and angle-of-sideslip range from -4° to $+10^\circ$.

MODEL

Detailed drawings of the model in figure 1 show the complete configuration and the geometric alterations of model components considered in this report. The complete configuration is shown in figure 2 and pertinent dimensions of the various model components are presented in table 1.

The model (fig. 1(a)) was derived from the analytical studies of reference 1 to represent an airbreathing, liquid-hydrogen fueled, turboramjet powered, hypersonic (M = 6) cruise aircraft having a gross weight of approximately a half-million pounds and a wing area of 6250 square feet. The scale of this model is 1 inch equals 16 feet.

The fuselage is circular in cross section and has a fineness ratio of 12 with a Sears-Haack profile extending back 11.13 inches from the nose. Aft of this station, the body opens into a cone frustum to permit entrance of the sting support. The vertical tail, mounted on the body center line, has a symmetrical diamond airfoil section with a maximum thickness-to-chord ratio of 4 percent located at midchord, and leading-edge and trailing-edge sweepback angles of 60° and 13°, respectively. The exposed area of the vertical tail is approximately one-fourth the wing reference area. The two-dimensional engine nacelles mounted on the wings (fig. 1(a)) have external contours that simulate a design containing two turboramjet engines per nacelle with an exit area twice the inlet area. The nacelles were placed in the wing compression field sufficiently outboard and aft to avoid jet impingement on the structure downstream of the engine exits. The nacelles have ducts of constant internal area and do not include inlet precompression ramps or provide for boundary-layer bypass. All the wings tested have delta planforms with 70° sweptback leading edges, aspect ratios of 1.46, maximum thicknesses of 4 percent ($t/c = 0.04$), and ridge lines (where applicable) at 30 and 70 percent of the local chords. In figure 1(a), the wing with a flat undersurface (positive camber) is shown mounted at zero incidence in a mid position on the body so that a plane containing the wing lower surface passes through the fuselage center line.

The wing vertical location on the body, the wing incidence and the wing airfoil shape were varied during this study. Figure 1(b) shows the three wing elevations investigated on the complete configuration (WBVN) with the positive-cambered wing and $i_w = 0^\circ$. The wing was moved up or down from its mid position until some point on the wing became tangent to the body surface, thus defining the high and low elevations. Small farings were used in the wing-fuselage juncture regions when the wing was in the high or low position to minimize corner flow problems. These filler sections fair into the body forward and aft of the wing.

The effect of wing incidence was investigated on the wing-body vertical-tail configuration without nacelles and with the positive-cambered wing mounted in the mid position as shown in figure 1(c). The wing was rotated about a point corresponding to the 25 percent point of the mean aerodynamic chord through angles of incidence of -2°, -1°, 0, $+1^\circ$, and $+2^\circ$.

Figure 1(d) presents details of the three wing airfoil sections studied. Each had a maximum thickness of 4 percent ($t/c = 0.04$) but one had positive camber, one had negative camber, and one had a symmetrical section. For this comparison, the wings were mounted in the mid position on the body at zero incidence. The wing with positive camber and the symmetrical wing were tested on the wing-body vertical-tail configuration, while the positive- and negative-cambered wings were compared on the wing-body combination.

TESTS

Experimental data were measured in the Ames 6- by 6-foot supersonic 1- by 3-foot supersonic, and 3.5-foot hypersonic wind tunnels over a Mach number range from 0.65 to 10.70. In the 6- by 6-foot tunnel, the Mach number was varied from 0.65 to 1.99, and in the 1- by 3-foot facility, from 1.99 to 4.81. Test Mach numbers were 5.31, 7.42, and 10.70 in the 3.5-foot hypersonic tunnel. To prevent liquefaction of air in the test section of the 3.5-foot facility, the stagnation temperature was maintained at 800° F for Mach numbers of 5.31 and 7.42 and at 1400° F for Mach number 10.70. Data were taken at a constant Reynolds number of 3.5×10^6 per foot at all Mach numbers except 1.99 and 10.70, where the Reynolds numbers were 2.5×10^6 and 2.0×10^6 per foot, respectively, because of wind-tunnel maximum pressure limitations.

The model was sting-mounted through the rear of the fuselage, and force and moment measurements were made with an internally mounted, six-component strain-gage balance. Test angles of attack ranged nominally from -4° to $+12^\circ$, and angles of sideslip ranged nominally from -4° to $+10^\circ$ at 0° angle of attack. Additional tests were conducted for the model in pitch at a constant angle of sideslip. The angles of attack and sideslip were corrected for both wind-tunnel flow alinement and for balance and sting deflections caused by the aerodynamic loads. Fuselage base-pressure was measured, and the drag data were adjusted to a condition corresponding to free-stream pressure on the base.

Since incremental variations in the aerodynamic coefficients were of primary interest in this report, the data were not corrected for internal drag of the flow through the nacelles nor for boundary-layer conditions on the

model. The effect of these corrections on the configuration drag and maximum L/D are shown in reference 5. The combination of nacelle internal and nacelle base drag coefficients was on the order of 16 percent of C_{D_o} at M - 1.10 and decreased to about 3 percent of C_{D_o} at M = 7.4. At Mach numbers to about 5 the boundary-layer flow over the model was mixed (laminar, transitional, and/or turbulent). At the hypersonic Mach numbers ($M \geq 5$) the flow was essentially laminar.

Based on repeatability of the data and known precision of the measuring equipment, the test Mach numbers and the dimensionless aerodynamic coefficients presented in this report are considered to be accurate within the following limits:

Mach number	Accuracy of aerodynamic coefficients, percent
0.65 through 4.81 $\pm$0.01	$\pm$2
5.31 through 10.70 $\pm$0.05	$\pm$3

The angles of attack and sideslip are considered to be accurate within $\pm 0.2^{\circ}$.

PRESENTATION OF RESULTS

The following table summarizes the purpose of each figure.

Figure	Model Configuration	Purpose of figure
3	WBVN - wing in high, mid, and low positions	Effect of wing elevation on logitudinal characteristics
4	Same as figure 3	Summary of results from figure 3 versus M
5	Same as figure 3	Effect of wing elevation on lateral-directional characteristics versus β
6	Same as figure 3	Summary of results from figure 5 versus M
7	Same as figure 3	Effect of wing elevation on lateral-directional characteristics versus α ($\beta = 4.4^{\circ}$ to 4.9°)

Figure	Model configuration	Purpose of figure
8	WBV - $i_w = +2^\circ, +1^\circ, 0, -1^\circ$, and -2°	Effect of wing incidence on longitudinal characteristics
9	Same as figure 8	Summary of results from figure 8 versus M
10	WBV - positive-cambered and symmetrical wings	Effect of wing camber on longitudinal characteristics
11	Same as figure 10	Summary of results from figure 10 versus M
12	Same as figure 10	Effect of wing camber on lateral-directional characteristics versus β
13	WB - positive-and negative-cambered wings	Effect of wing camber on longitudinal characteristics
14	Same as figure 13	Summary of results from figure 13 versus M

In summary, figures 3 through 7 present the effects of wing elevation while the effects of wing incidence are shown in figures 8 and 9. The effects of wing camber are presented in figures 10 through 14.

RESULTS AND DISCUSSION

Throughout the study the wing thickness was held constant at 4 percent ($t/c = 0.04$). The angle of attack in all cases was referenced to the center line of the fuselage, and the values of $(L/D)_{max}$ as presented in this report are for untrimmed configurations. All logitudinal aerodynamic centers presented herein were evaluated at maximum lift-drag ratio. The general increase in drag coefficient above $M = 7.4$ is primarily a consequence of the lower test Reynolds number at $M = 10.70$.

Wing Elevation

The complete configuration consisting of wing, body, vertical tail, and nacelles was used for this study as shown in figure 1. (For clarity, the nacelles are not shown on figure 1(b).) The wing with a positive-cambered airfoil section was mounted at zero incidence in three different vertical positions on the body (fig. 1(b)).

Longitudinal characteristics- The vertical location of the wing had little or no effect on C_{L_α} throughout the speed range of the tests (figs. 3 and 4). All three configurations exhibited the familiar decrease in C_{L_α} with increasing supersonic Mach number (fig. 4). However, the low-wing configuration had the highest C_{L_o} up to and including a Mach number of 2, and the mid-wing model the lowest (fig. 3). The configuration with the wing in the mid position had the lowest C_{D_o} at all Mach numbers; the low-wing model had the highest. At a given Mach number, all three wing elevations resulted in essentially the same $(L/D)_{max}$ except at Mach numbers less than 1 where the high wing was slightly superior.

The vertical position of the wing had little effect on the pitching moment at zero lift (fig. 4). The C_{m_o} varied from large negative values at the lower speeds to essentially zero at the highest speeds. At all three wing positions the longitudinal aerodynamic center traveled forward with increasing supersonic Mach number and gradually moved rearward as the speeds became hypersonic. This forward travel amounted to approximately 19 percent of the mean aerodynamic chord and was greatest with the wing in the low position.

Lateral-directional characteristics- Variations in wing elevation significantly affected the directional stability at most Mach numbers of the study. At low angles of attack and at most Mach numbers, the static directional stability was largest for the low-wing position and least for the high-wing position (figs. 5 and 6). There was a significant reduction in C_{n_β} with increasing supersonic Mach number (fig. 6). As shown in figure 7, changes in angle of attack had little effect on the yawing moment through a Mach number of 2, with the low-wing model maintaining the greatest C_n. At hypersonic speeds C_n decreased with increasing angle of attack. The configuration with the high wing exhibited a less negative C_n at Mach number 7.4 and at the higher angles of attack, as shown in figure 7(f).

Varying the wing elevation changed the lateral stability at all Mach numbers of the investigation (fig. 5). The high-wing configuration produced the greatest effective dihedral $(-C_{l_\beta})$ at all Mach numbers and the low-wing the least. As shown in figure 6, there was a gradual decrease in effective dihedral with increasing supersonic Mach number. Changes in angle of attack had little effect on C_l through a Mach number of 2, but above this speed, C_l increased (became more negative) with increasing angle of attack (fig. 7).

Throughout the Mach number range of the tests, the low-wing configuration exhibited the largest side-force parameter (C_{Y_β}), as shown in figures 5 and 6. The side-force coefficient was relatively unaffected by changes in angle of attack at all test Mach numbers (fig. 7).

Wing Incidence

For these tests, the model consisted of a wing, body, and vertical tail (nacelles off) with the wing having a positive-cambered airfoil section

mounted in the mid position on the fuselage. The wing was tested at incidence angles of -2°, -1°, 0, $+1^{\circ}$ and $+2^{\circ}$ as shown in figure 1(c).

At all test Mach numbers, variations in wing incidence significantly affected lift at zero angle of attack, with positive incidence producing the higher values of C_{L_o} (fig. 8). The effect on lift-curve slope, however, was slight at all Mach numbers and angles of attack, and except at M = 1.59 and below, the effect on C_{D_o} was essentially zero (fig. 9).

Changes in wing incidence had a large effect on C_{m_o} for the test Mach number range with little or no reduction in $(L/D)_{max}$ at supersonic and hypersonic speeds (fig. 9). A wing incidence of -1 caused a favorable positive shift in C_{m_o} at all speeds with a small reduction in static-longitudinal stability above a Mach number of 2. A wing incidence of -2° drastically decreased the longitudinal stability, and the aerodynamic center moved forward to 19 percent of the mean aerodynamic chord.

Wing Camber

Positive cambered and symmetrical wings- The wing with positive camber and the symmetrical wing (fig. 1(d)) were tested in the mid position with zero incidence on the wing-body-vertical tail combination (nacelles off).

The C_{L_α} of the two wings was essentially the same at all test Mach numbers (fig. 11), but the positive cambered wing produced a negative C_{L_o} at the higher speeds (fig. 10). At Mach number 2.93, there was an increase in C_{D_o} due to camber, but since the symmetrical wing had a higher drag rise with increasing lift coefficient, the $(L/D)_{max}$ was the same for the two wings. The drag due to camber was greatly reduced at the higher speeds, and the $(L/D)_{max}$ for the two wings was essentially equal.

The major effect of wing camber occurred in the pitching-moment characteristics. At the lower speeds, the unfavorable negative C_{m_o} associated with the positive-cambered wing was eliminated by the symmetrical airfoil section at no loss in $(L/D)_{max}$. However, at the hypersonic Mach numbers, wing camber had little effect on C_{m_o}, and the positive-cambered wing had a more rearward a.c. location than the symmetrical wing (fig. 11).

An examination of the lateral and directional characteristics for Mach numbers of 1.99 and 7.42 (fig. 12) indicates that camber had only slight effects on these parameters for the mid-wing position on the wing-body-vertical-tail combination at low angles of attack.

Positive and negative cambered wings- At supersonic speeds C_{m_o} was more positive with the symmetrical wing than with the positive-cambered wing with no loss in $(L/D)_{max}$ (fig. 11). Because measurements were not obtained for the symmetrical wing at the low Mach numbers, the effects of camber at the lower speeds is based on a comparison of the positive and negative camber (fig. 1(d)) studied throughout the entire test range of Mach numbers (figs. 13

and 14) for the mid-wing position on the wing-body combination. The results (fig. 14) indicate no difference in C_{L_α} between the two wings above a Mach number of 1, but at the subsonic Mach numbers C_{L_α} was slightly lower for the positive-cambered wing. At the lower speeds, C_{L_o} was higher for the wing with positive camber but above the Mach number at which the wing leading edge experienced supersonic flow (M = 2.92), C_{L_o} was larger for the wing with negative camber. Both wings produced equal levels of C_{D_o} throughout the test range of Mach numbers.

For the wings with positive and negative camber, tested in the presence of the body only, C_{m_o} was of equal magnitude but opposite algebraic sign (fig. 14), as expected. The positive values of C_{m_o} for the wing with negative camber below a Mach number of 6 are favorable to achieving longitudinal trim, but were accompanied by significantly reduced levels of $(L/D)_{max}$ (fig. 14). At hypersonic speeds, the wing with negative camber had slightly lower values of $(L/D)_{max}$, higher drag at positive lift coefficients, slightly negative values of C_{m_o}, and a more forward a.c. location in comparison to the positive-cambered wing.

CONCLUSIONS

An experimental investigation of the effects of wing elevation, wing incidence, and wing camber on the aerodynamic characteristics of a representative hypersonic cruise configuration has been conducted at Mach numbers from 0.65 to 10.70. The wings were tested in high, mid, and low positions at zero incidence on the body, and the incidence angle was varied from -2° to $+2^\circ$ for the mid position. Wings with positive cambered, symmetrical, and negative cambered airfoil sections were studied in the mid position at zero incidence. The results warrant the following comments:

1. Wing elevation on the body had little effect on the lift and pitching-moment characteristics throughout the test Mach number range.

2. The low-wing configuration had the greatest directional stability at most test Mach numbers at the lower angles of attack.

3. The high-wing configuration exhibited the greatest effective dihedral throughout the Mach number range of the investigation.

4. Changes in angle of attack had little effect on the lateral and directional characteristics at Mach numbers of 2 and below for the three wing elevations, but above M = 2 increasing angle of attack reduced the directional stability and increased the effective dihedral.

5. Variations in wing incidence changed the pitching moment at zero lift for the entire test Mach number range, with little or no reduction in the maximum lift-drag ratio at supersonic and hypersonic speeds.

6. Varying the wing camber significantly affected the pitching moment at zero lift at transonic and supersonic speeds, but had a very small effect on this parameter at hypersonic Mach numbers.

7. The aerodynamic center was farther rearward on the positive-cambered wing than on the symmetrical or negative-cambered wings at hypersonic speeds and at maximum lift-drag ratio.

Ames Research Center
National Aeronautics and Space Administration
Moffett Field, Calif., 94035, June 23, 1970

REFERENCES

1. Gregory, Thomas J.; Petersen, Richard H.; and Wyss, John A.: Performance Trade-Offs and Research Problems for Hypersonic Transports. J. Aircraft, vol. 2, no. 4, 1965, pp. 266-271.

2. Petersen, Richard H.; Gregory, Thomas J.; and Smith, Cynthia L.: Some Comparisons of Turboramjet-Powered Hypersonic Aircraft for Cruise and Boost Missions. J. Aircraft, vol. 3, no. 5, 1966, pp. 398-405.

3. General Dynamics/Convair Division: Performance Potential of Hydrogen Fueled, Airbreathing Cruise Aircraft. Rep. GDC-DCB-66-004 (Contract NAS2-3180), May and Sept. 1966.

4. Lockheed-California Company: Study of Advanced Airbreathing Launch Vehicles with Cruise Capability. Rep. LR 21042 (Contract NAS2-4084), Feb. 1968.

5. Nelms, Walter P., Jr.; and Axelson, John A.: Longitudinal Aerodynamic Characteristics of Three Representative Hypersonic Cruise Configurations At Mach Numbers From 0.65 to 10.70. NASA TM X-2113

TABLE 1 - MODEL GEOMETRY

[Dimensions are in inches; areas are in square inches]

Fuselage	
Length, l	17.81
Maximum diameter, d_{max}	1.48
Wing	
Span, b	5.96
Aspect ratio	1.46
Center-line chord	8.19
Mean aerodynamic chord, $\bar{c}$	5.46
Planform area, S	24.41
Maximum t/c	0.04
Leading-edge sweep	70°
Trailing-edge sweep	0°
Vertical Tail	
Exposed span	2.48
Exposed root chord	4.33
Tip chord	0.60
Exposed area	6.40
Maximum t/c	0.04
Leading-edge sweep	60°
Trailing-edge sweep	13°
Nacelles	
Length	2.19
Inlet area, total	0.28

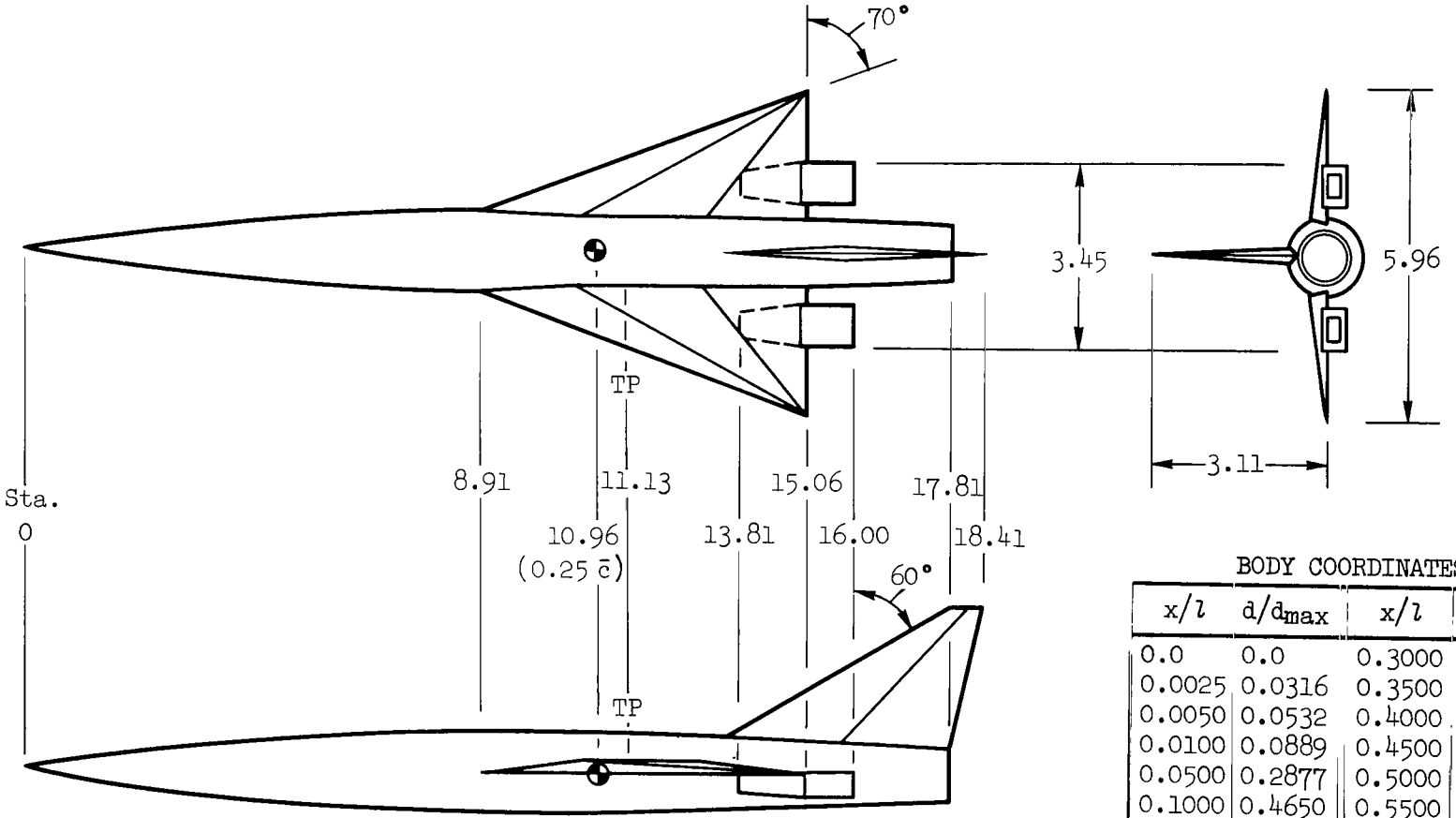

BODY COORDINATES

x/l	d/d_{max}	x/l	d/d_{max}
0.0	0.0	0.3000	0.8774
0.0025	0.0316	0.3500	0.9326
0.0050	0.0532	0.4000	0.9703
0.0100	0.0889	0.4500	0.9926
0.0500	0.2877	0.5000	1.0000
0.1000	0.4650	0.5500	0.9926
0.1500	0.6038	0.6000	0.9703
0.2000	0.7156	0.6250	0.9535
0.2500	0.8059	1.0000	0.6739

d_{max} = 1.48
l = 17.81

(a) Complete configuration (WBVN); mid-wing elevation; positive cambered wing; $i_w = 0°$.

Figure 1.- Model drawing; all dimensions are in inches.

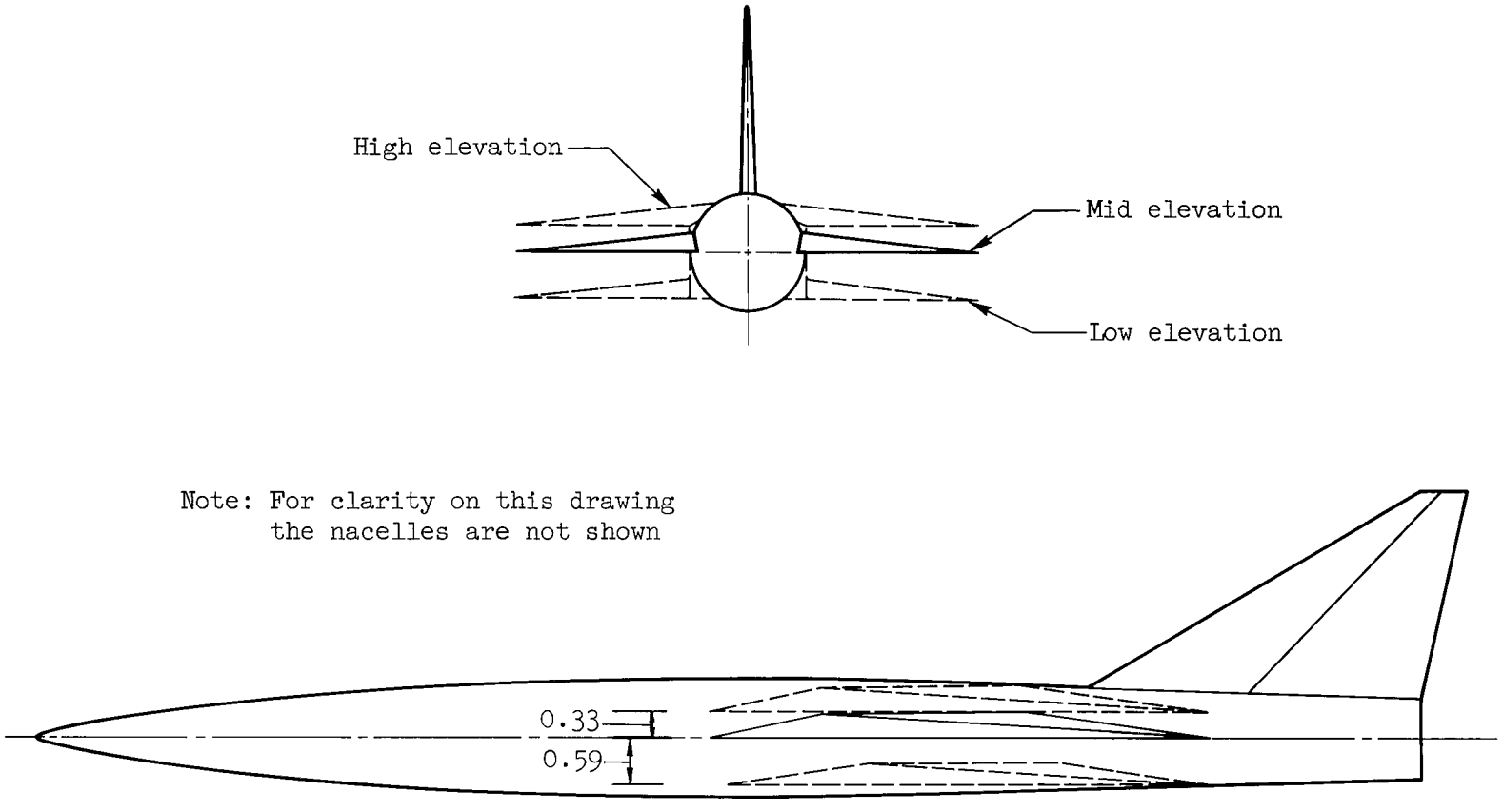

(b) Sketch showing wing elevations; WBVN configuration; positive cambered wing; $i_w = 0°$.

Figure 1.- Continued.

Note: For clarity on this drawing the wing incidence angle has been exaggerated

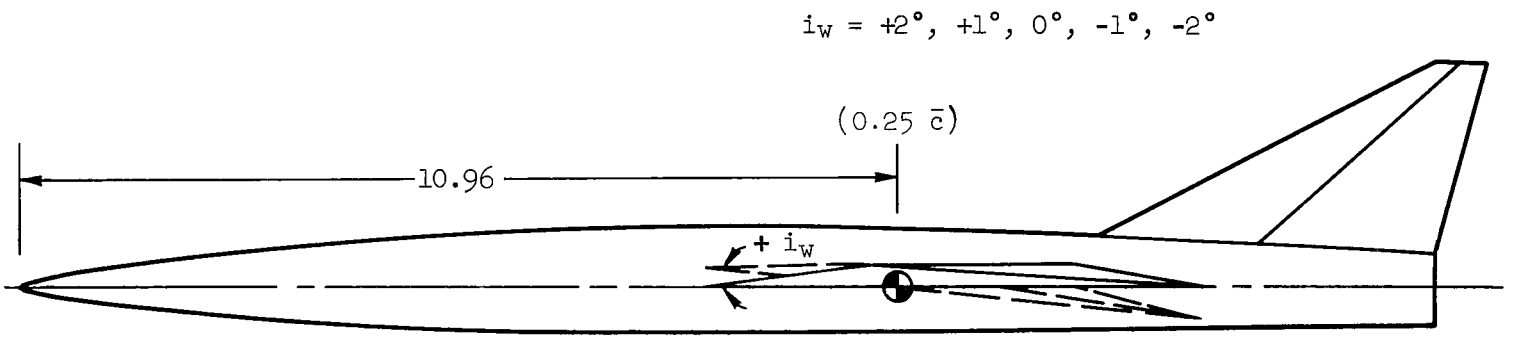

(c) Sketch showing wing incidence; WBV configuration; mid-wing elevation; positive cambered wing.

Figure 1.- Continued.

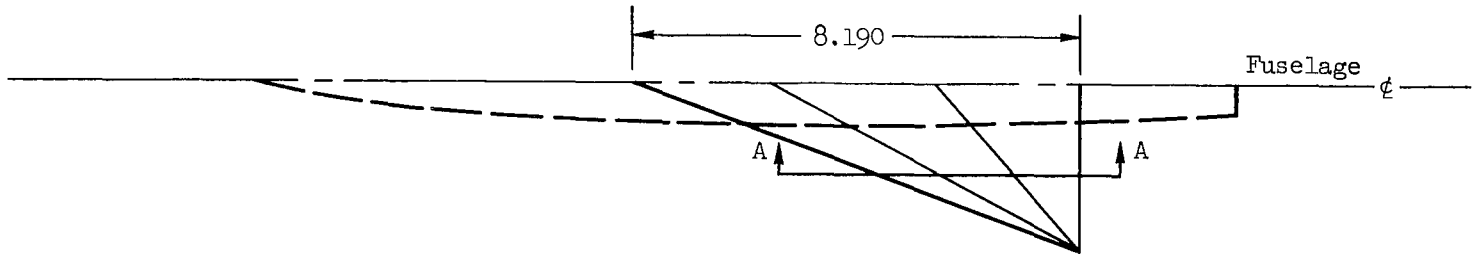

Typical A-A sections
(Not to scale)

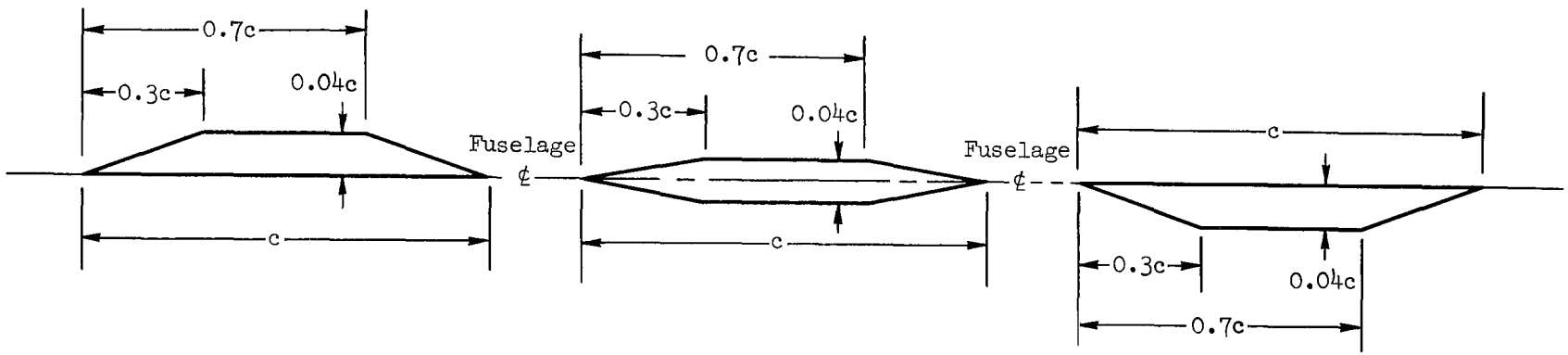

Positive camber | Symmetrical | Negative camber

(d) Details of cambered and symmetrical wings; WB and WBV configurations; mid-wing elevation; $i_w = 0°$.

Figure 1.- Concluded.

Three-quarter top view

Three-quarter bottom view A-39626-5

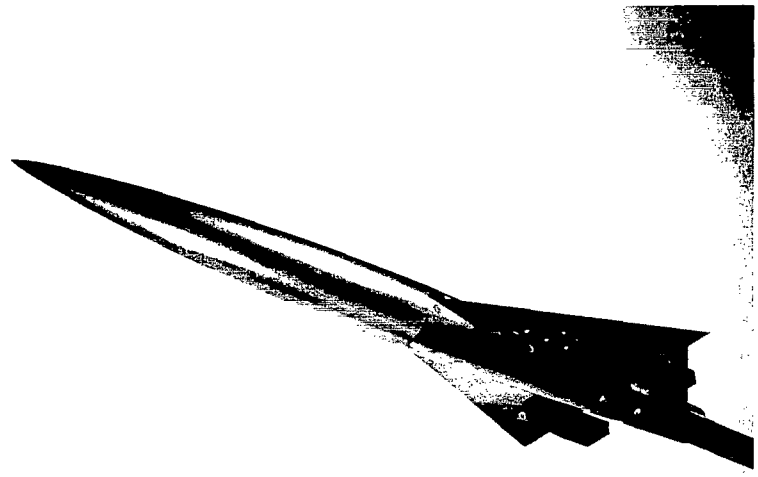

A-39626-6

Figure 2.- Photographs of model; WBVN configuration; mid-wing elevation; positive cambered wing; $i_w = 0°$.

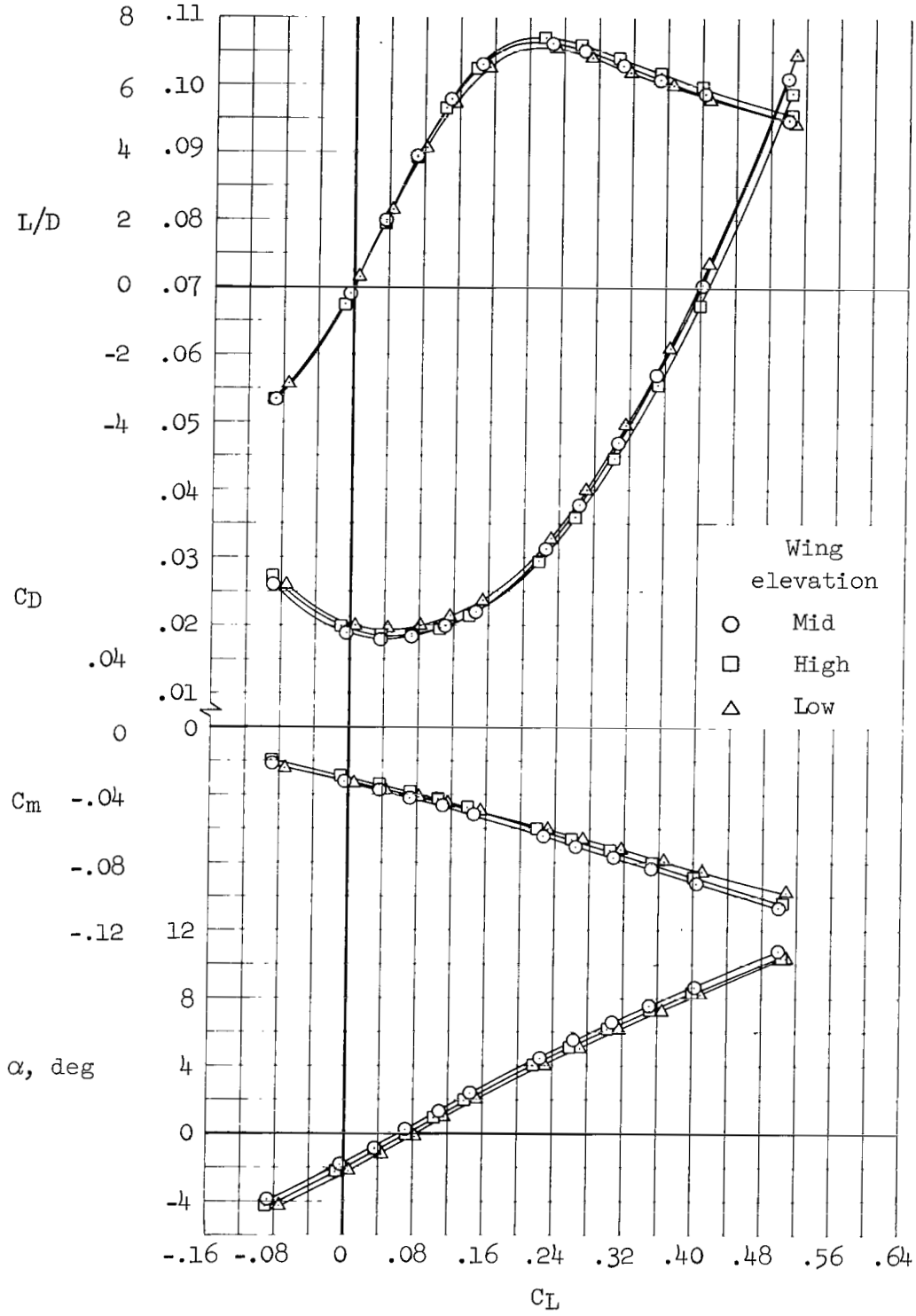

(a) M = 0.65

Figure 3.- Effect of wing elevation on the longitudinal aerodynamic characteristics; WBVN configuration, positive cambered wing, $i_w = 0°$.

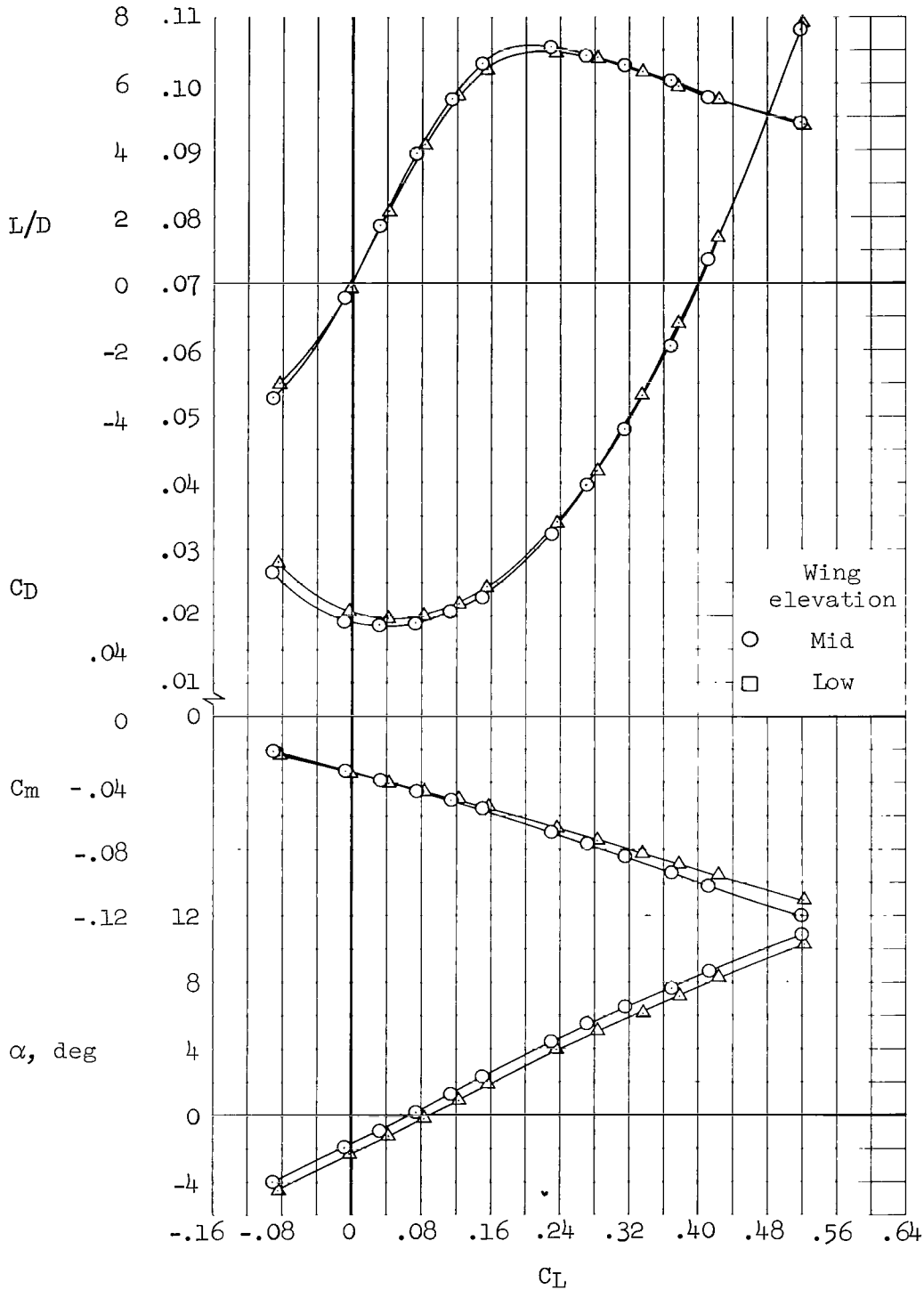

(b) M = 0.80

Figure 3.- Continued.

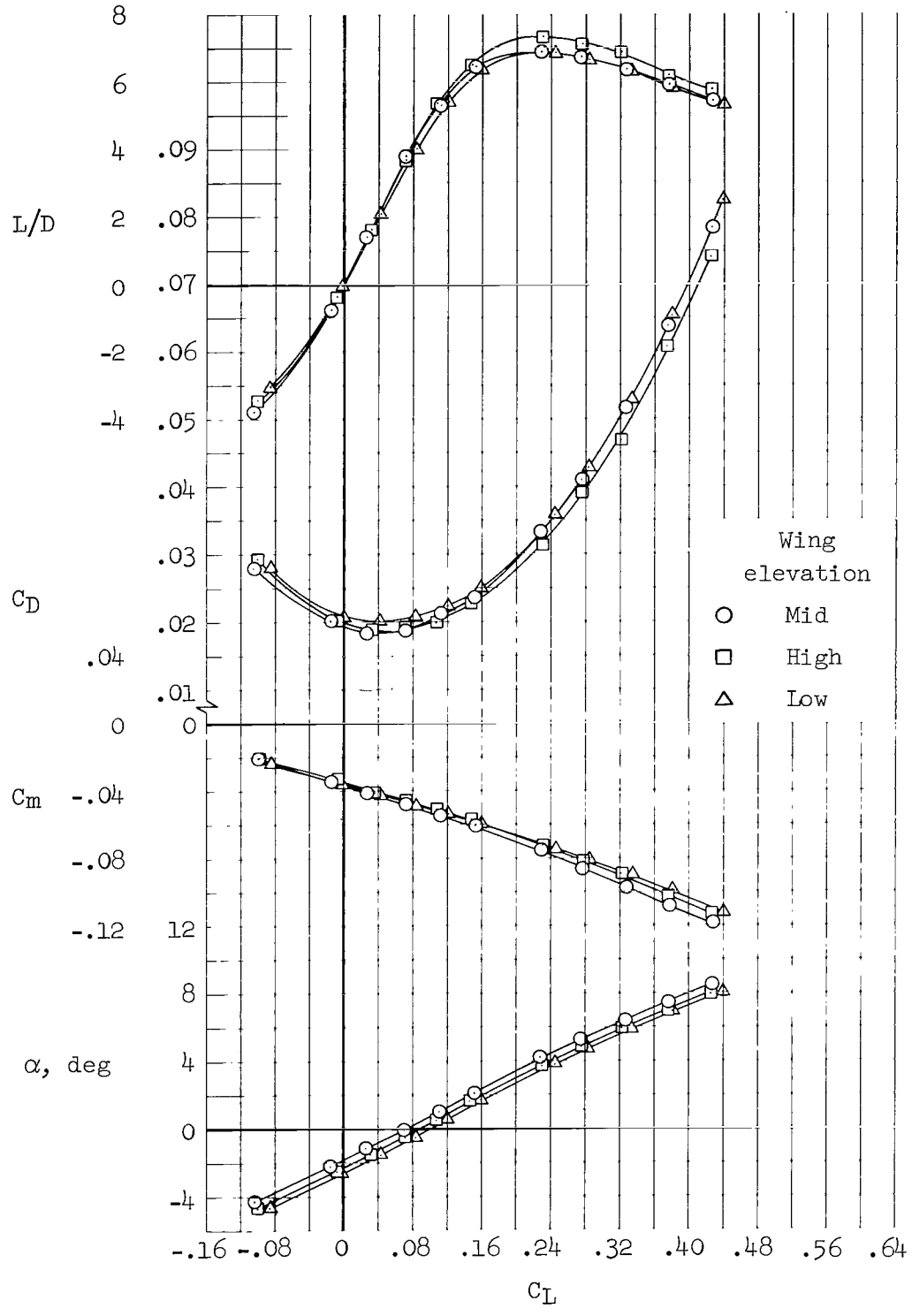

(c) M = 0.90

Figure 3.- Continued.

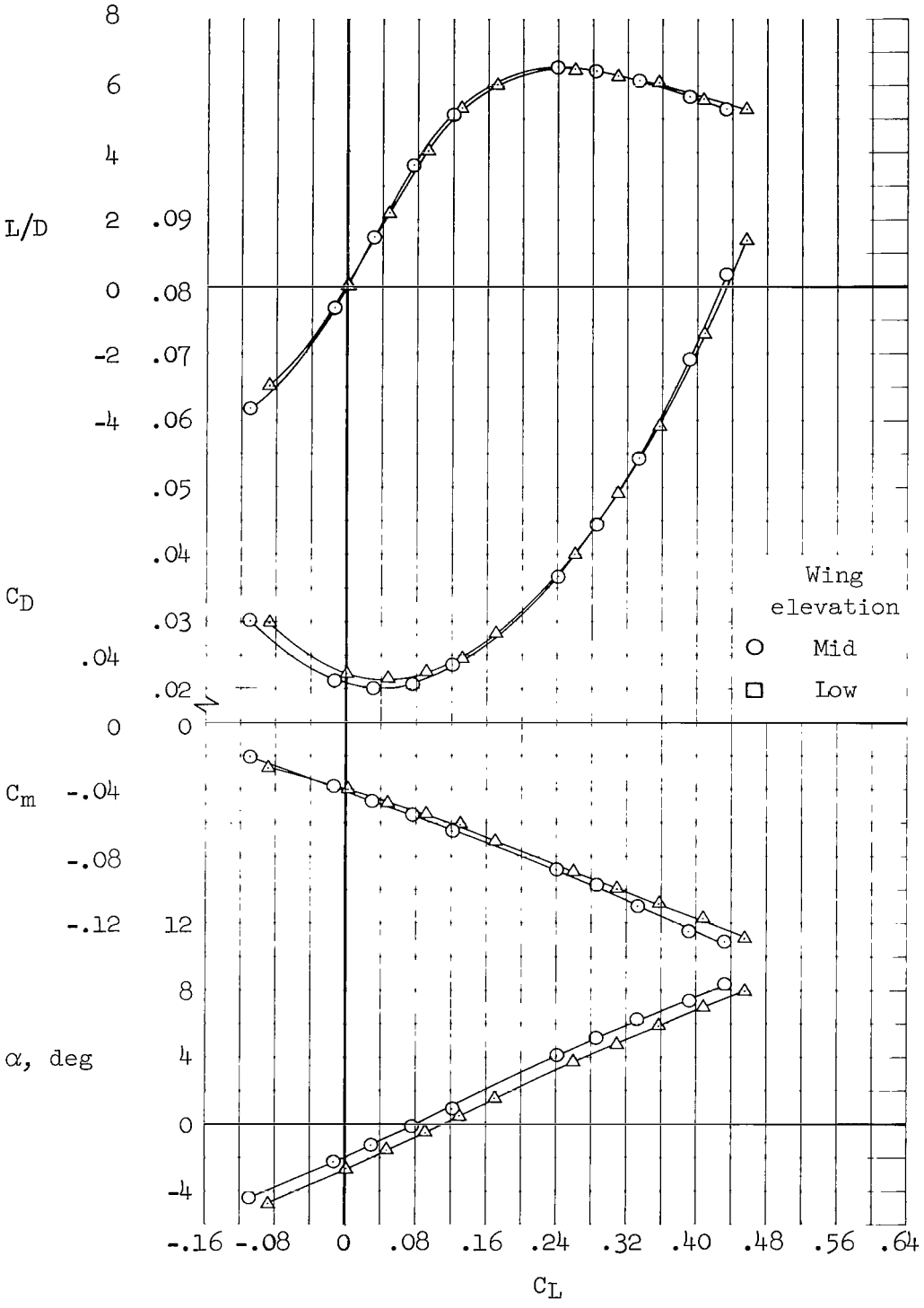

(d) M = 0.95

Figure 3.- Continued.

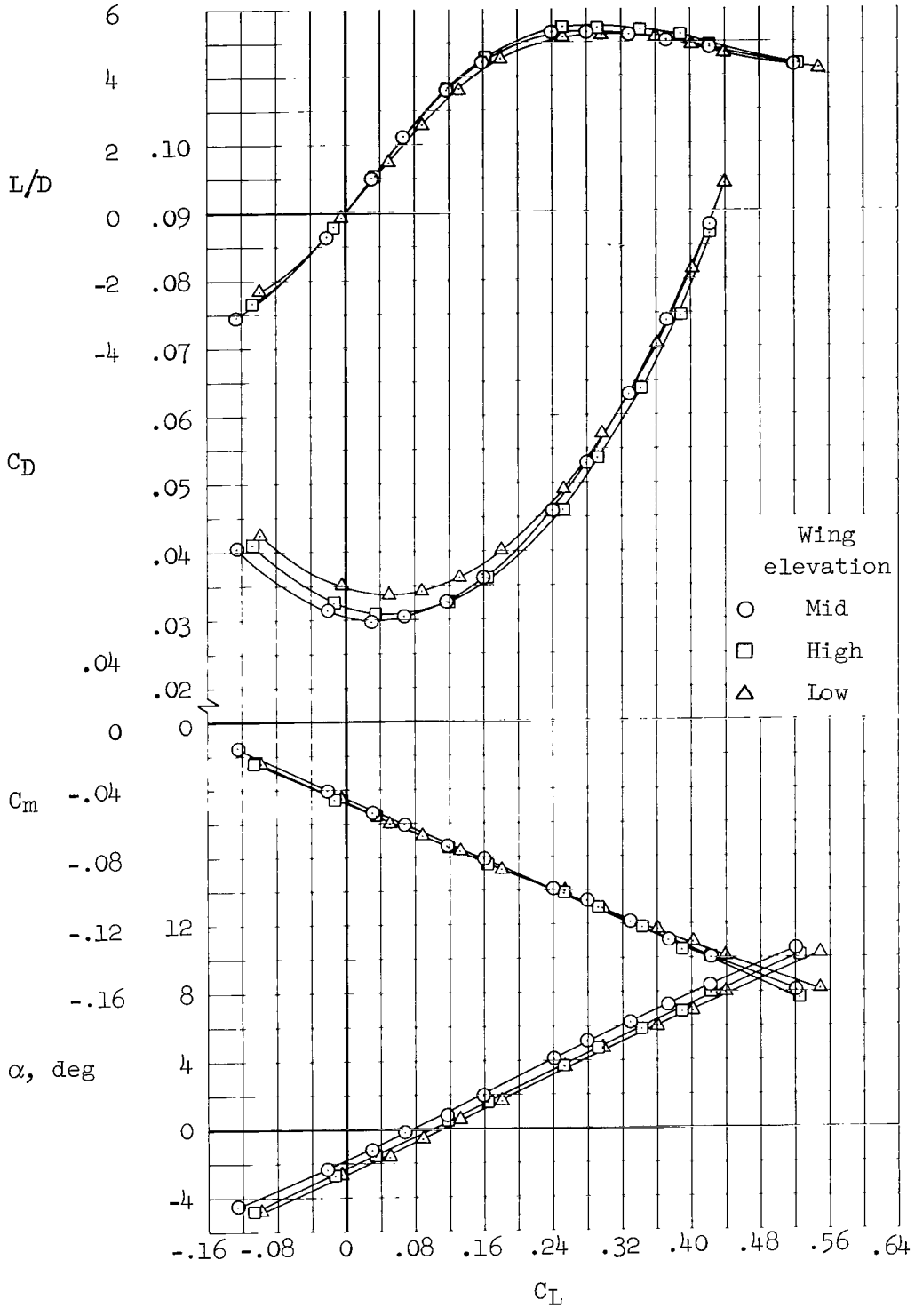

(e) M = 1.10

Figure 3.- Continued.

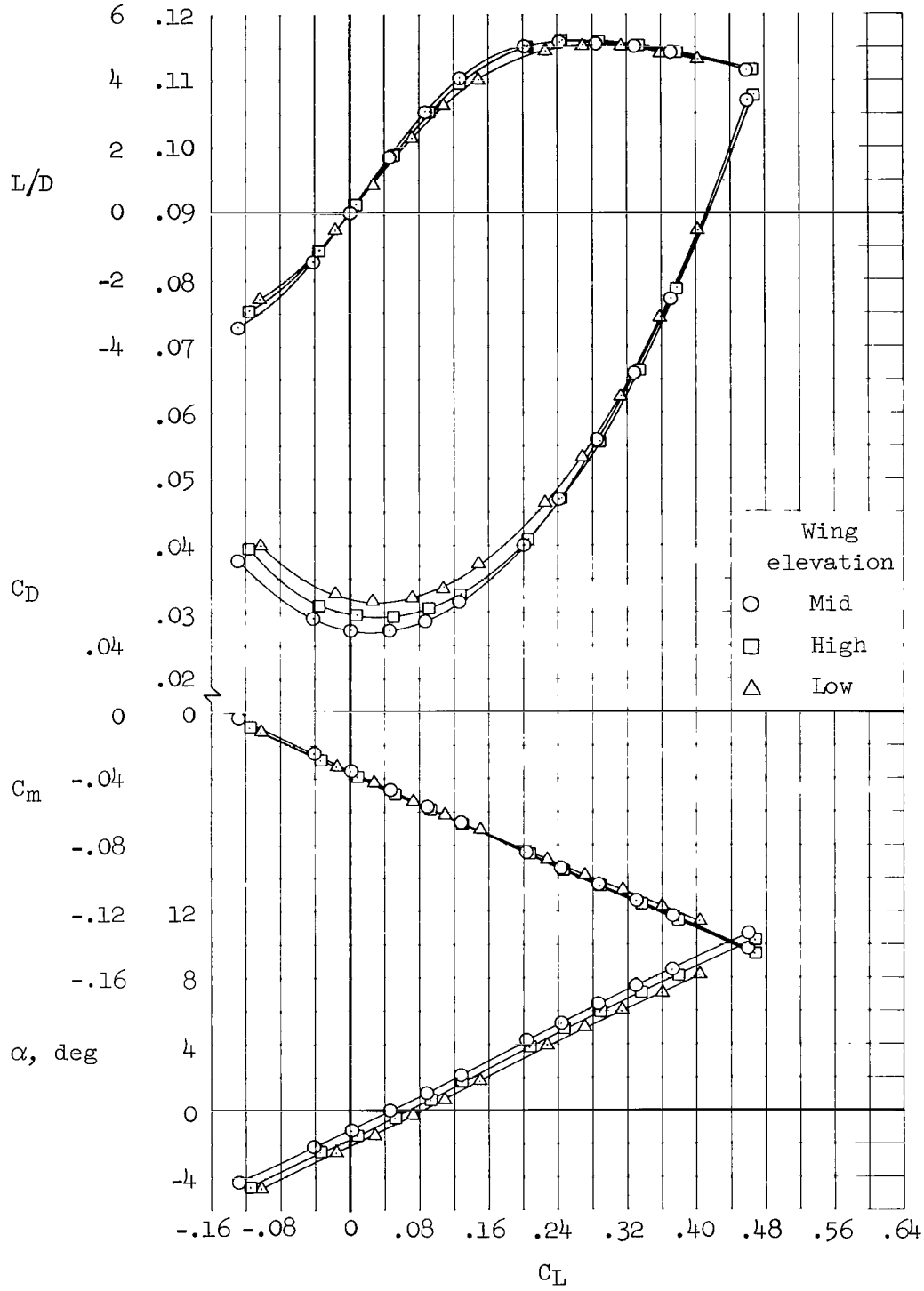

(f) M = 1.30

Figure 3.- Continued.

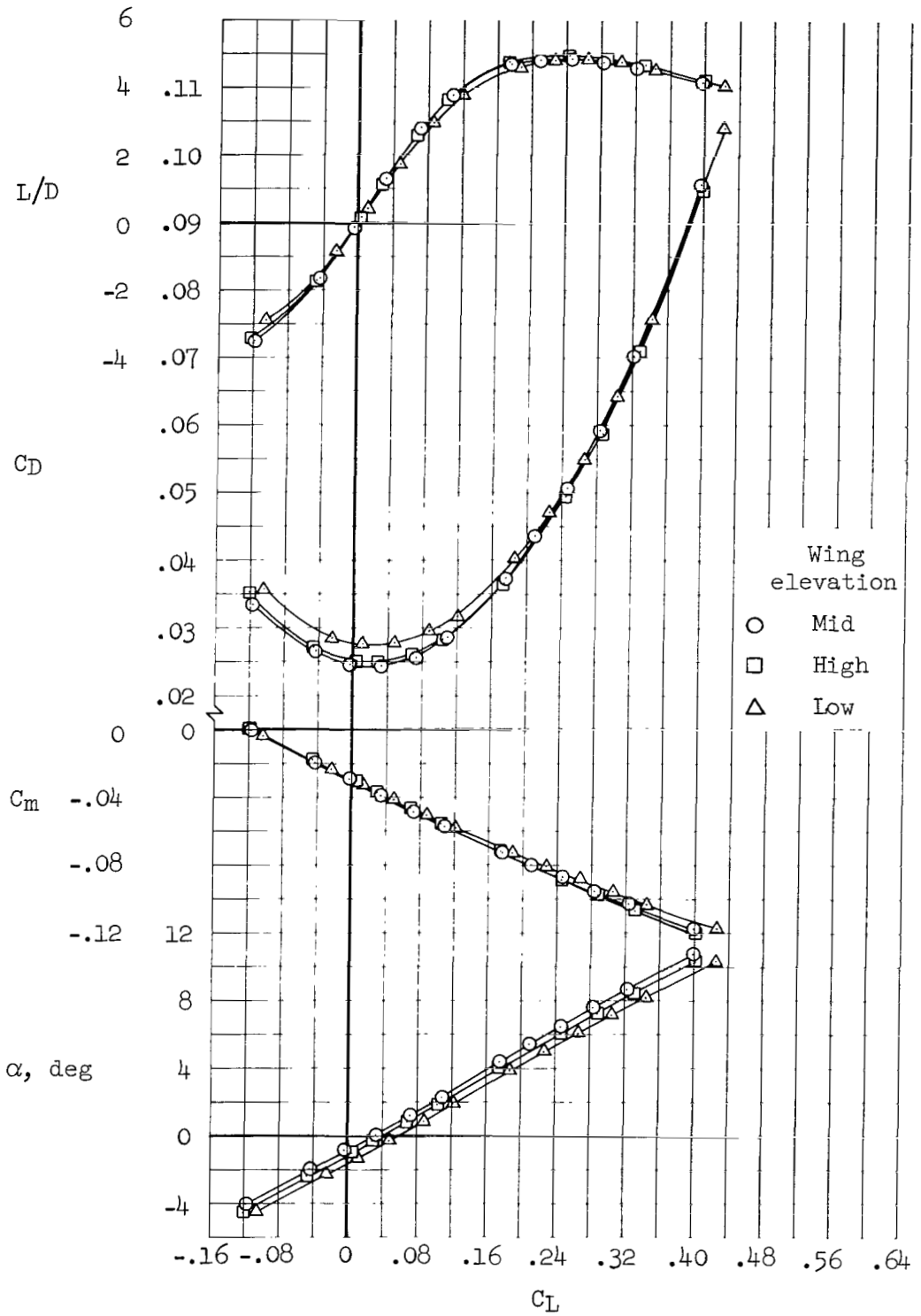

(g) M = 1.59

Figure 3.- Continued.

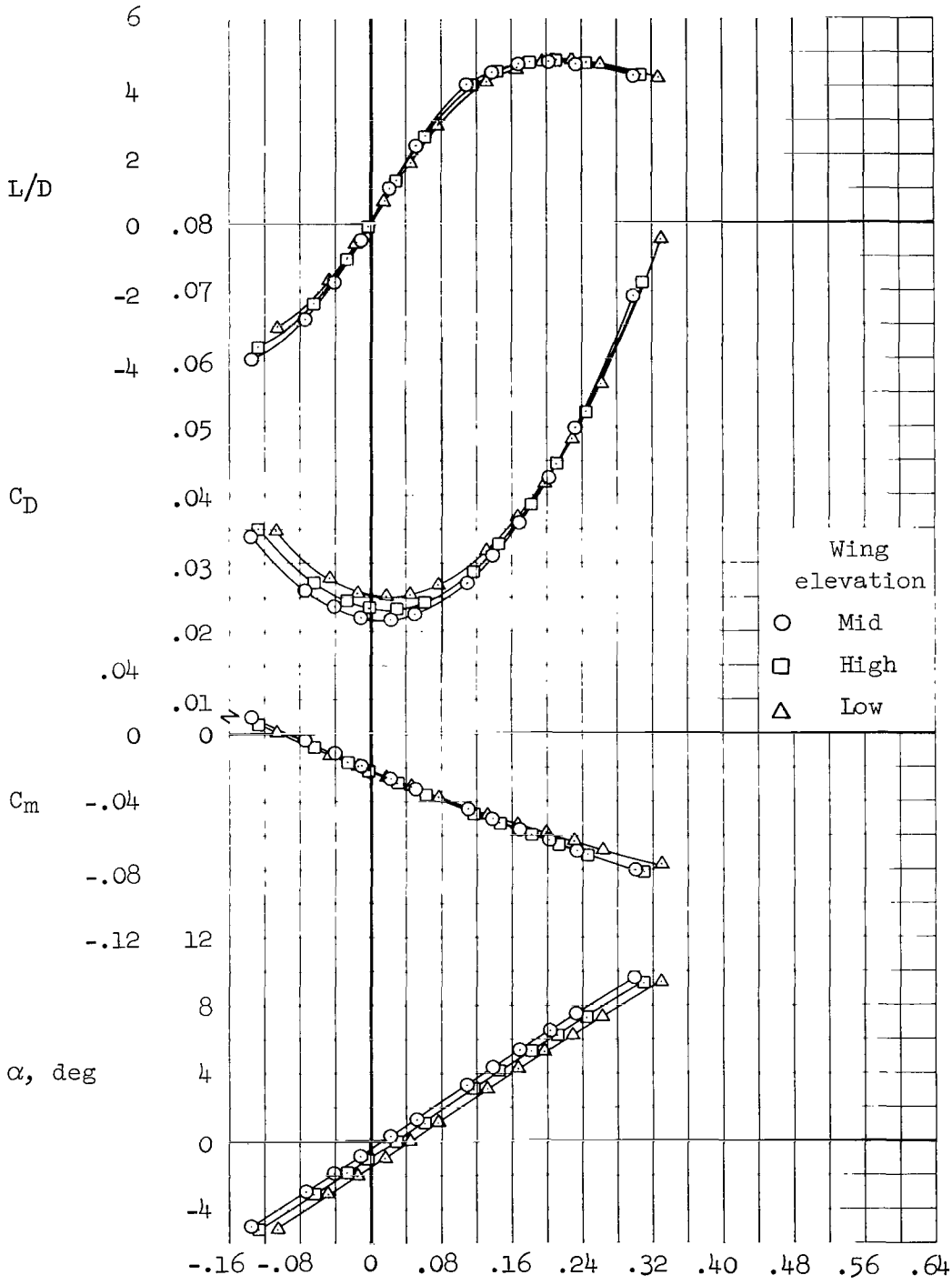

(h) M = 1.99

Figure 3.- Continued.

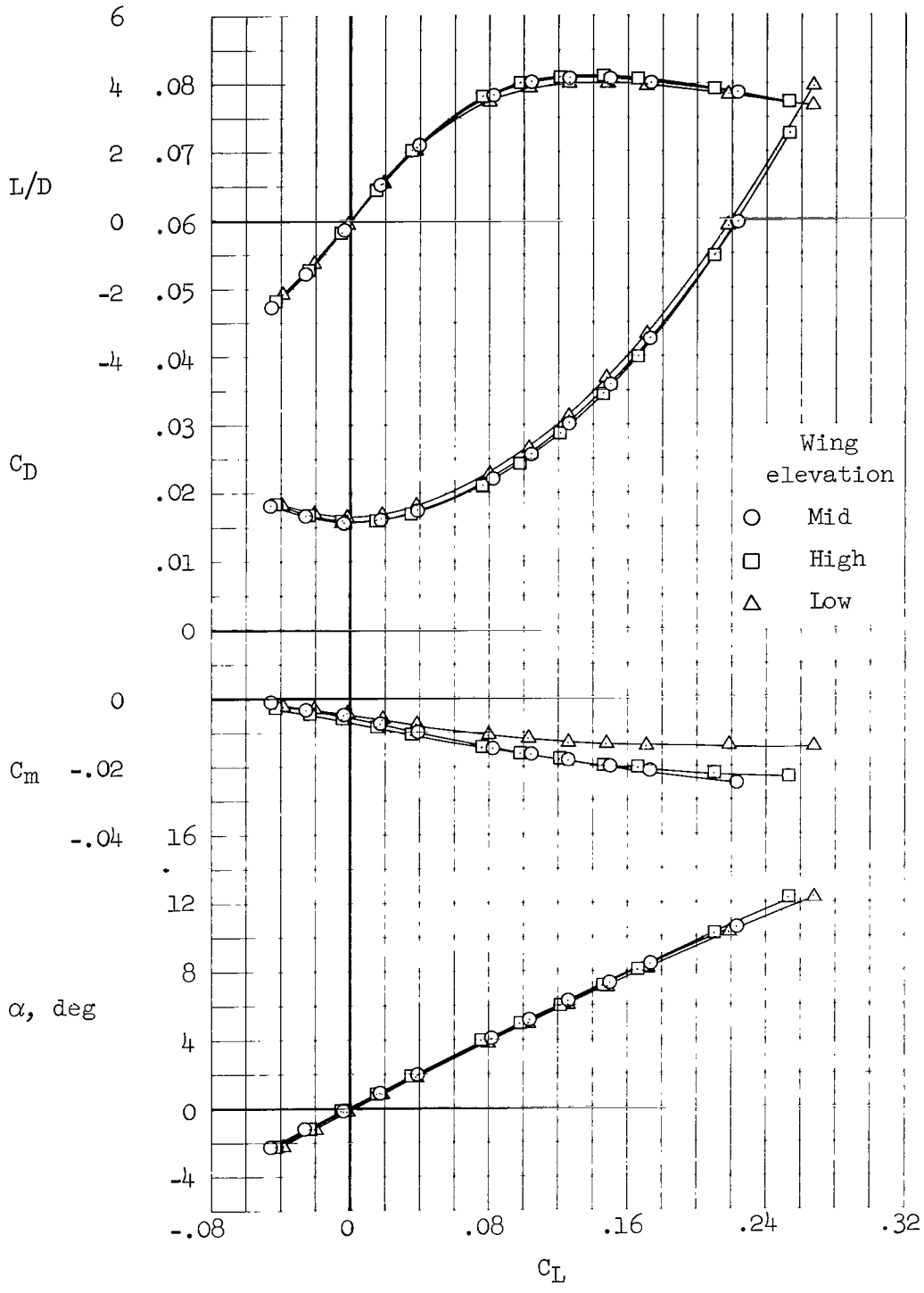

(i) M = 3.88

Figure 3.- Continued.

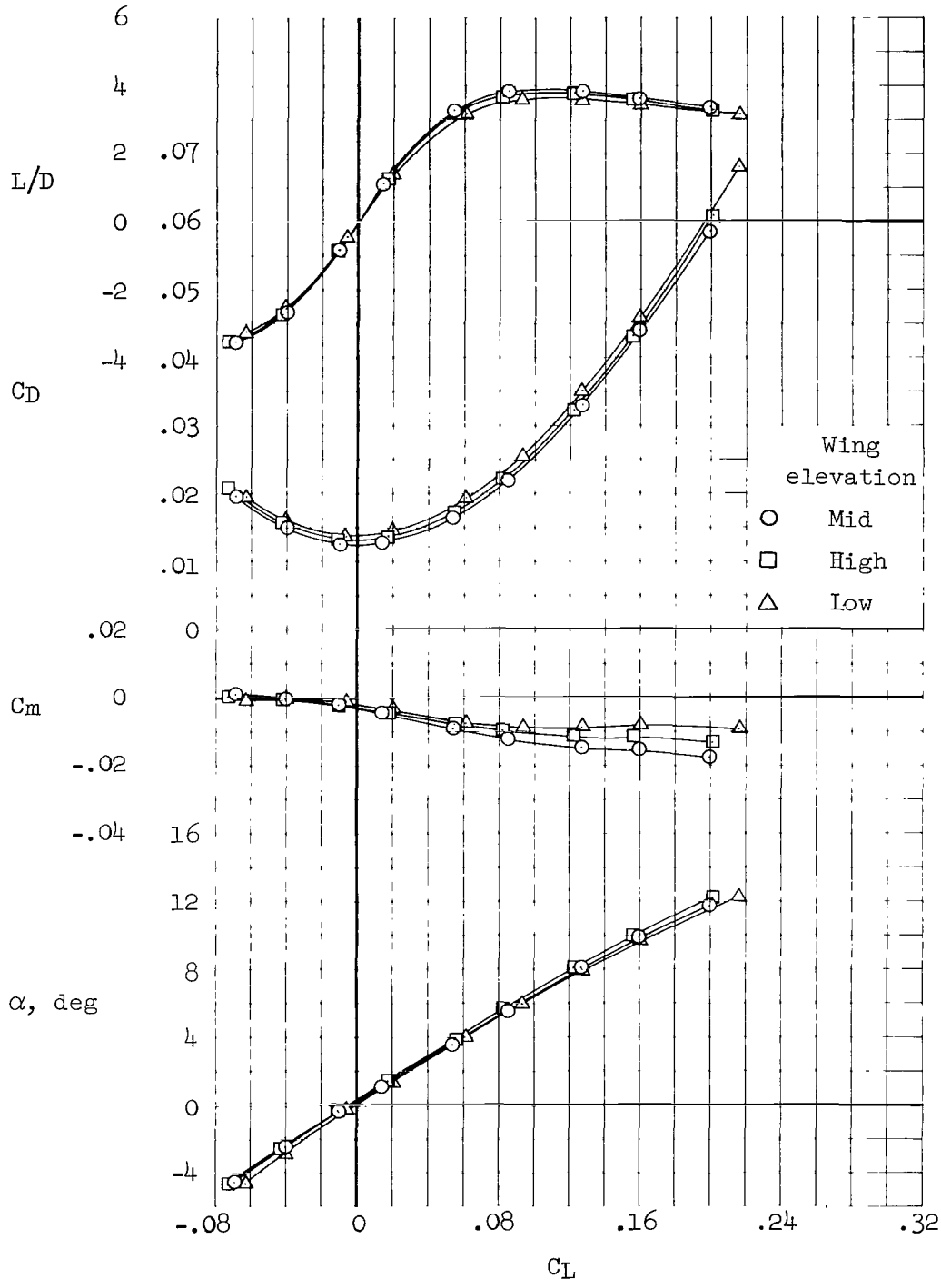

(j) M = 5.31

Figure 3.- Continued.

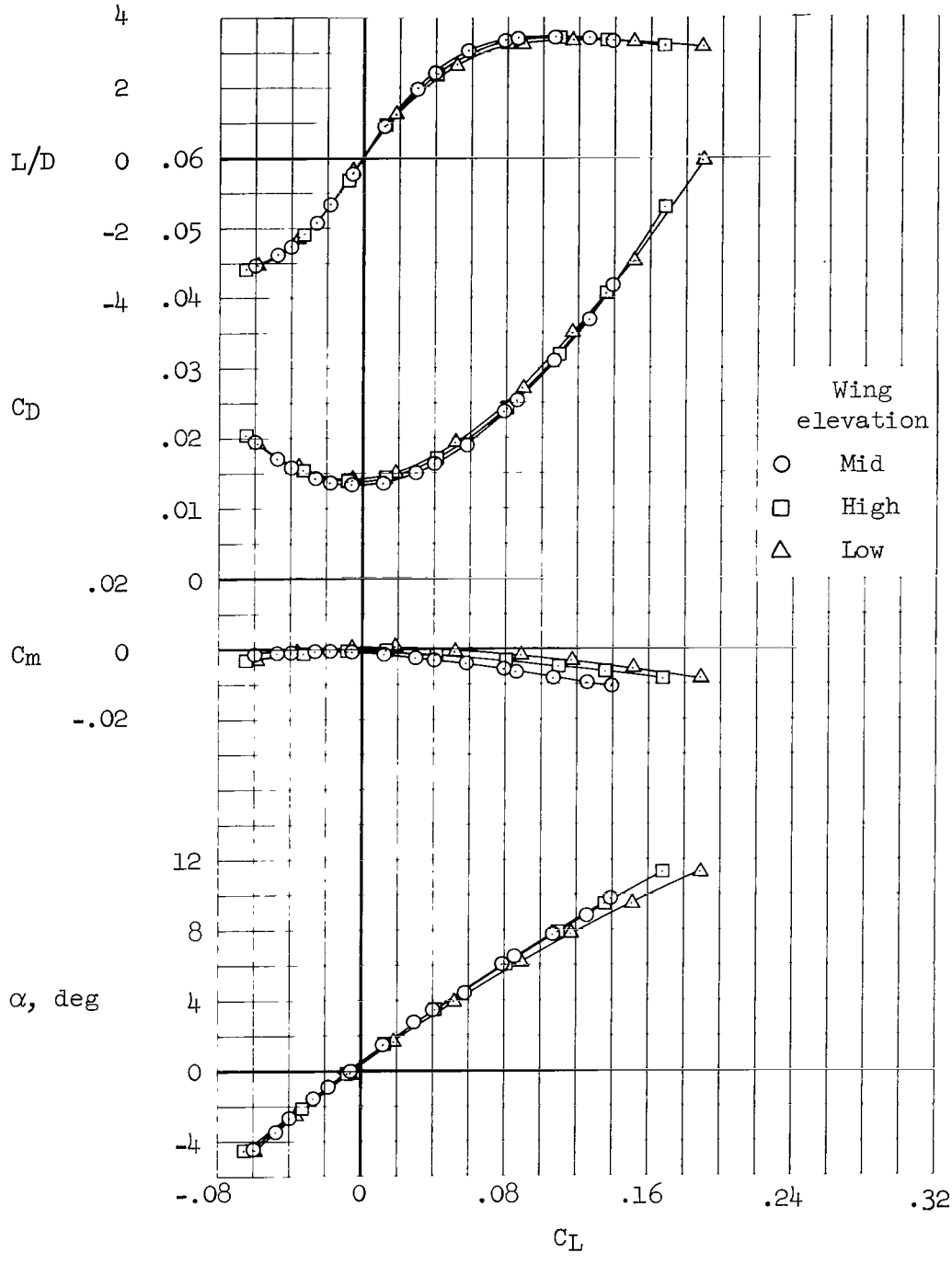

(k) M = 7.42

Figure 3.- Continued.

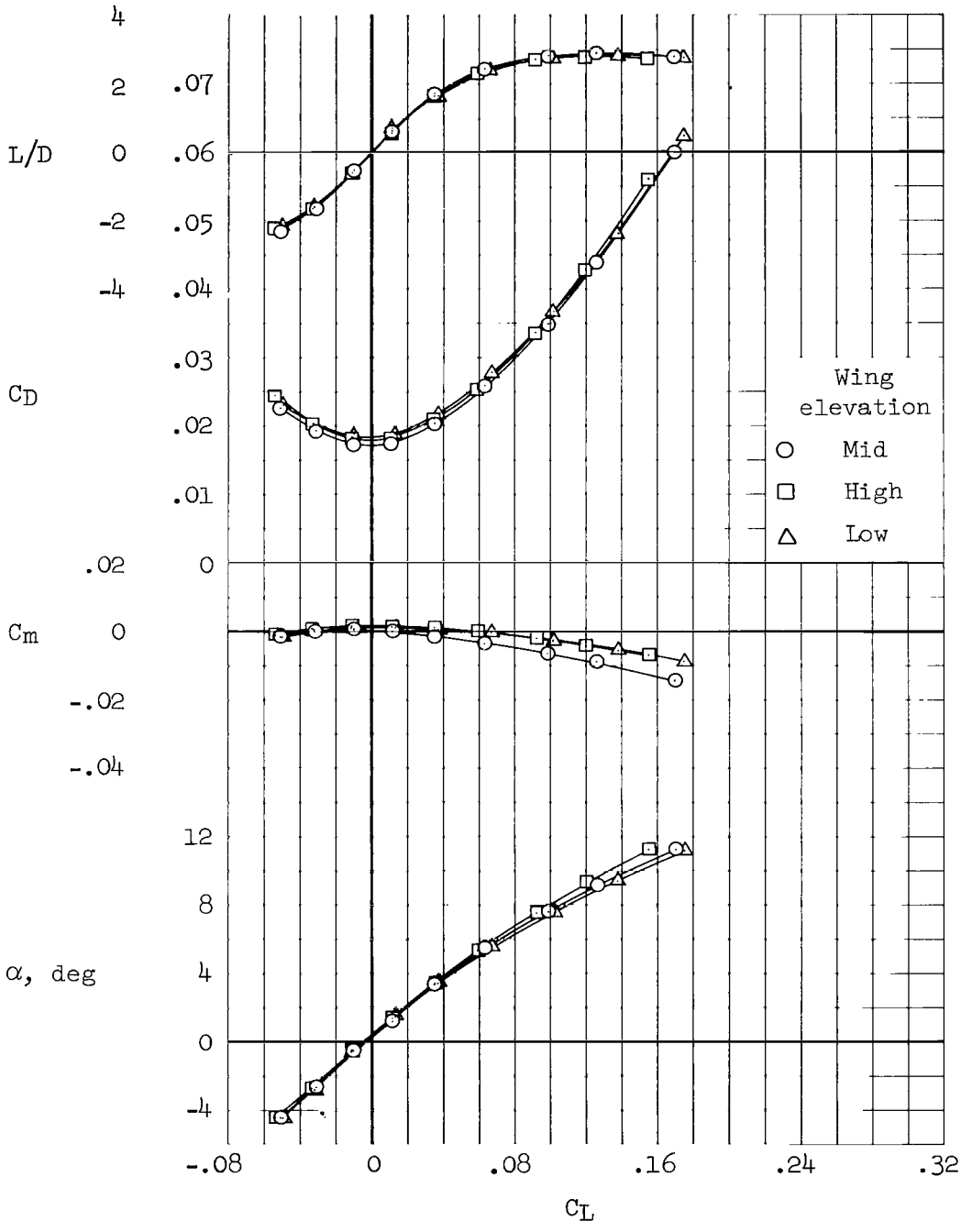

(1) M = 10.70

Figure 3.- Concluded.

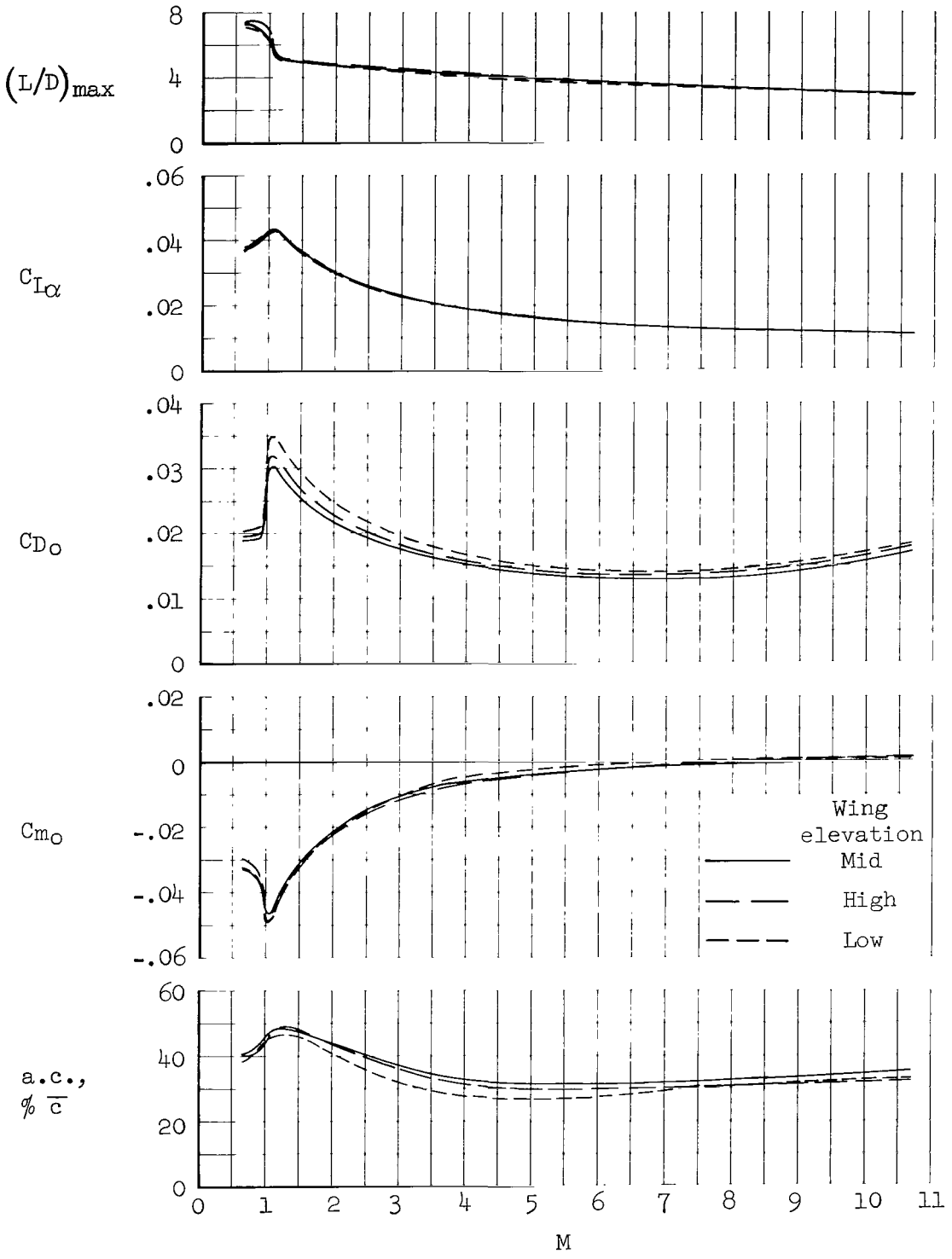

Figure 4.- Variation with Mach number of the effect of wing elevation on the longitudinal aerodynamic characteristics; WBVN configuration, positive cambered wing, $i_w = 0°$.

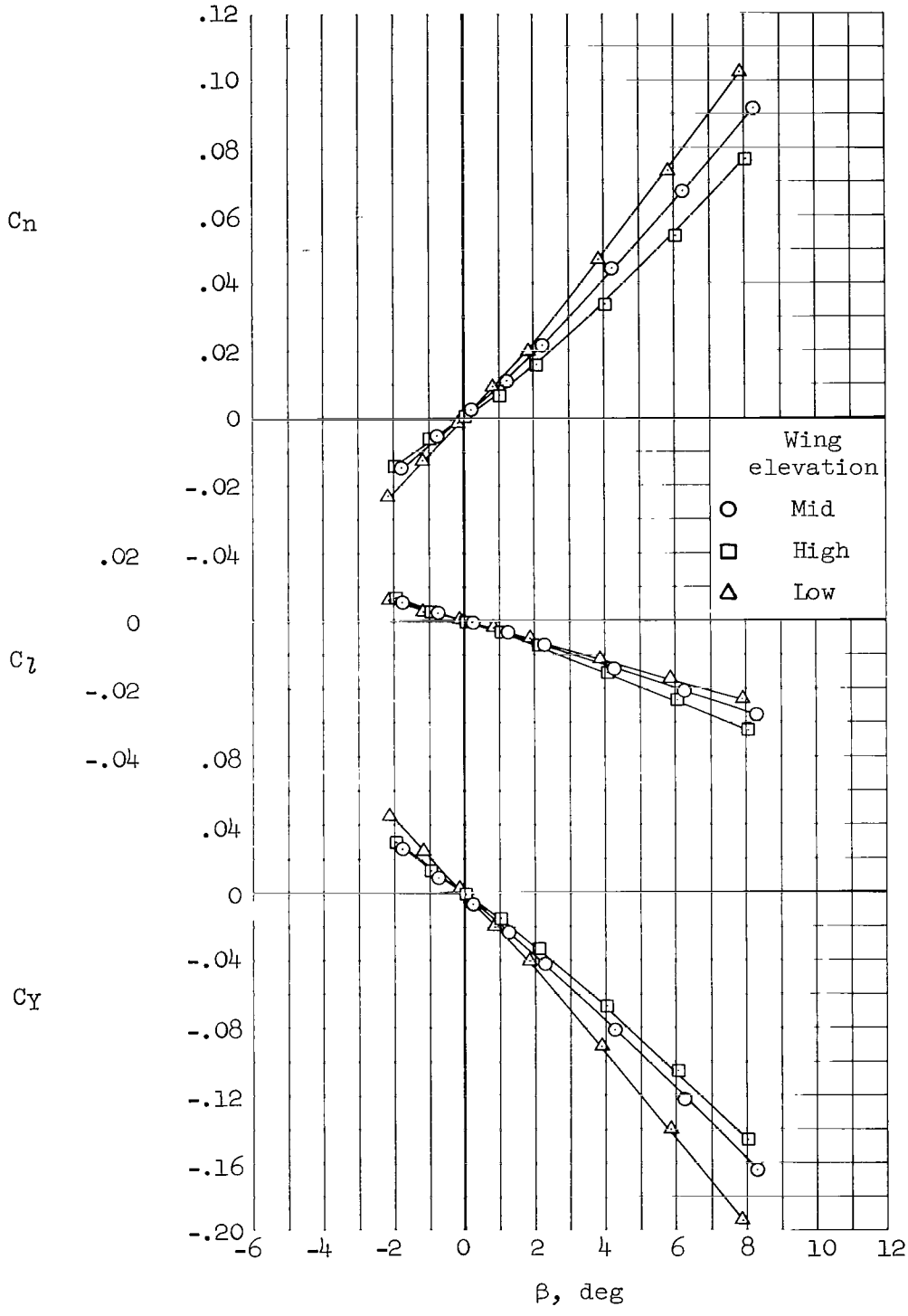

(a) M = 0.65; α = 0°

Figure 5.- Effect of wing elevation on the lateral and directional aerodynamic characteristics as a function of angle of sideslip; WBVN configuration, positive cambered wing, i_w = 0°.

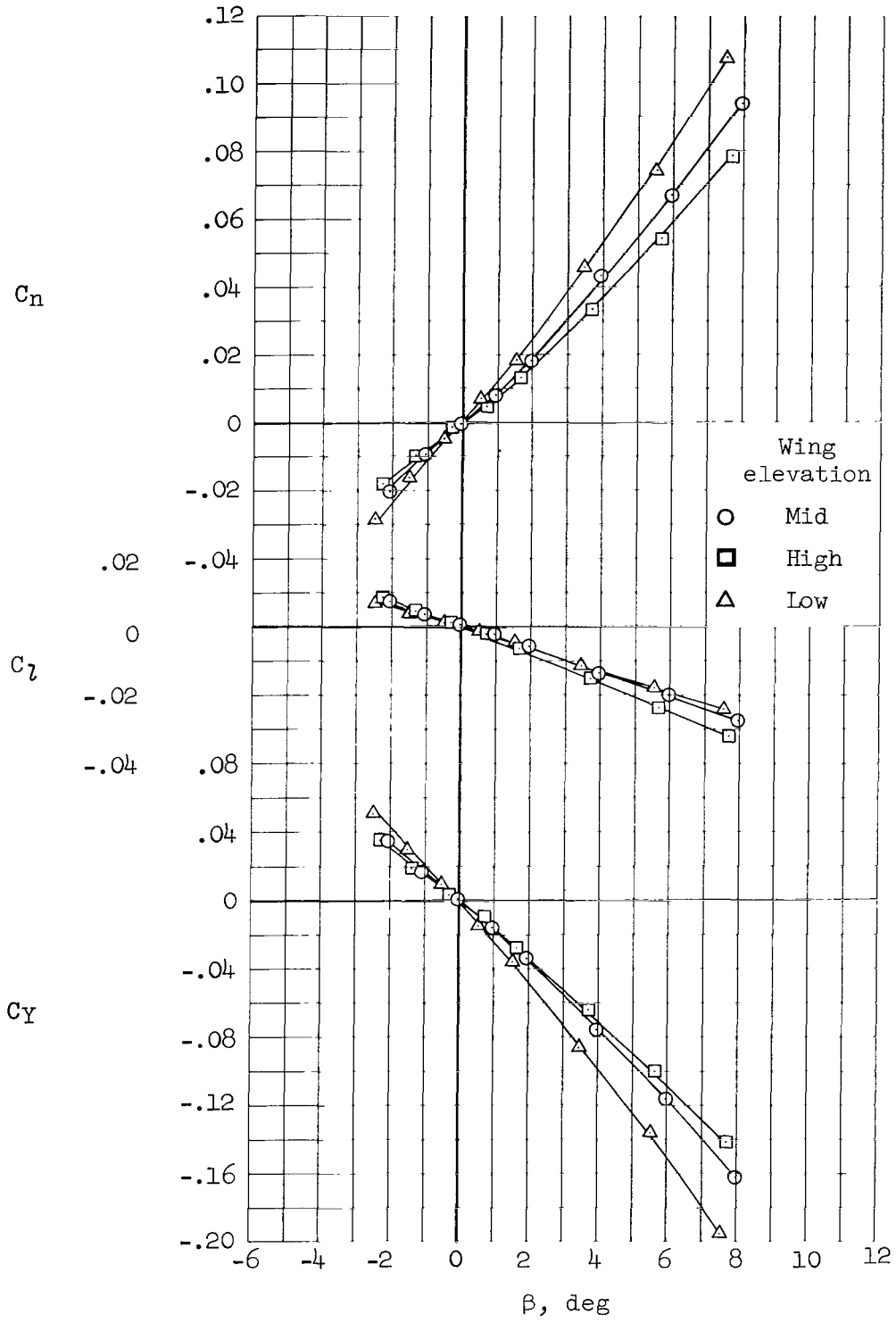

(b) M = 0.90; α = 0°

Figure 5.- Continued.

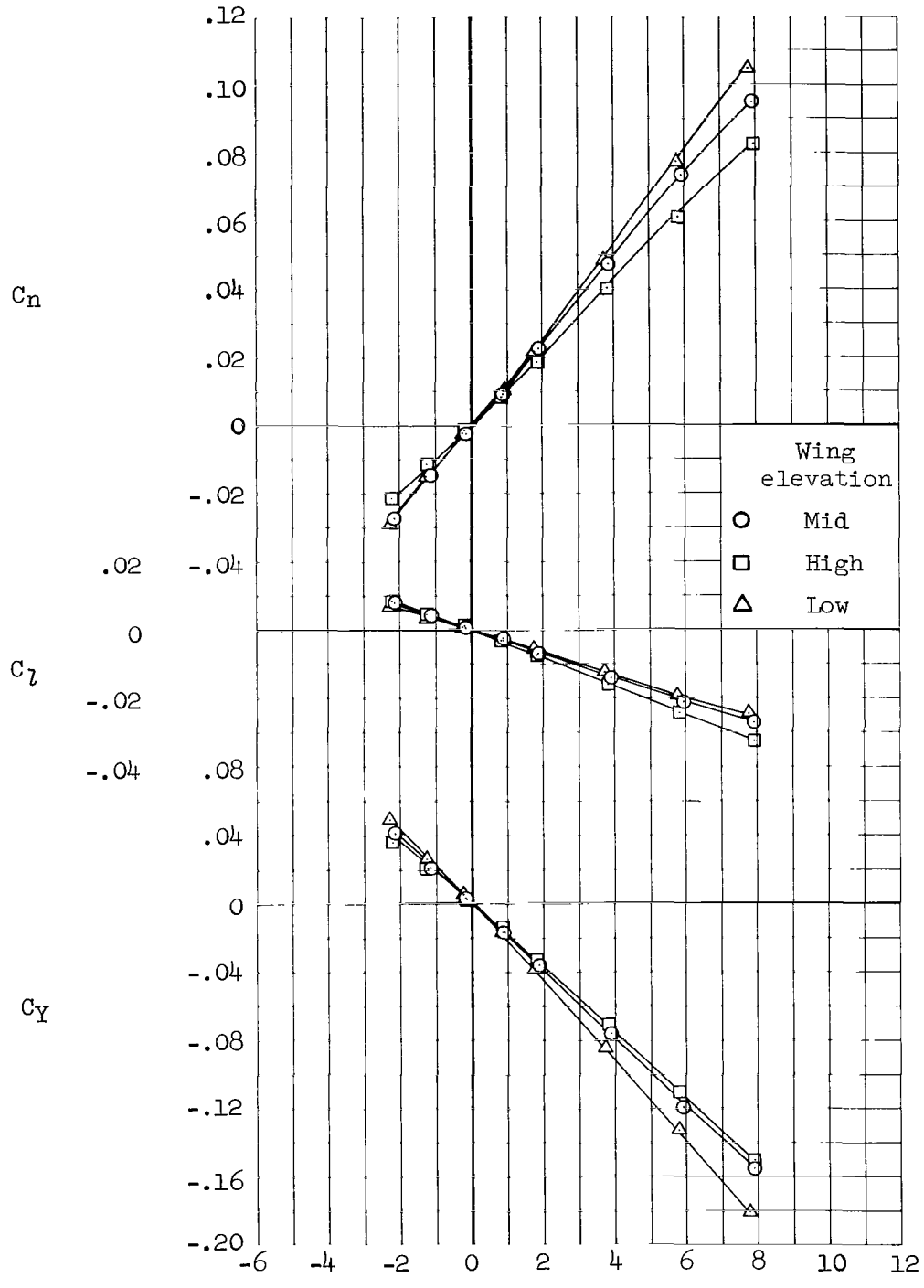

(c) M = 1.30; $\alpha = 0°$

Figure 5.- Continued.

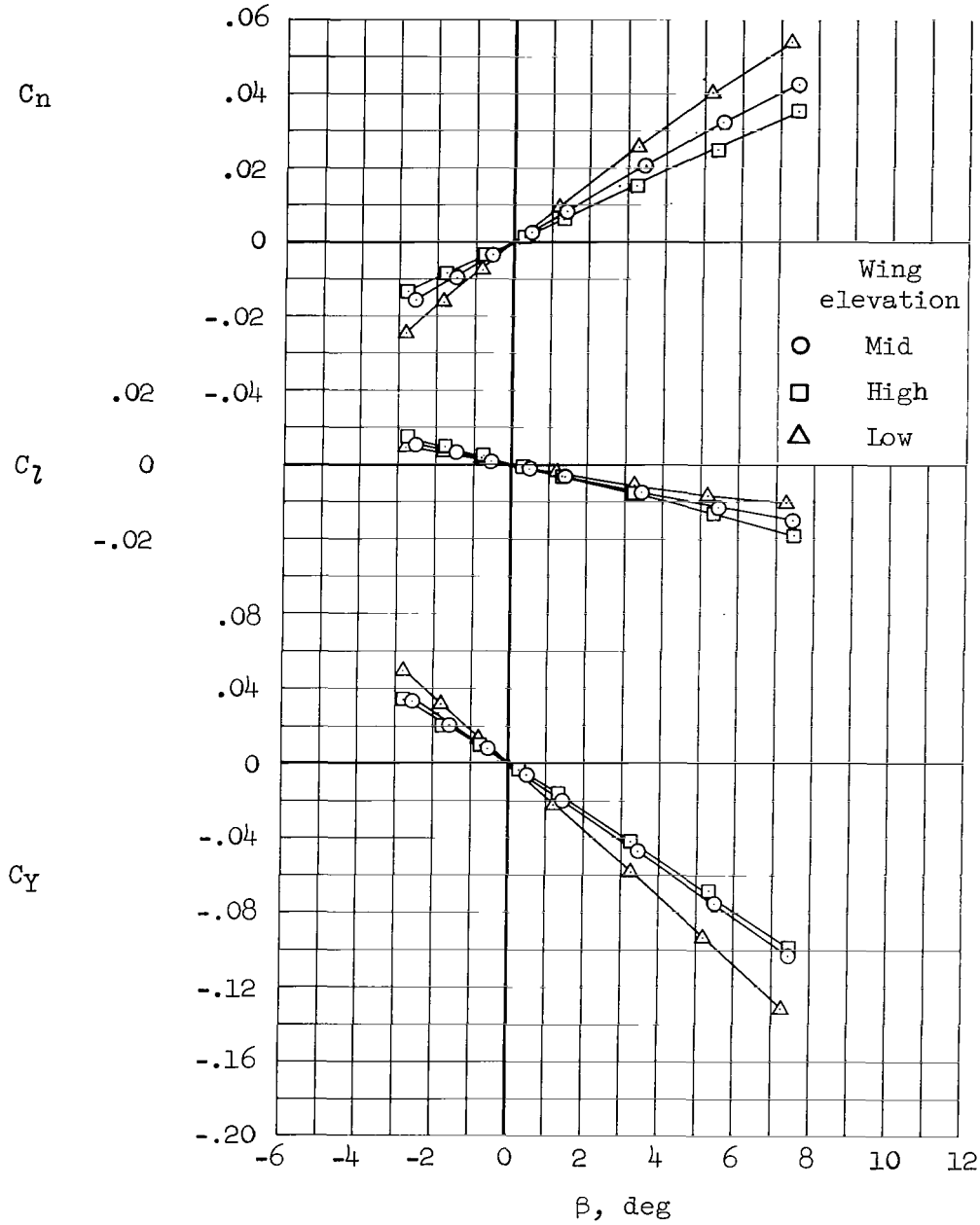

(d) M = 1.99; α = 0°

Figure 5.- Continued.

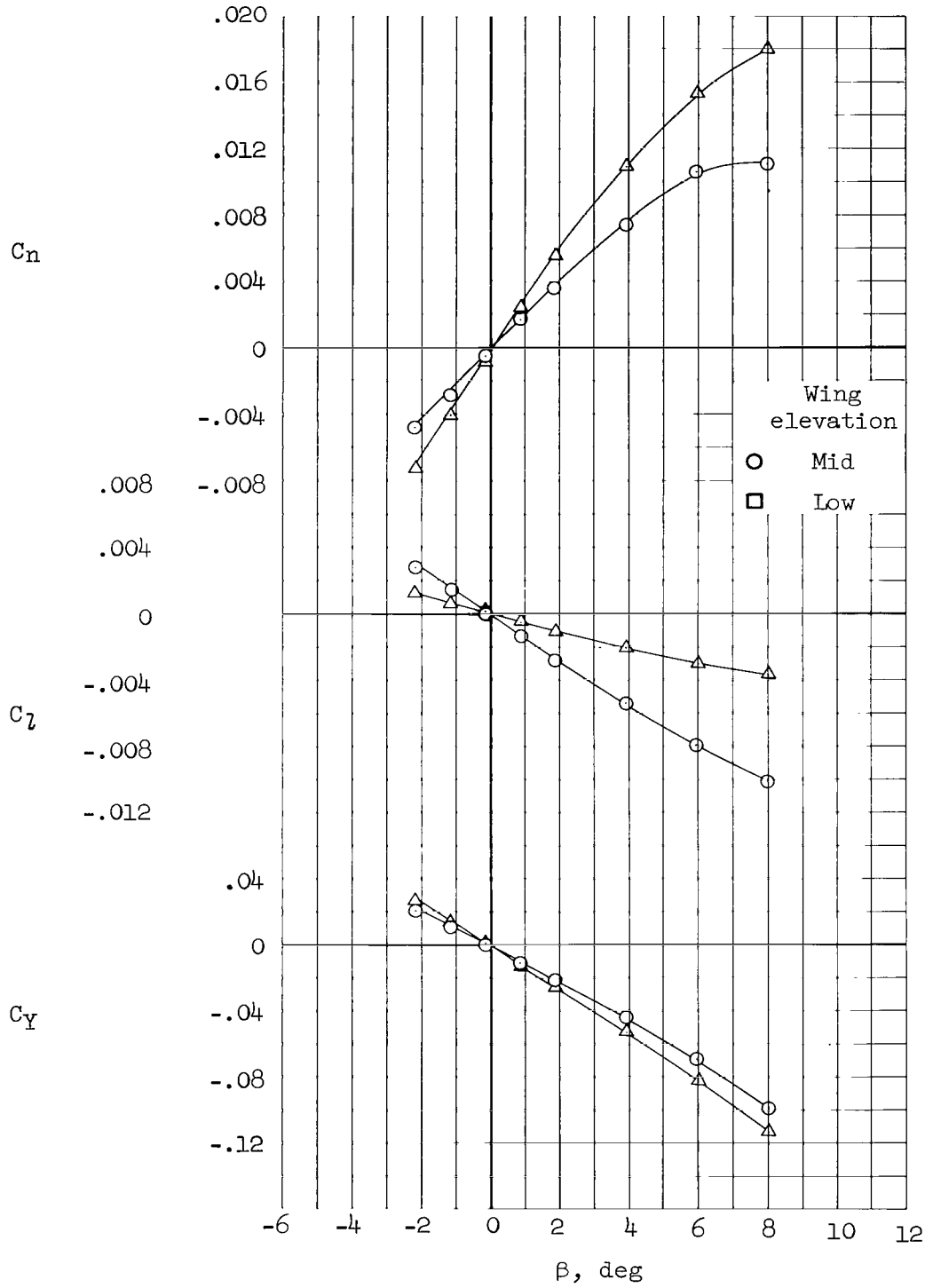

(e) M = 3.88; α = 0°

Figure 5.- Continued.

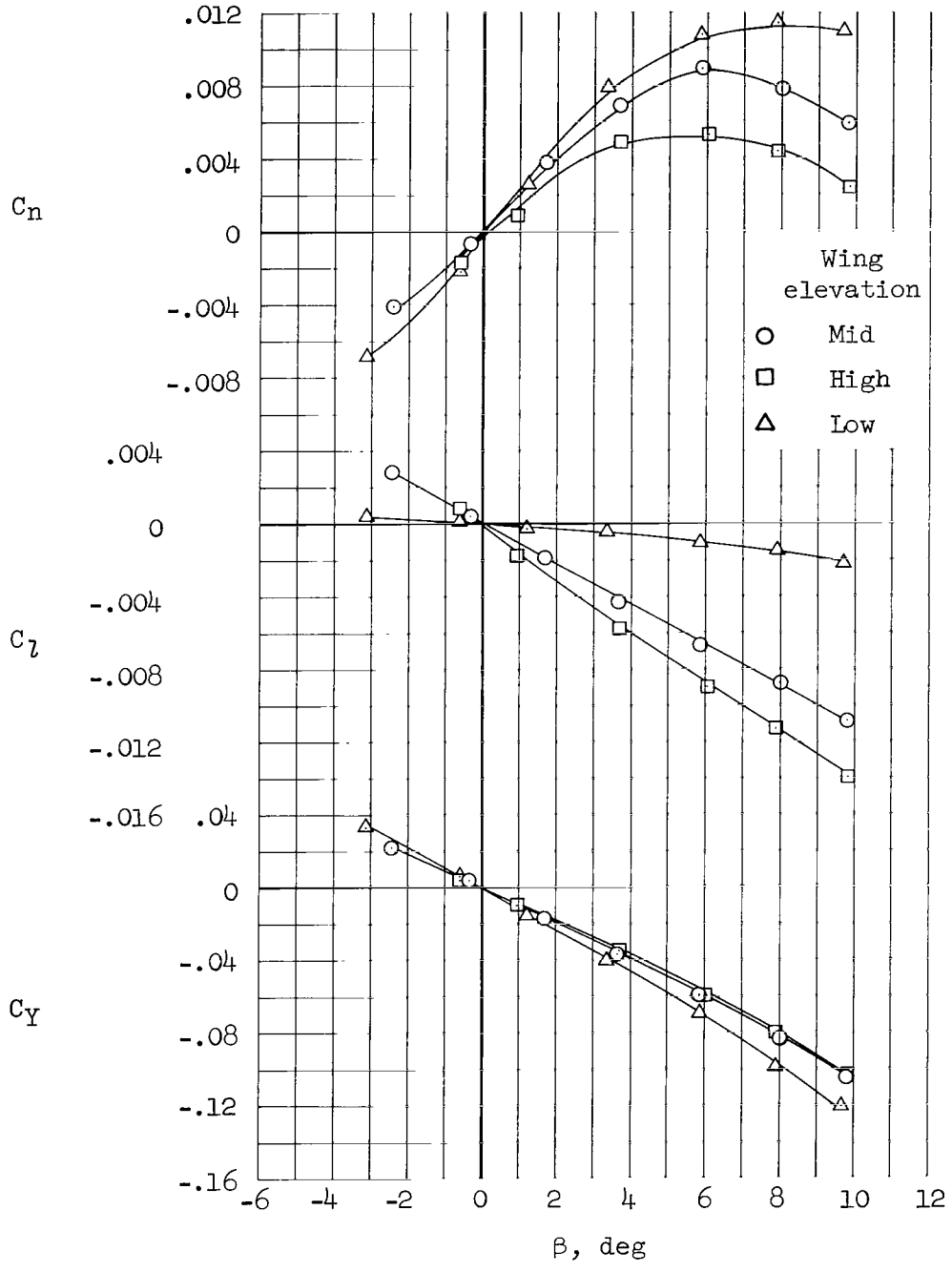

(f) M = 5.31; $\alpha = 0°$

Figure 5.- Continued.

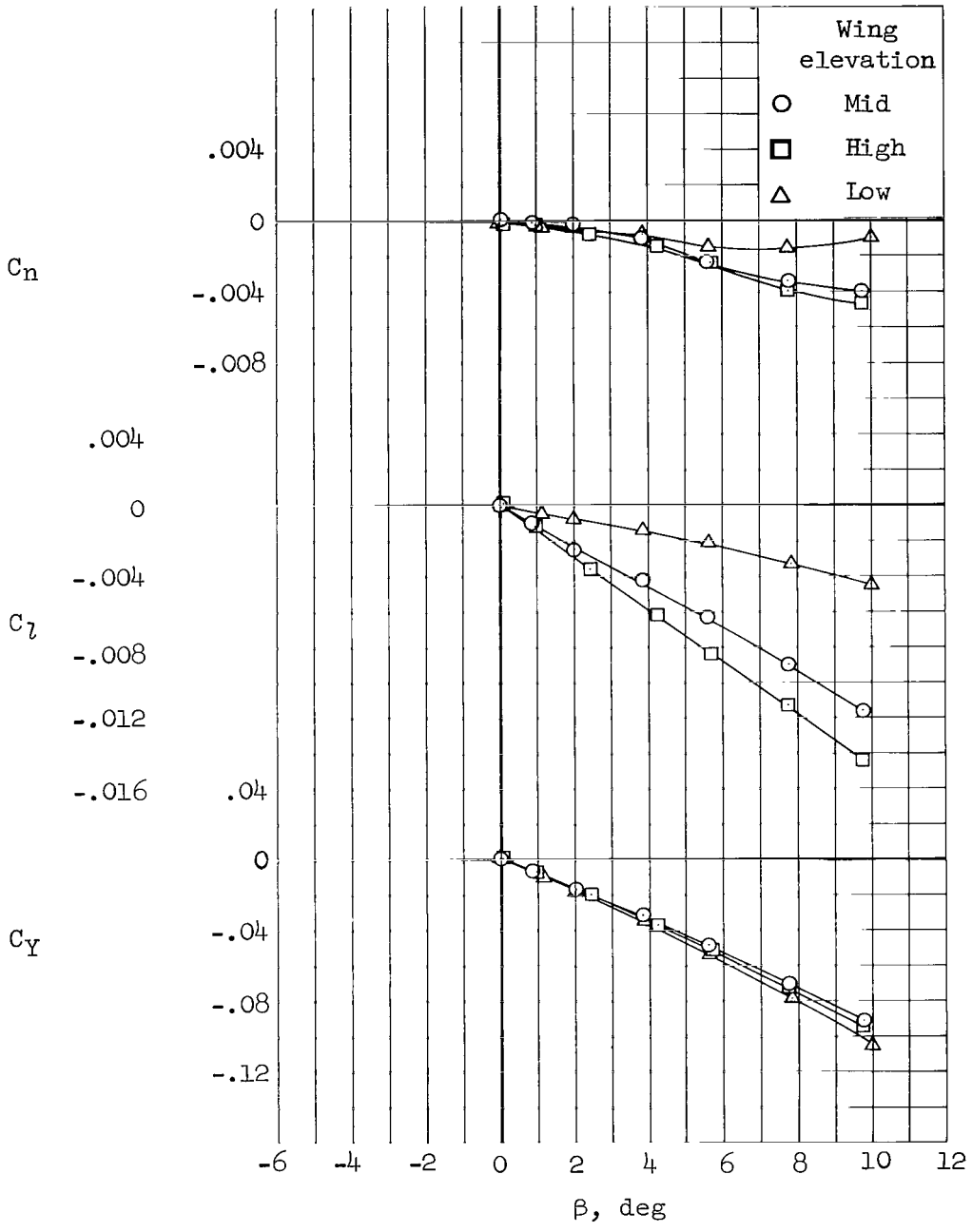

(g) M = 7.42; α = 3.9°

Figure 5.- Continued.

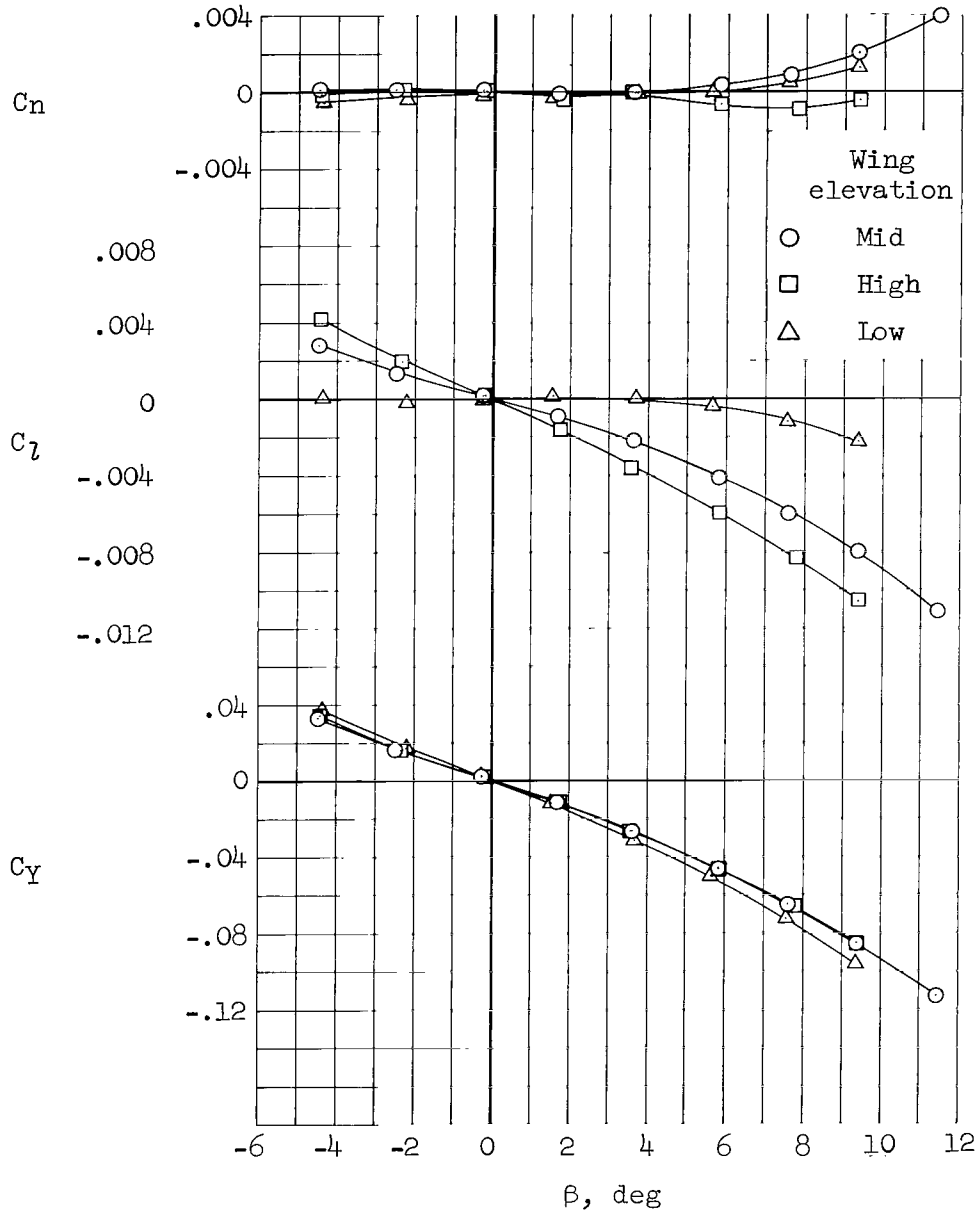

(h) M = 10.70; $\alpha = 0°$

Figure 5.- Concluded.

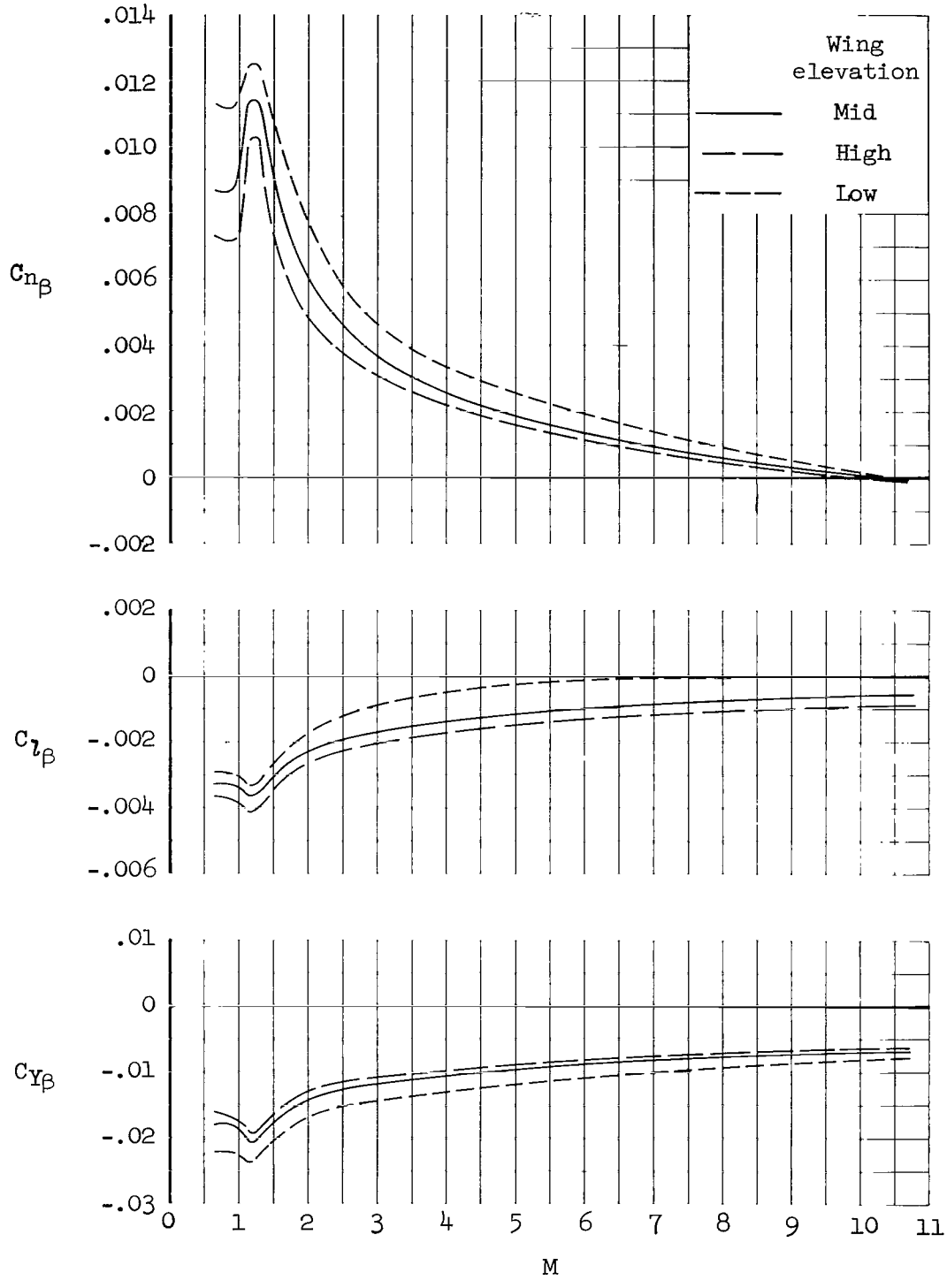

Figure 6.- Variation with Mach number of the effect of wing elevation on the lateral and directional aerodynamic characteristics; WBVN configuration, positive cambered wing, $i_w = 0°$, $\alpha = 0°$.

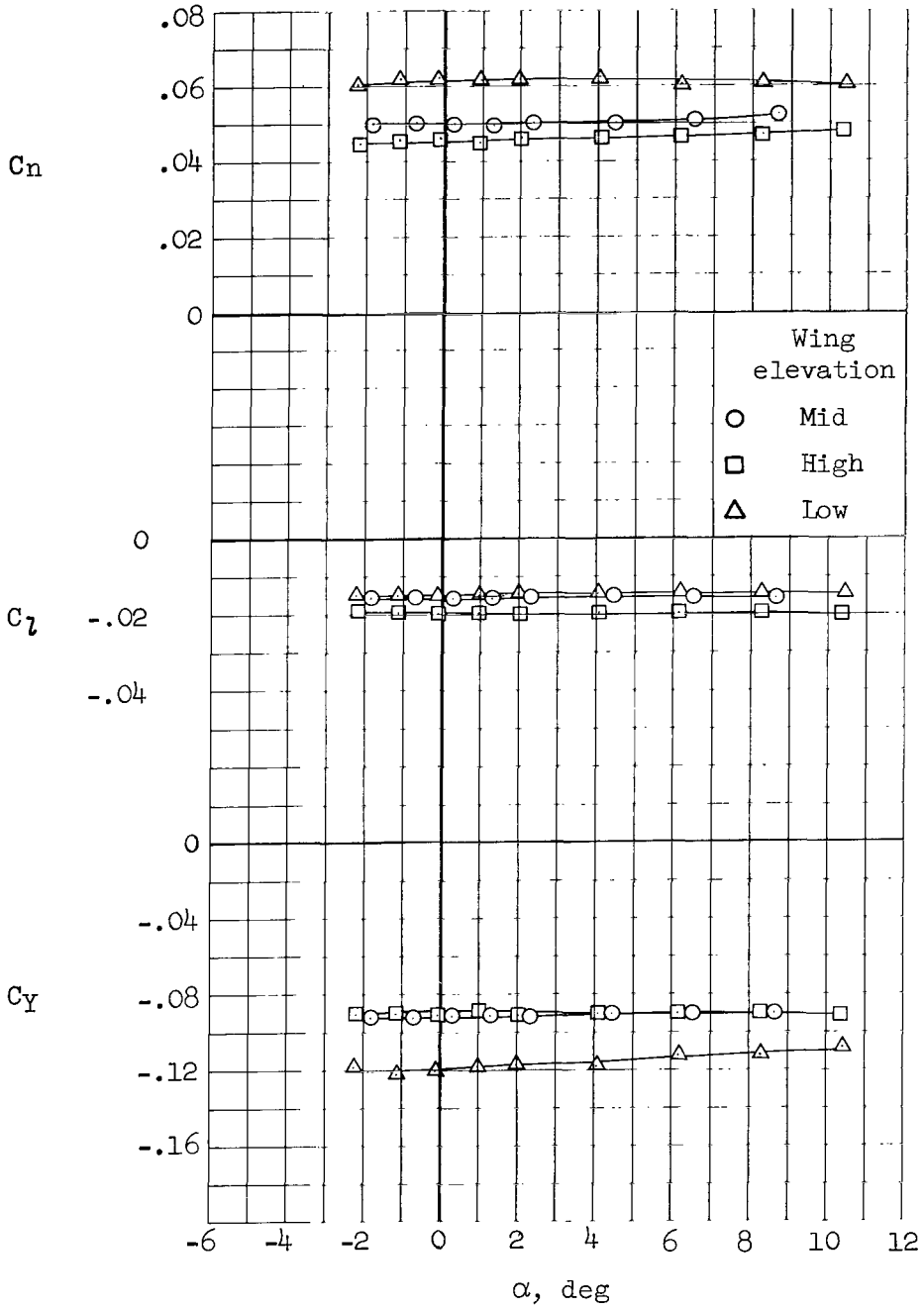

(a) M = 0.65; β = 4.9°

Figure 7.- Effect of wing elevation on the lateral and directional aerodynamic characteristics as a function of angle of attack; WBVN configuration, positive cambered wing, $i_w = 0°$.

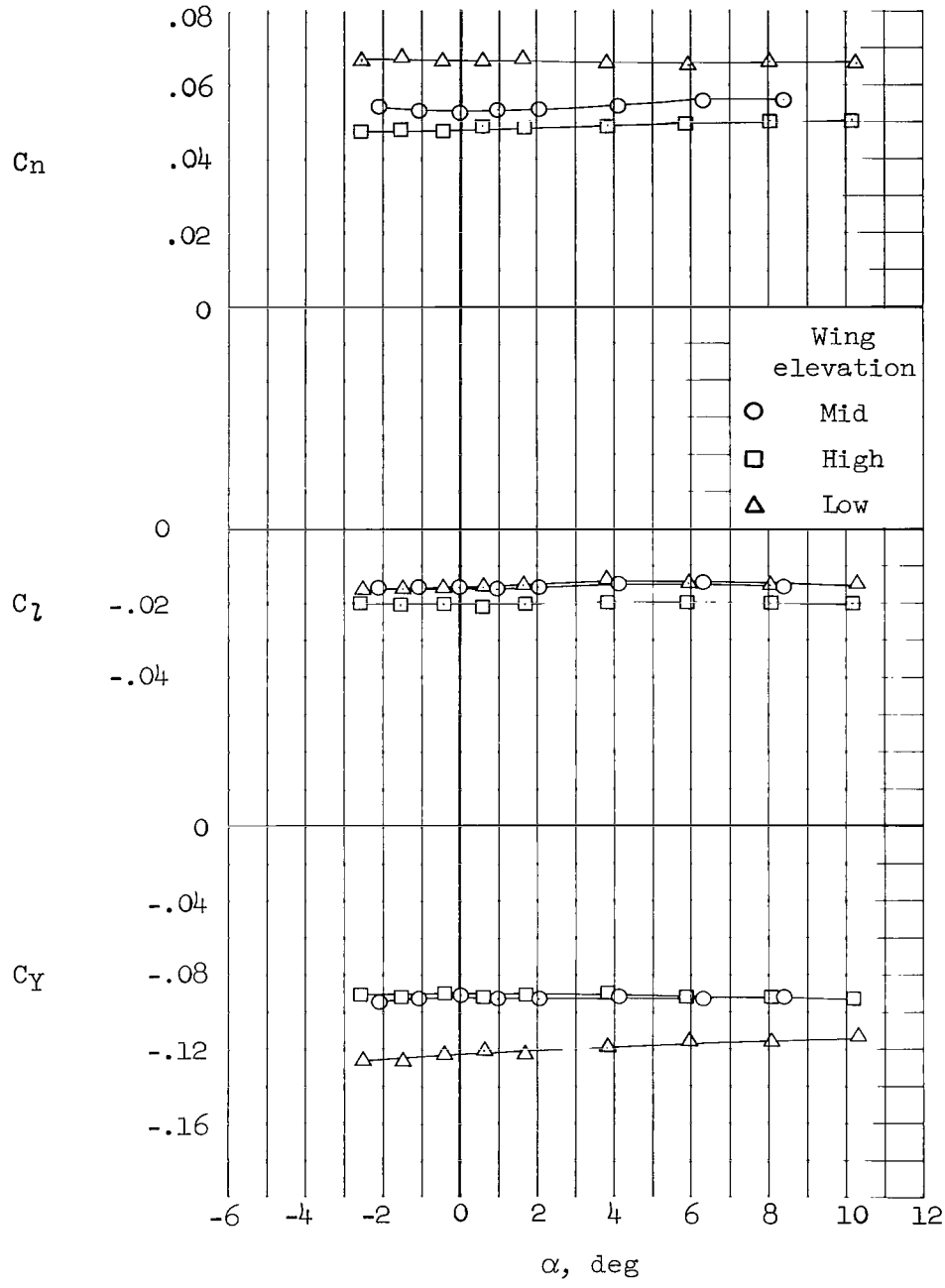

(b) M = 0.90; β = 4.9°

Figure 7.- Continued.

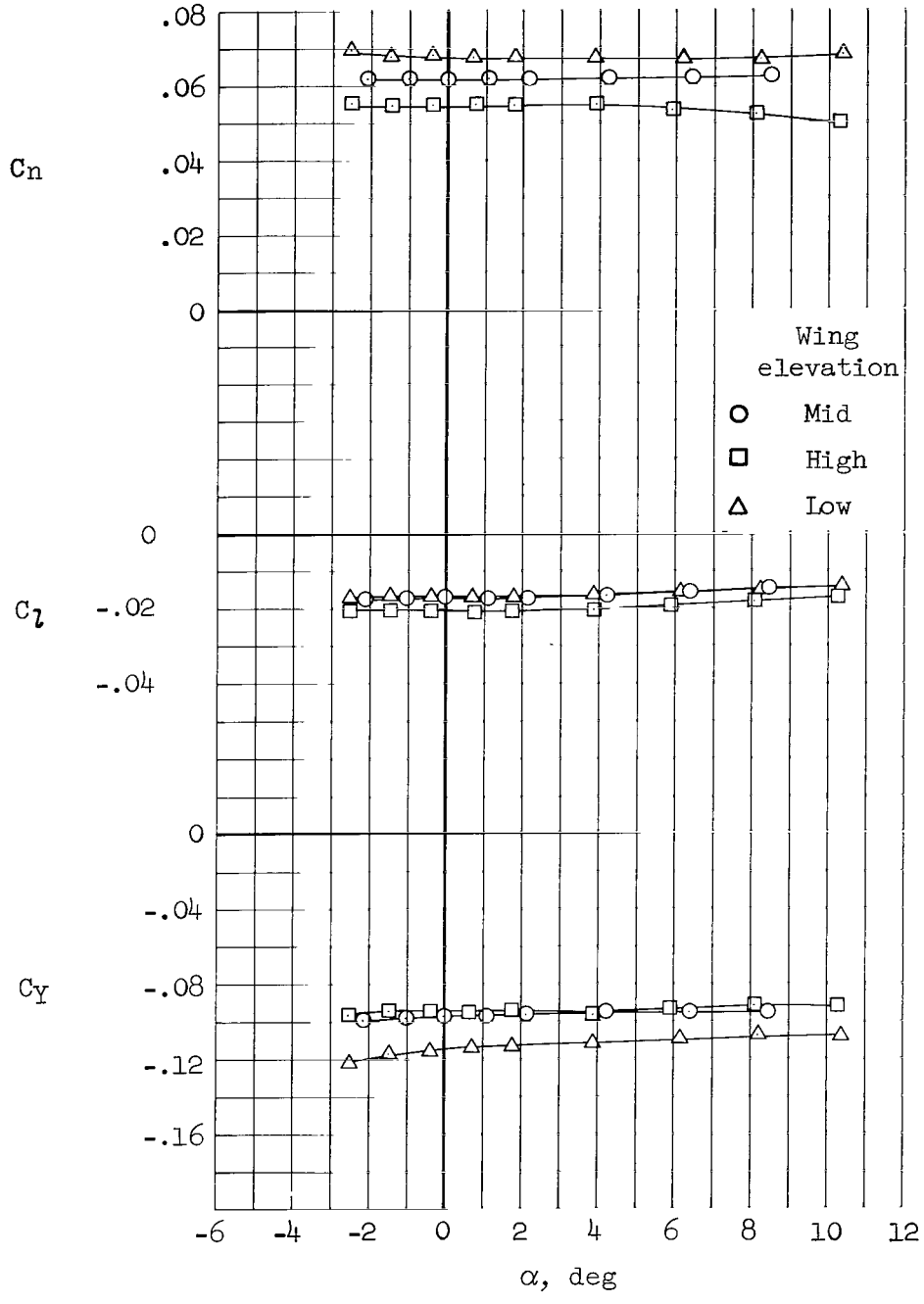

(c) M = 1.30; β = 4.9°

Figure 7.- Continued.

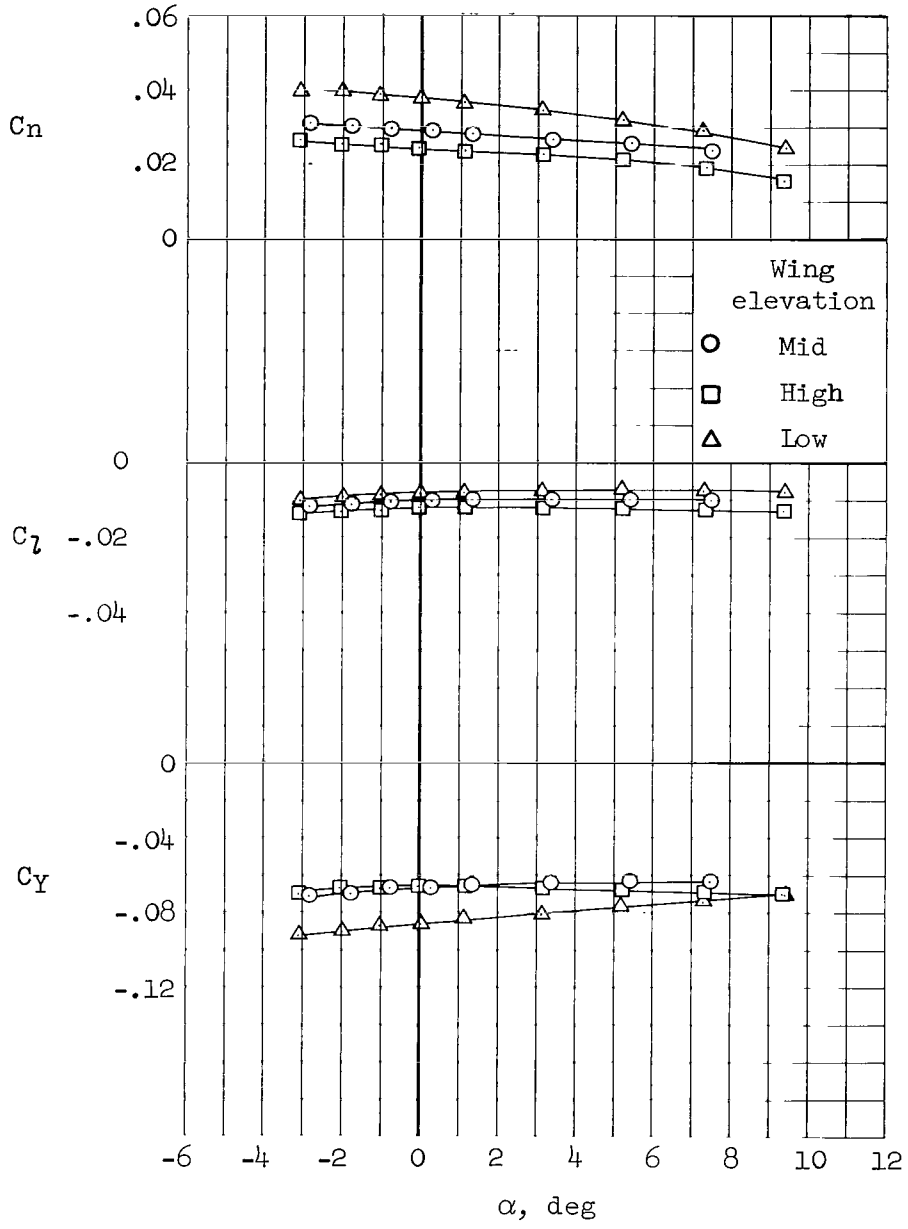

(d) M = 1.99; β = 4.9°

Figure 7.- Continued.

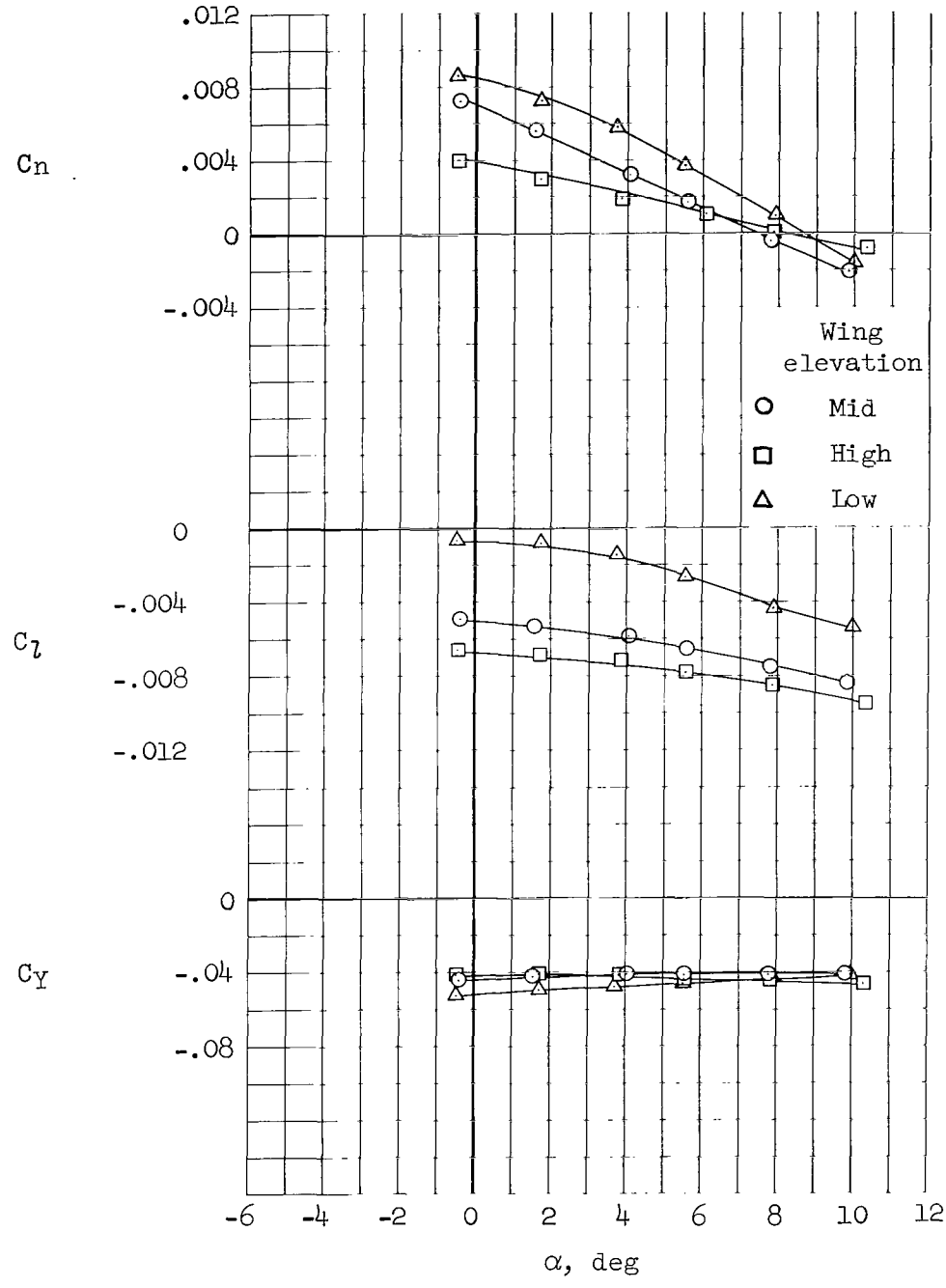

(e) M = 5.31; β = 4.7°

Figure 7.- Continued.

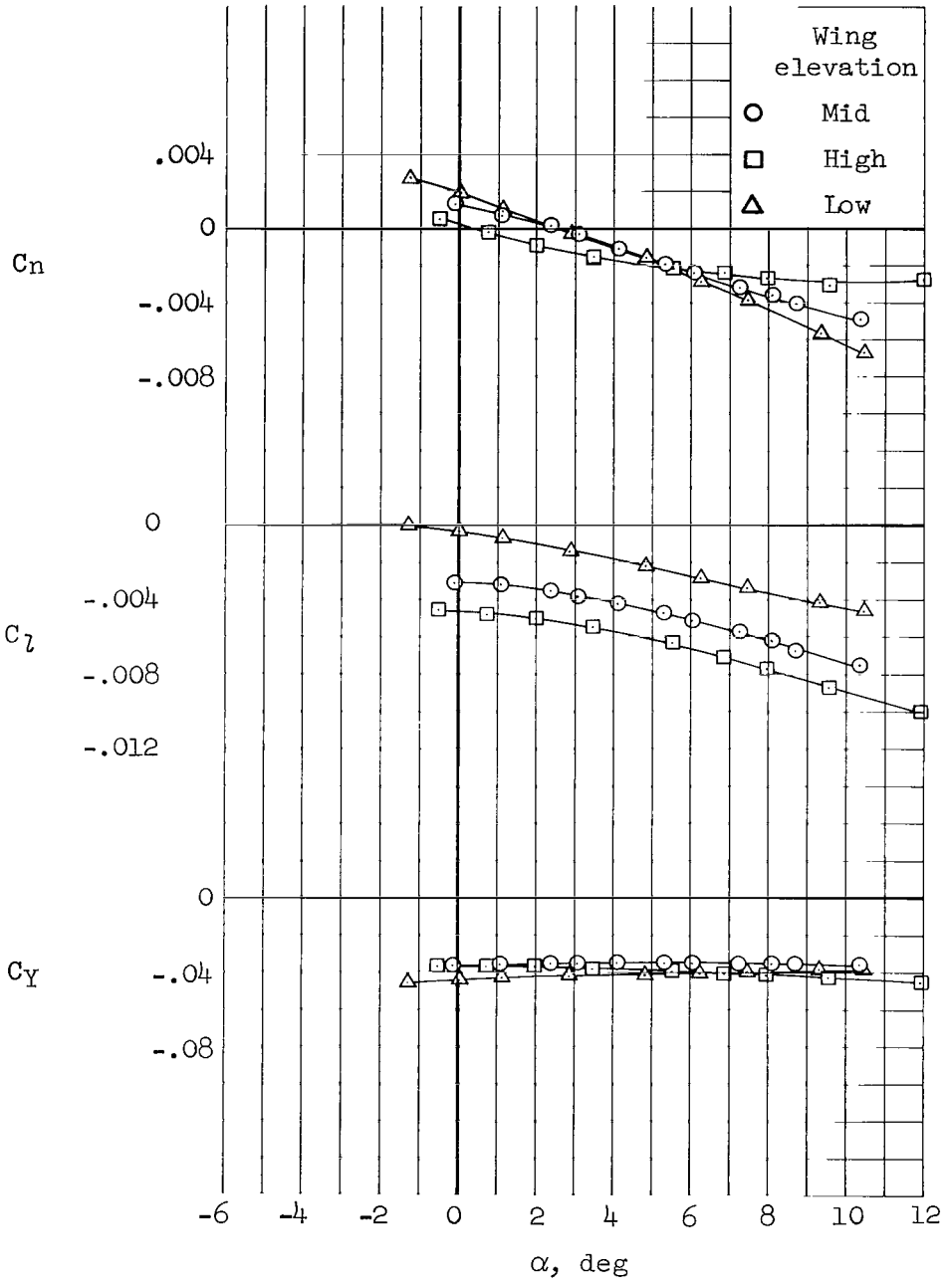

(f) M = 7.42; β = 4.4°

Figure 7.- Concluded.

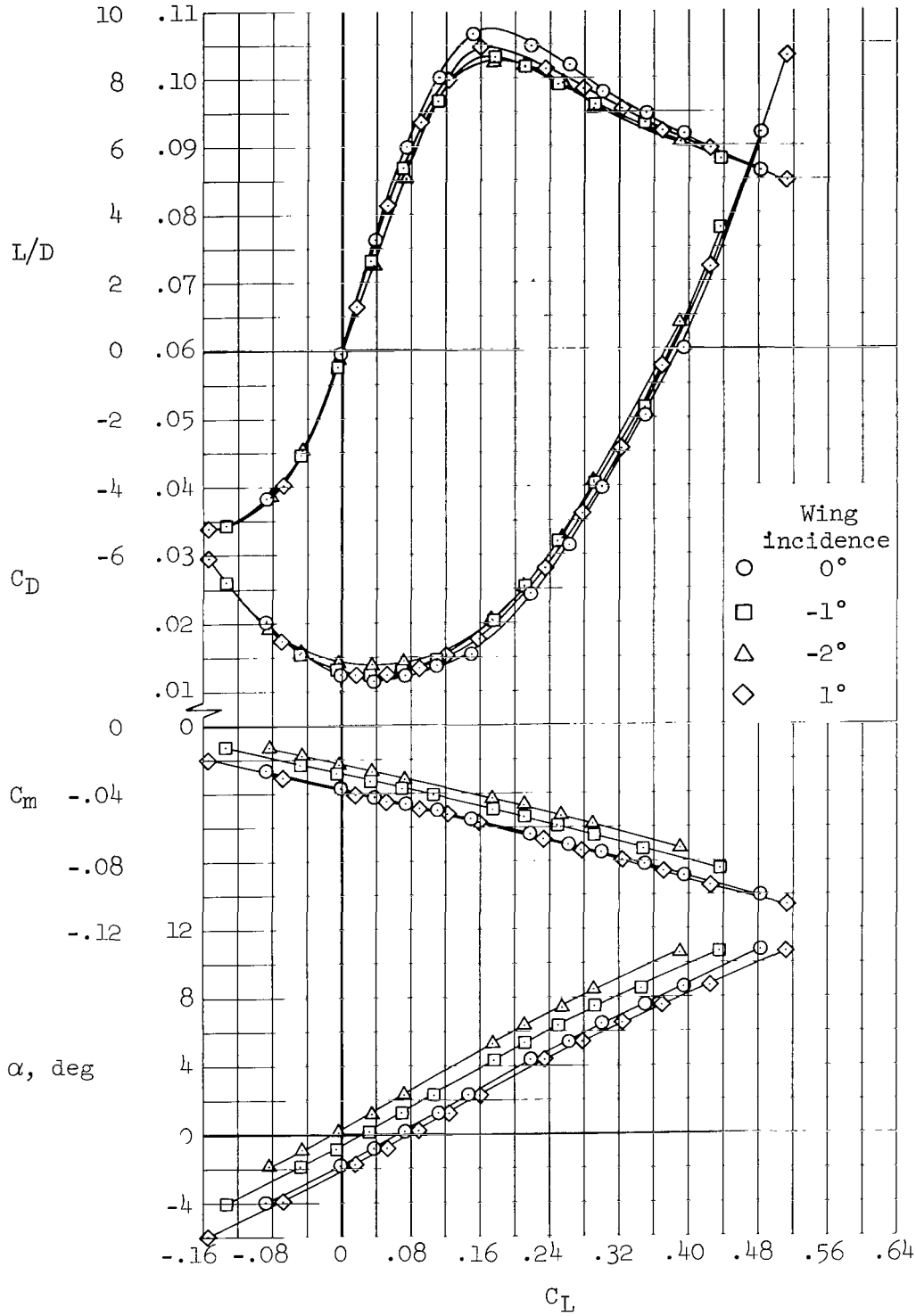

(a) M = 0.65

Figure 8.- Effect of wing incidence on the longitudinal aerodynamic characteristics; WBV configuration, positive cambered wing, mid-wing elevation.

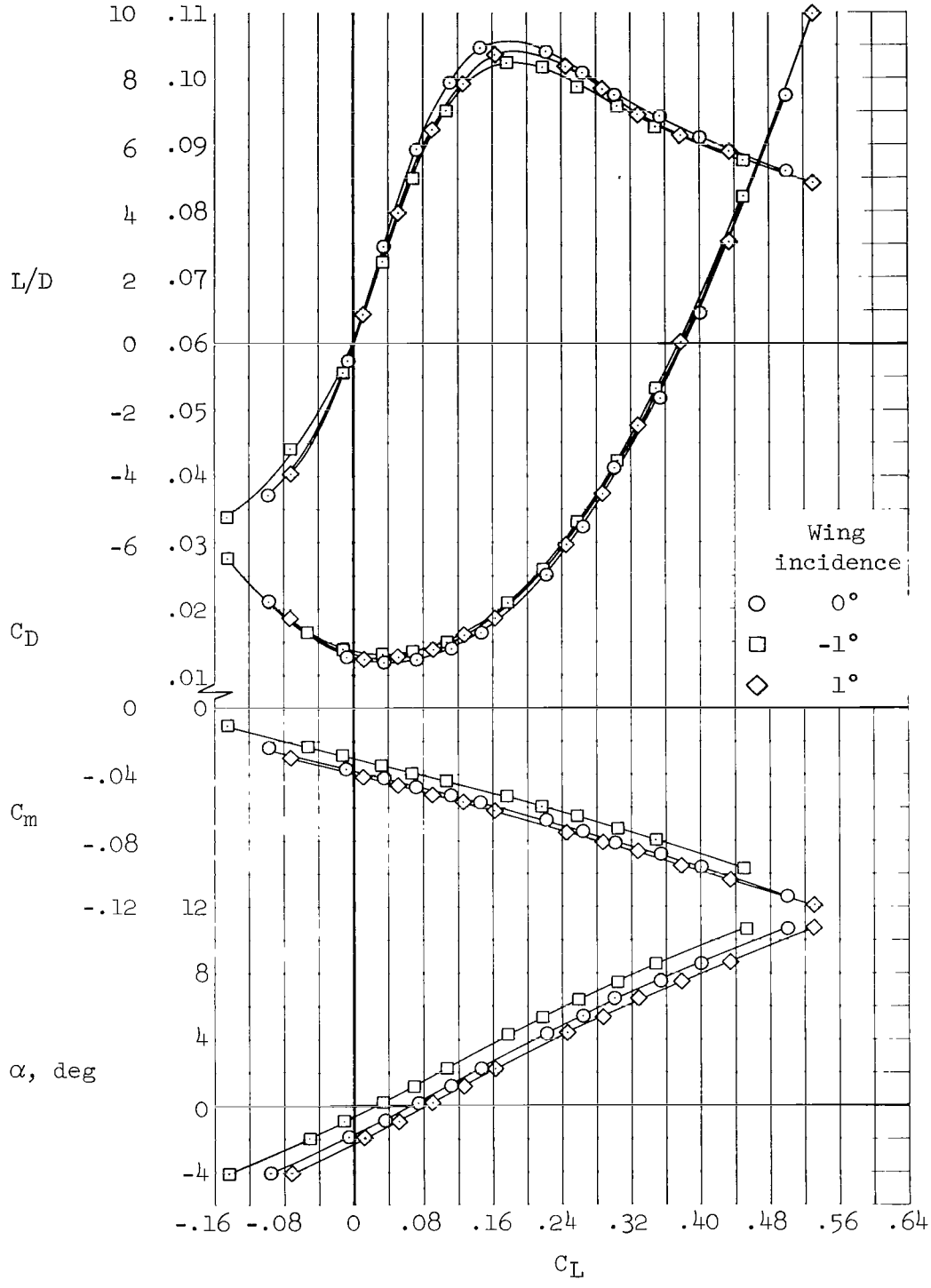

(b) M = 0.80

Figure 8.- Continued.

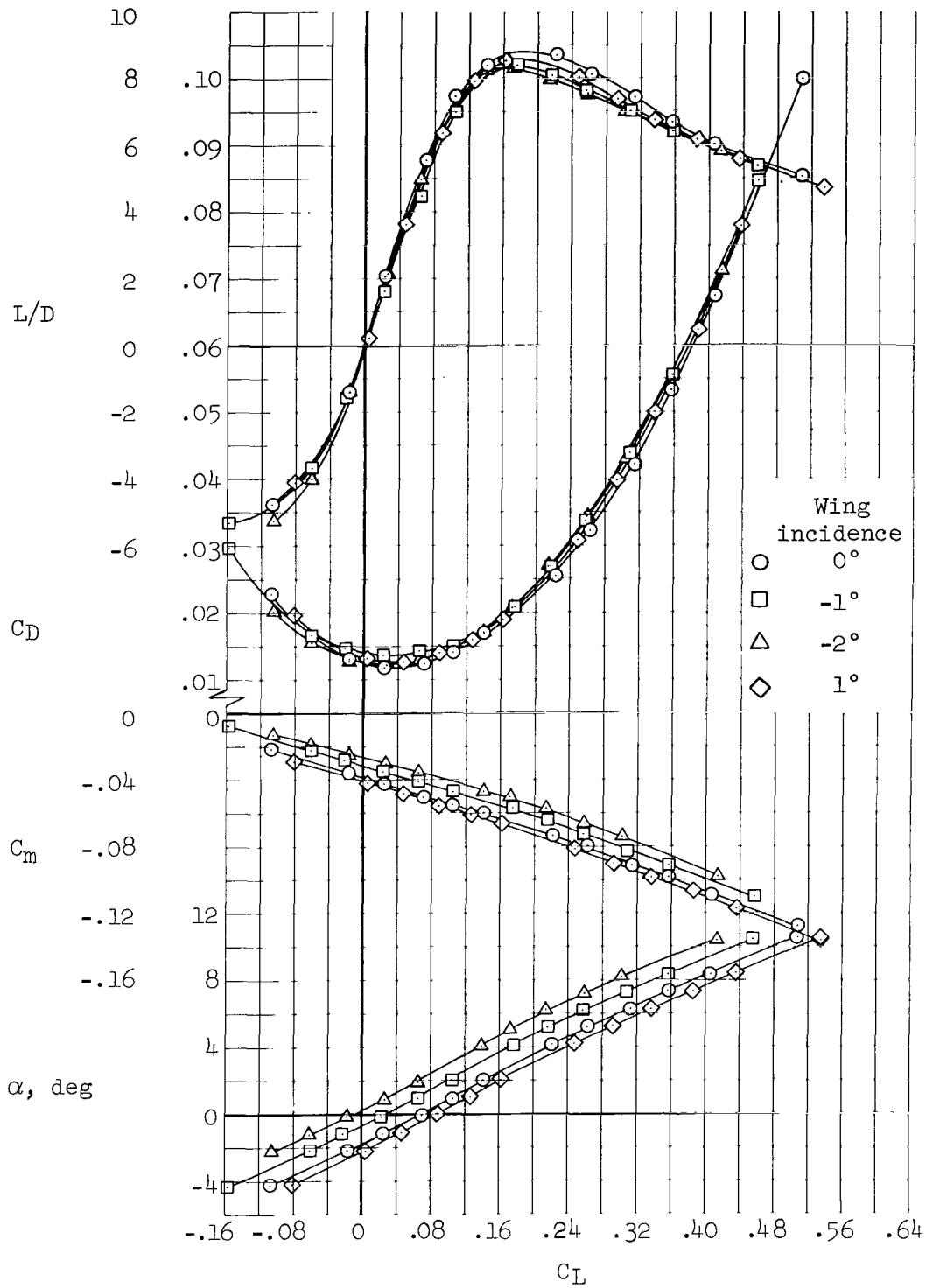

(c) M = 0.90

Figure 8.- Continued.

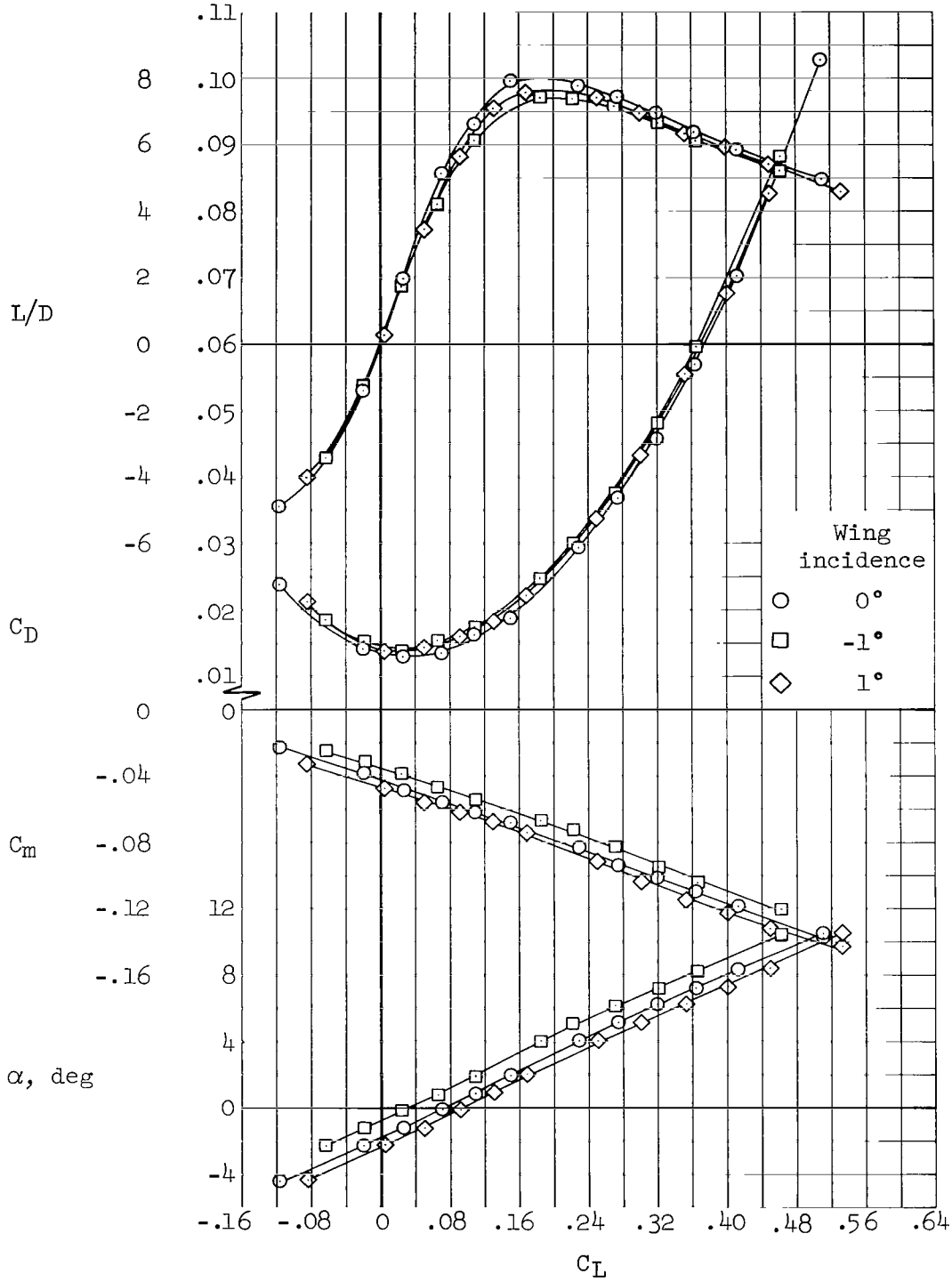

(d) M = 0.95

Figure 8.- Continued.

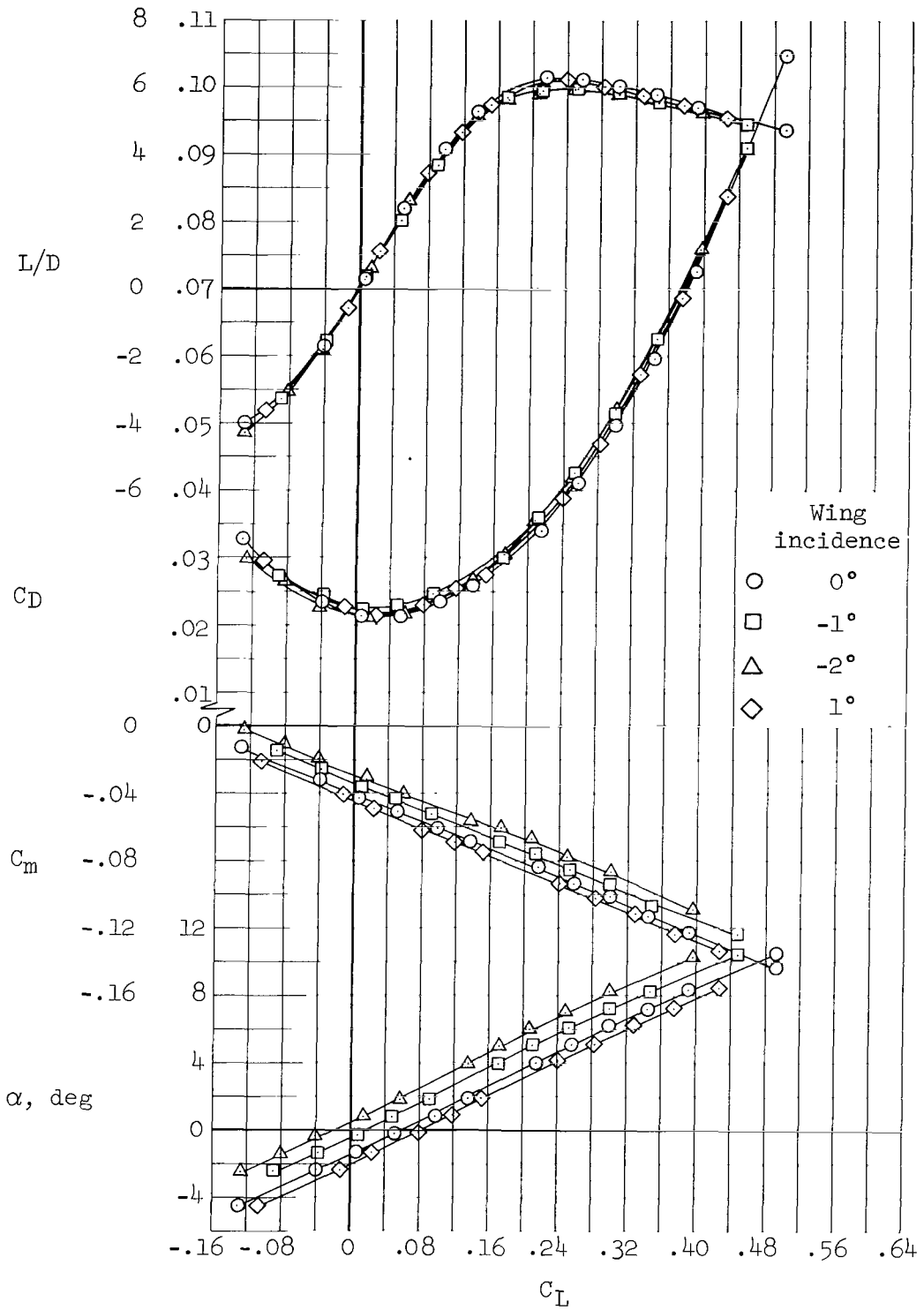

(e) M = 1.10

Figure 8.- Continued.

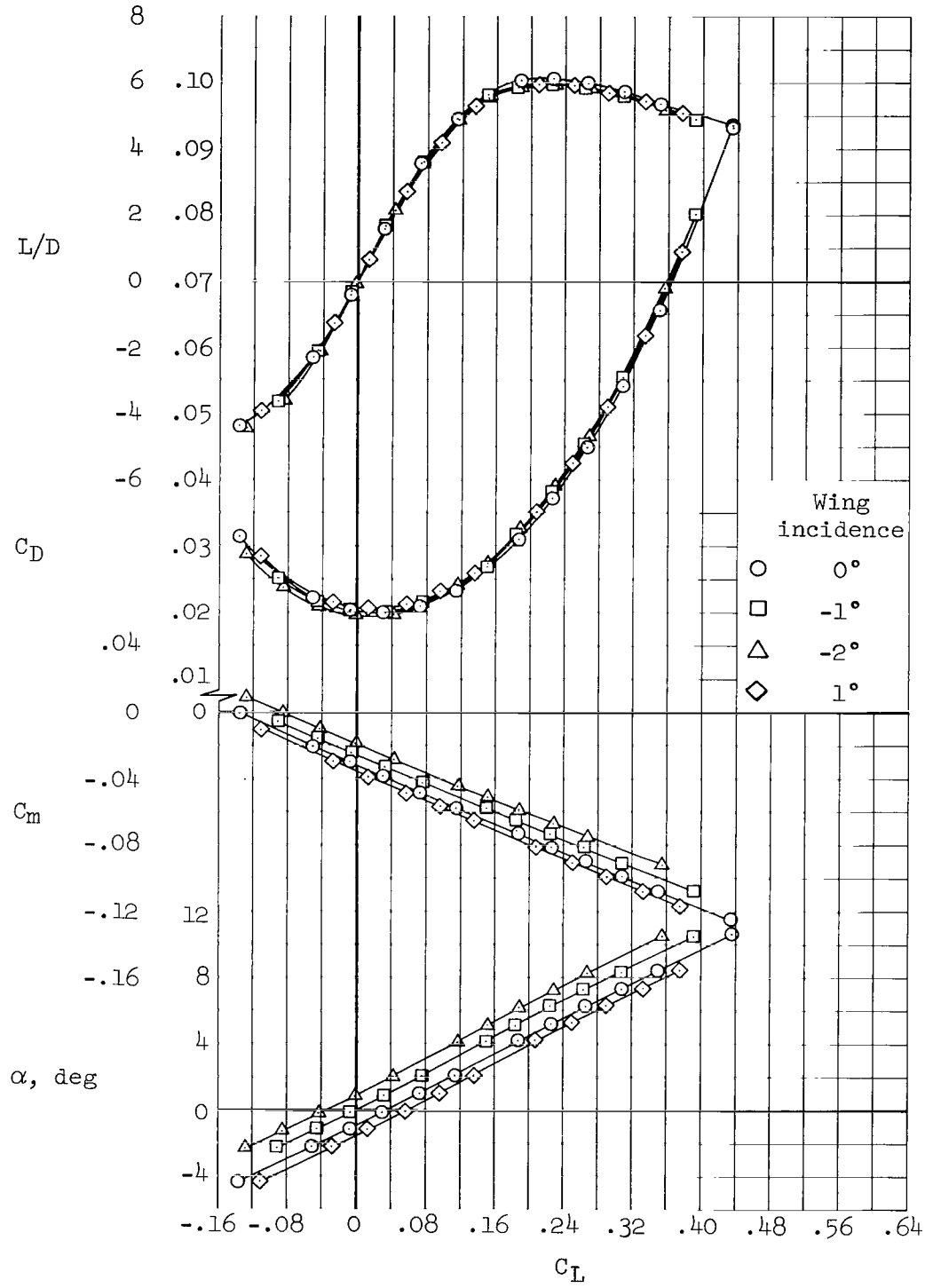

(f) M = 1.30

Figure 8.- Continued.

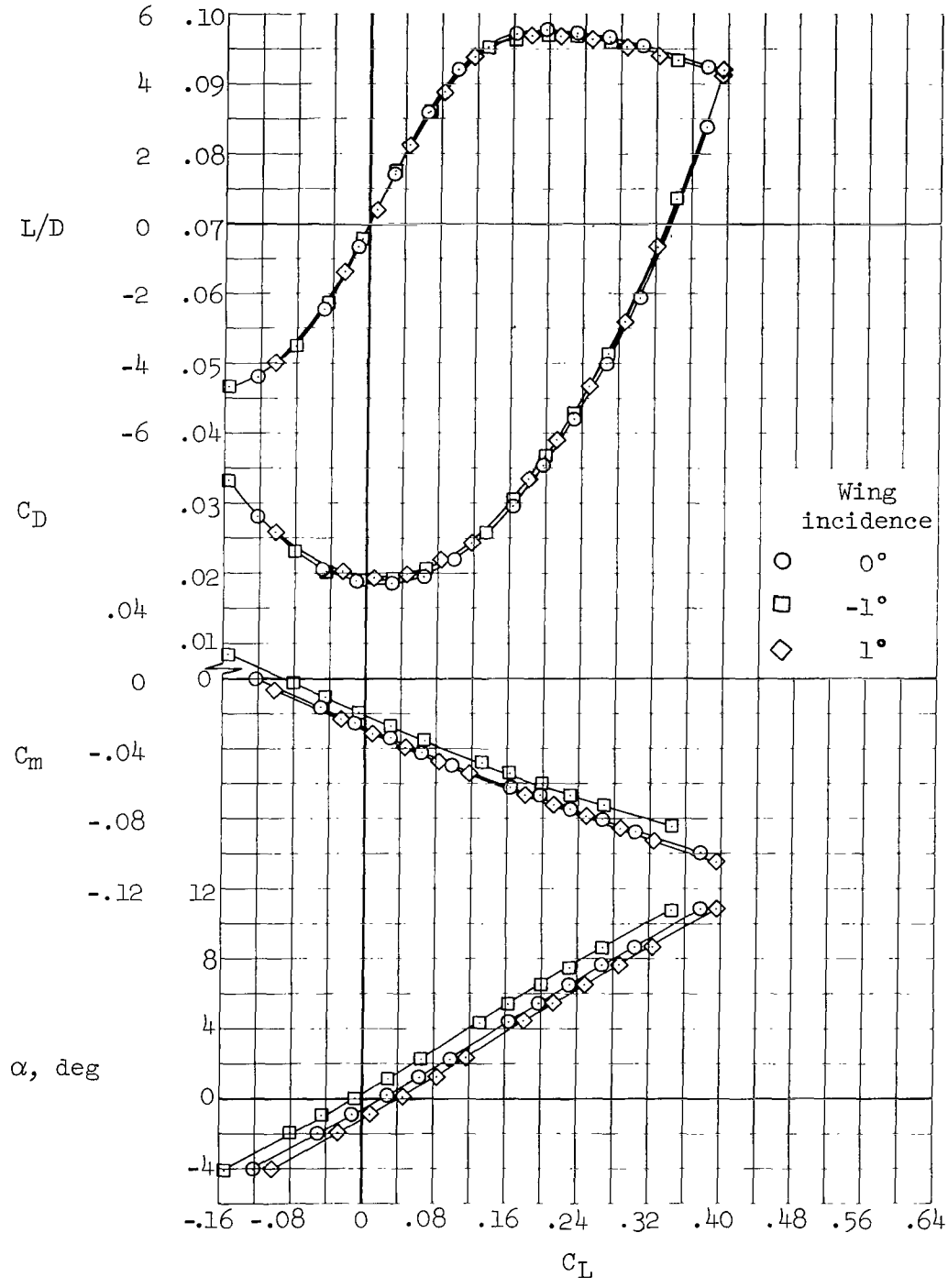

(g) M = 1.59

Figure 8.- Continued.

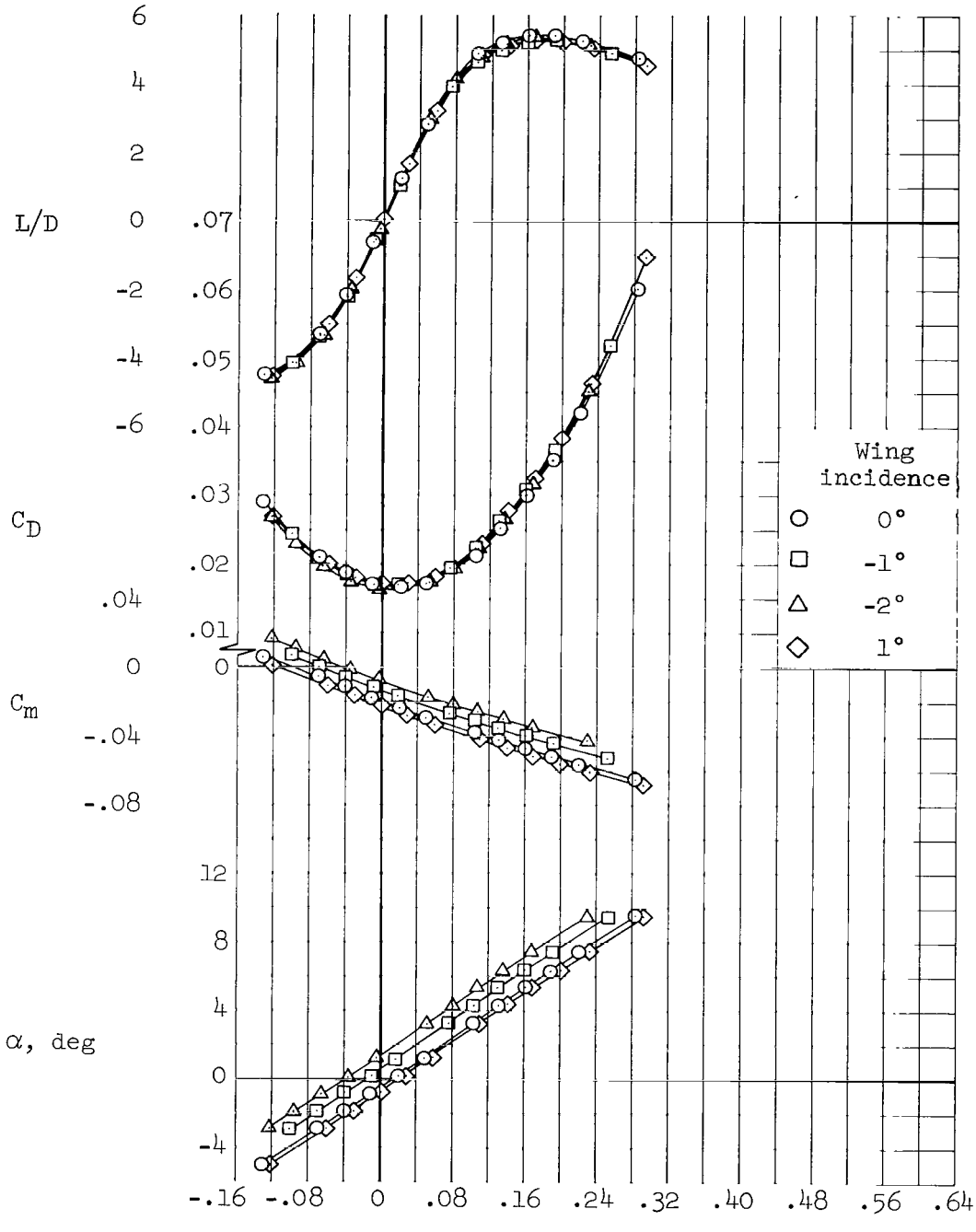

(h) M = 1.99

Figure 8.- Continued.

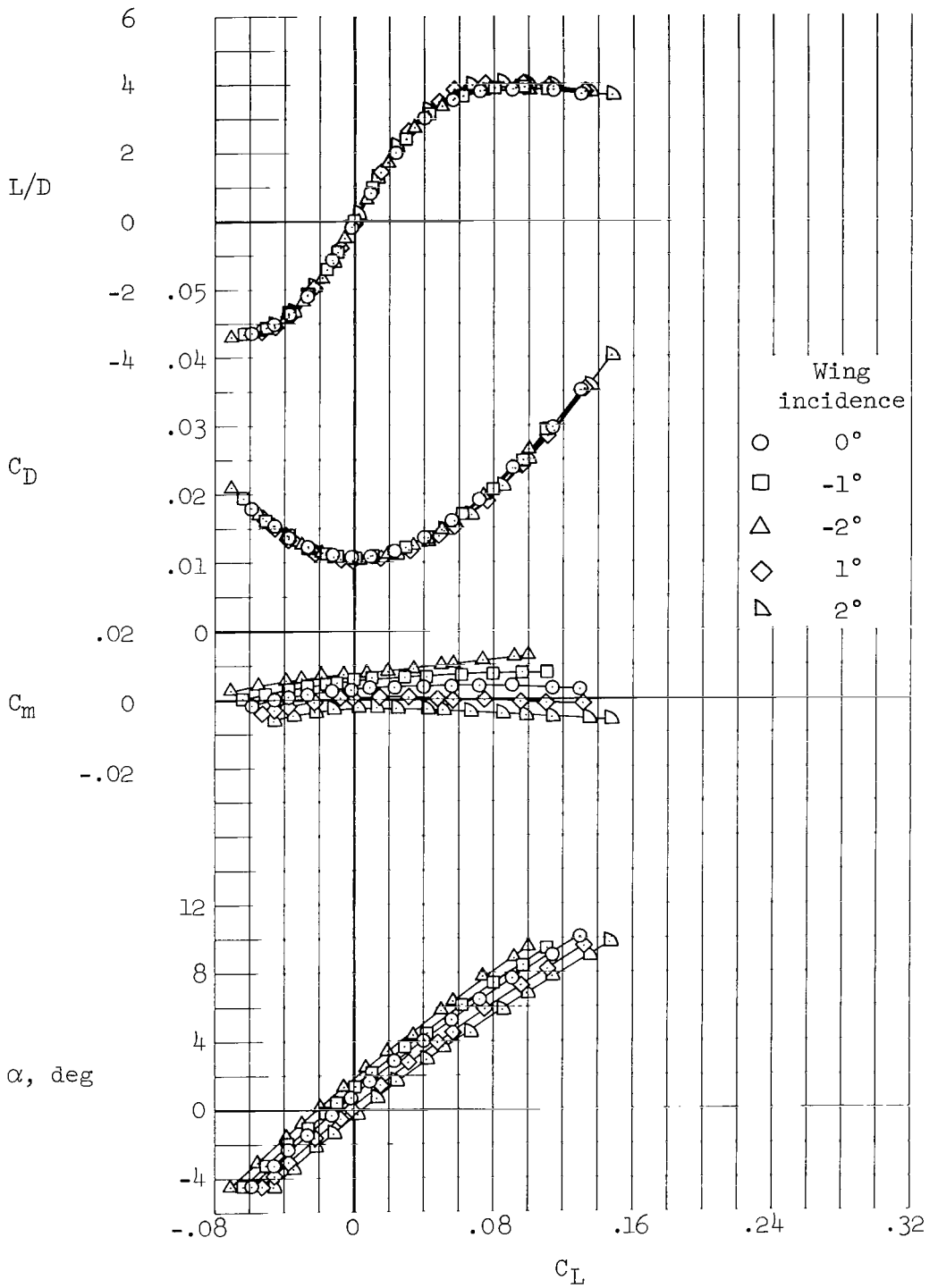

(i) M = 7.42

Figure 8.- Concluded.

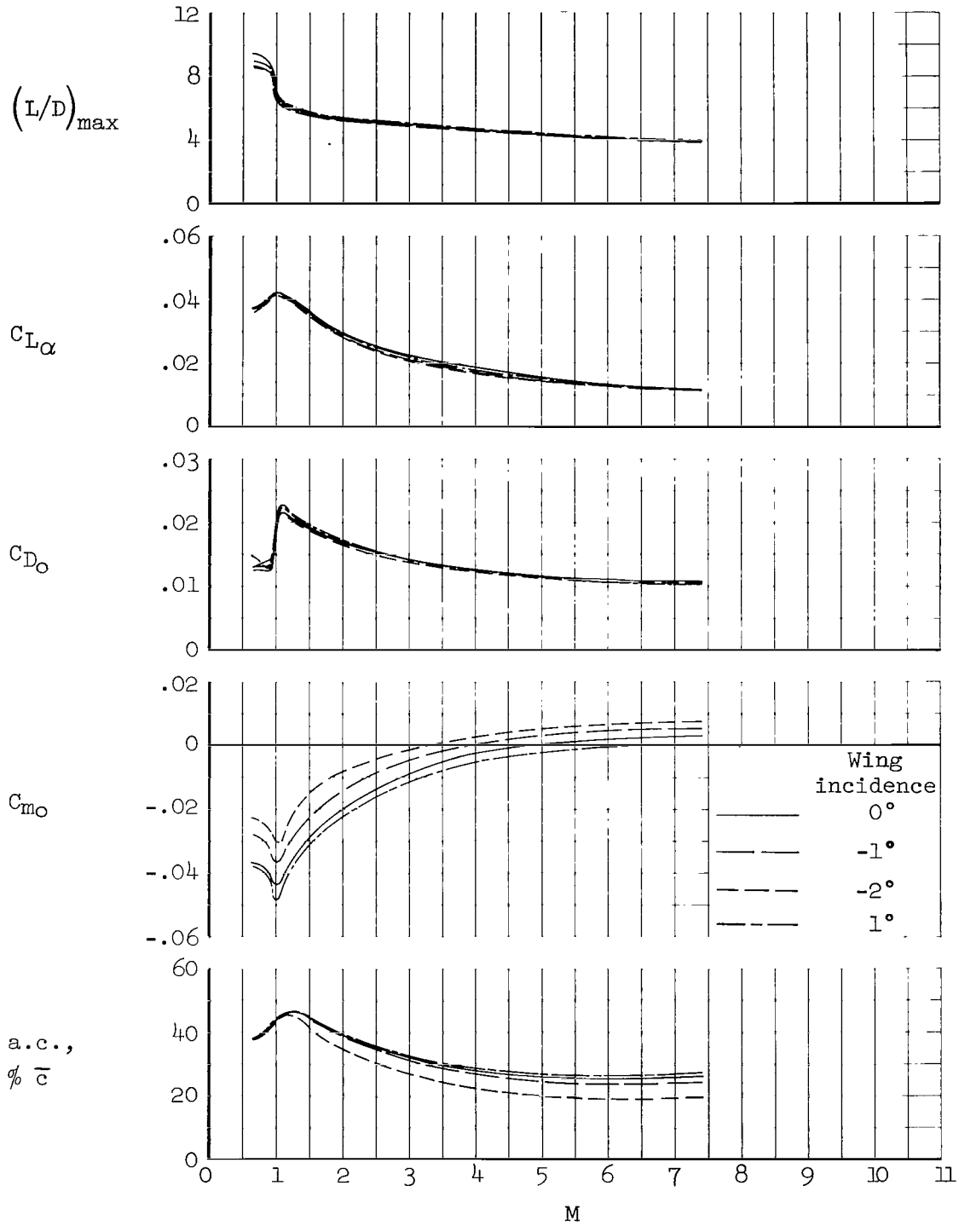

Figure 9.- Variation with Mach number of the effect of wing incidence on the longitudinal aerodynamic characteristics; WBV configuration, positive cambered wing, mid-wing elevation.

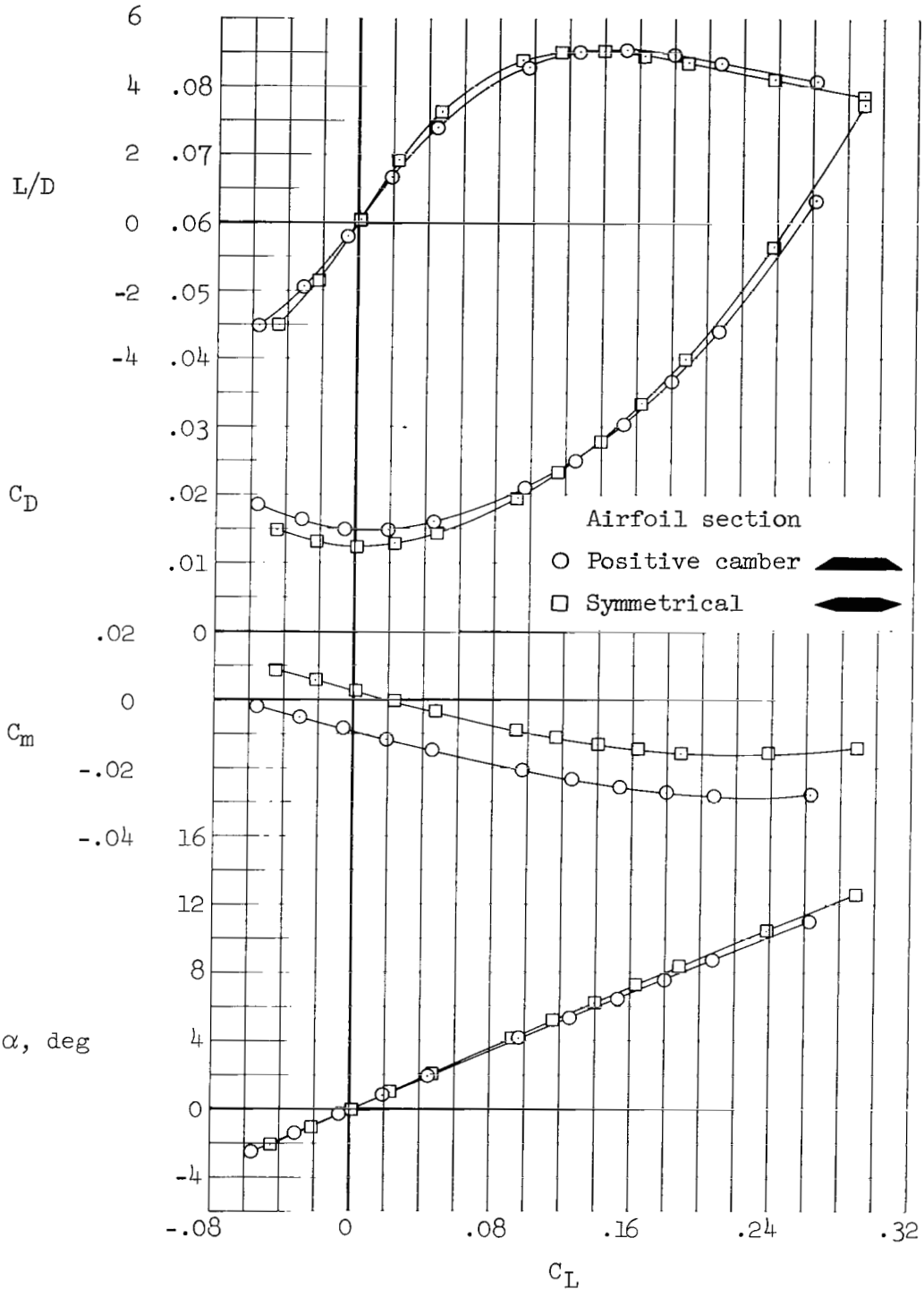

(a) M = 2.93

Figure 10.- Effect of wing camber on the longitudinal aerodynamic characteristics; positive cambered and symmetrical airfoil sections, WBV configuration, mid-wing elevation, $i_w = 0°$.

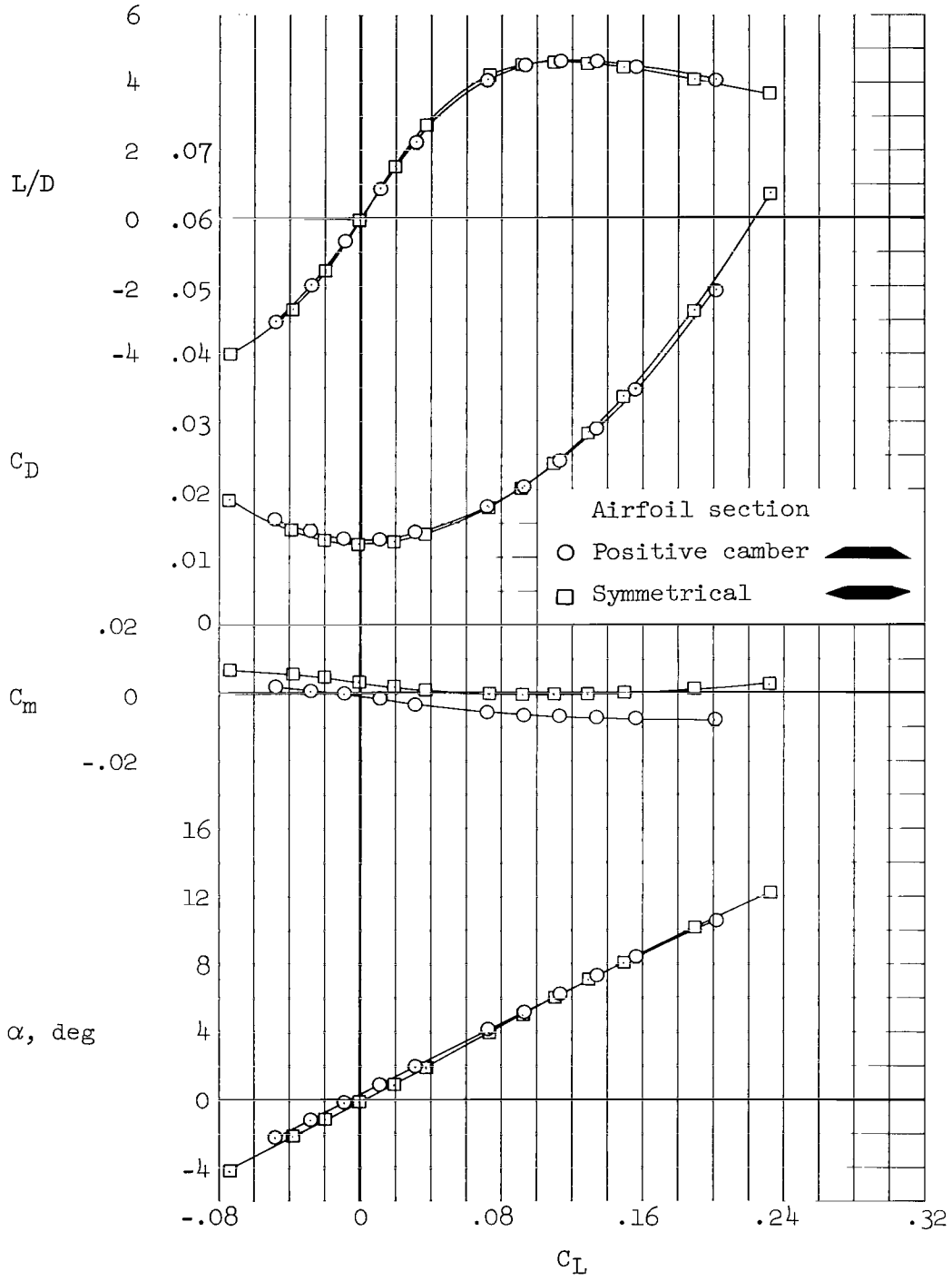

(b) M = 3.88

Figure 10.- Continued.

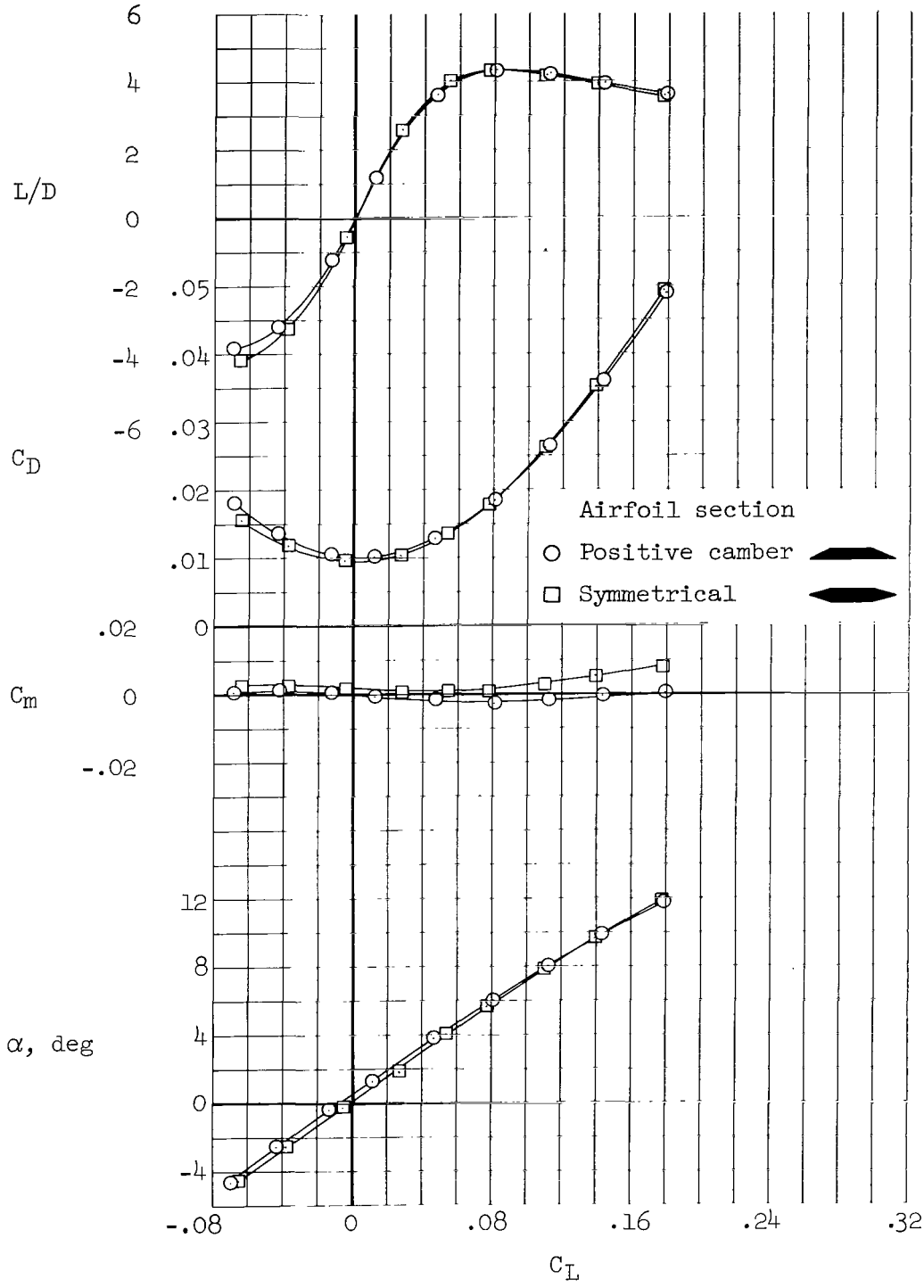

(c) M = 5.31

Figure 10.- Continued.

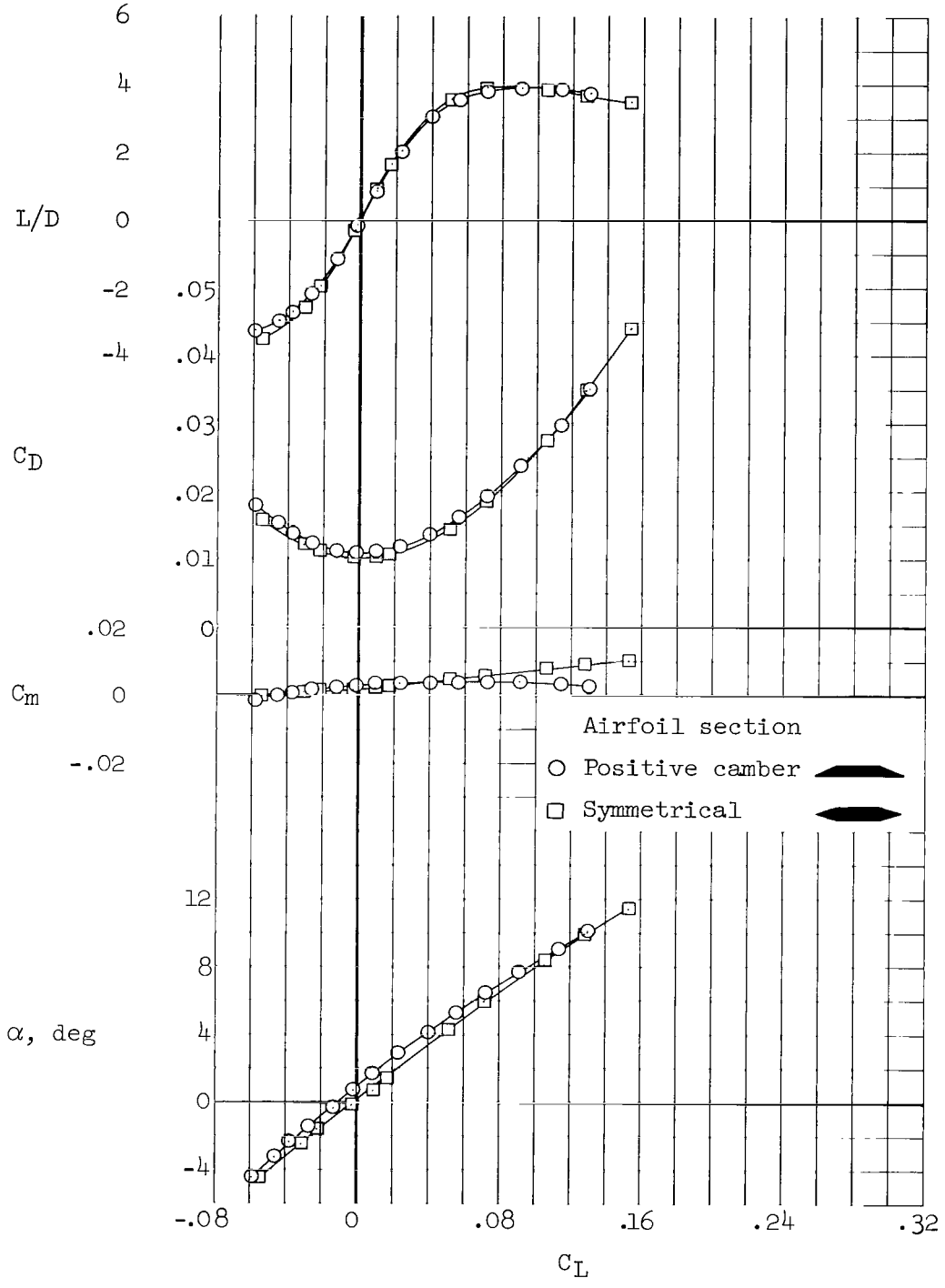

(d) M = 7.42

Figure 10.- Continued.

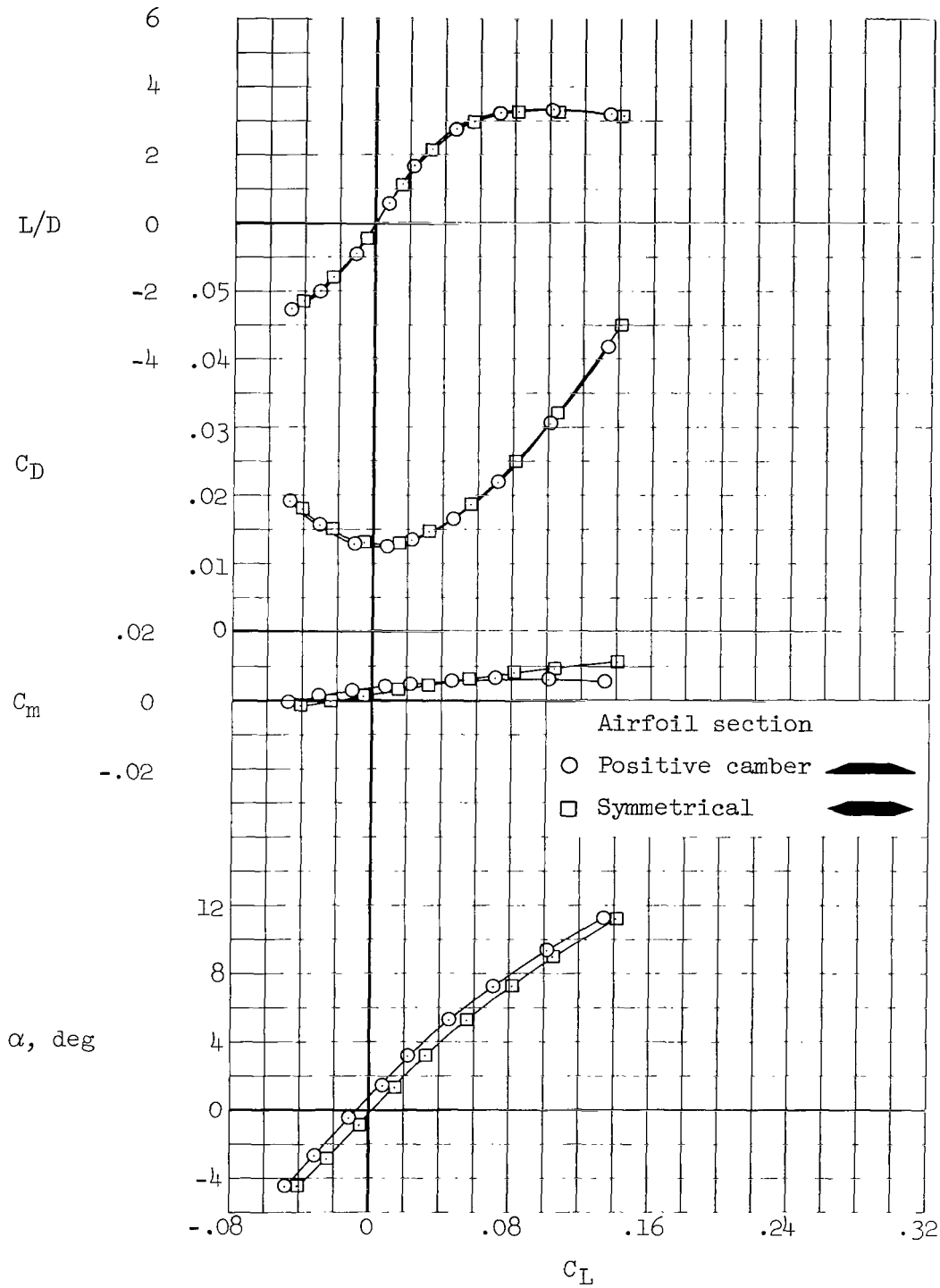

(e) M = 10.70

Figure 10.- Concluded.

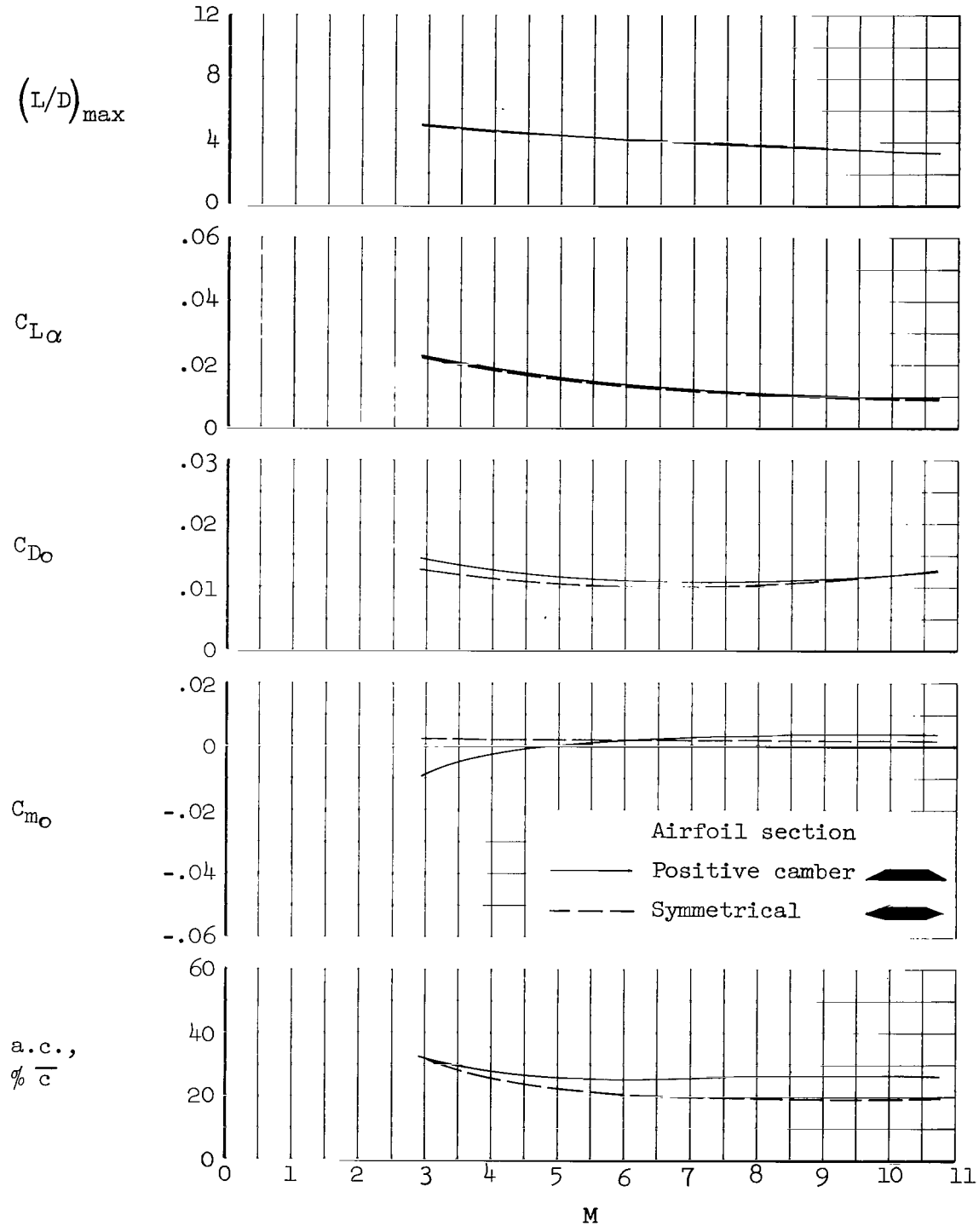

Figure 11.- Variation with Mach number of the effect of wing camber on the longitudinal aerodynamic characteristics; positive cambered and symmetrical airfoil sections, WBV configuration, mid-wing elevation, $i_w = 0°$.

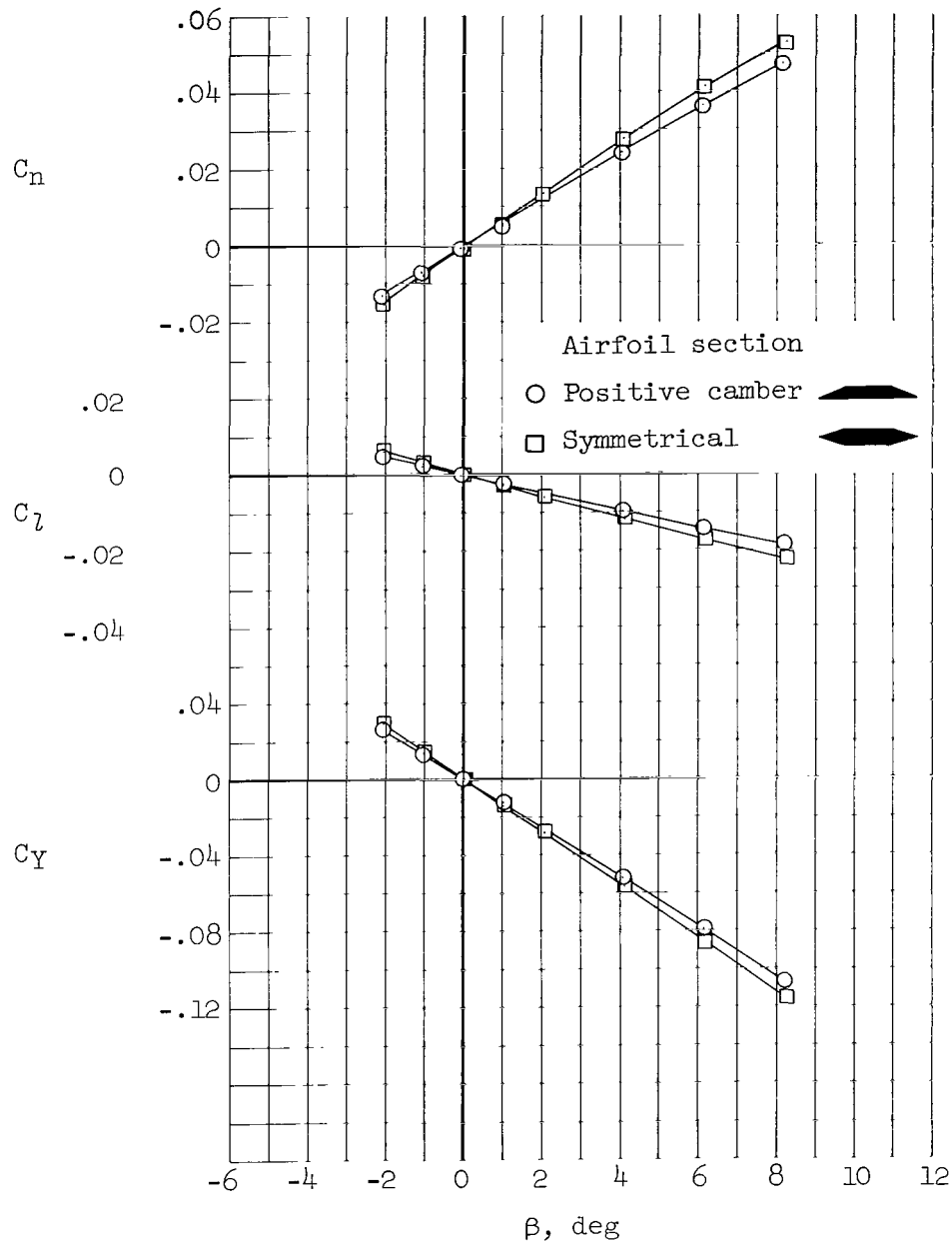

(a) M = 1.99

Figure 12.- Effect of wing camber on the lateral and directional aerodynamic characteristics; positive cambered and symmetrical airfoil sections, WBV configuration, mid-wing elevation, $i_w = 0°$, $\alpha = 0°$.

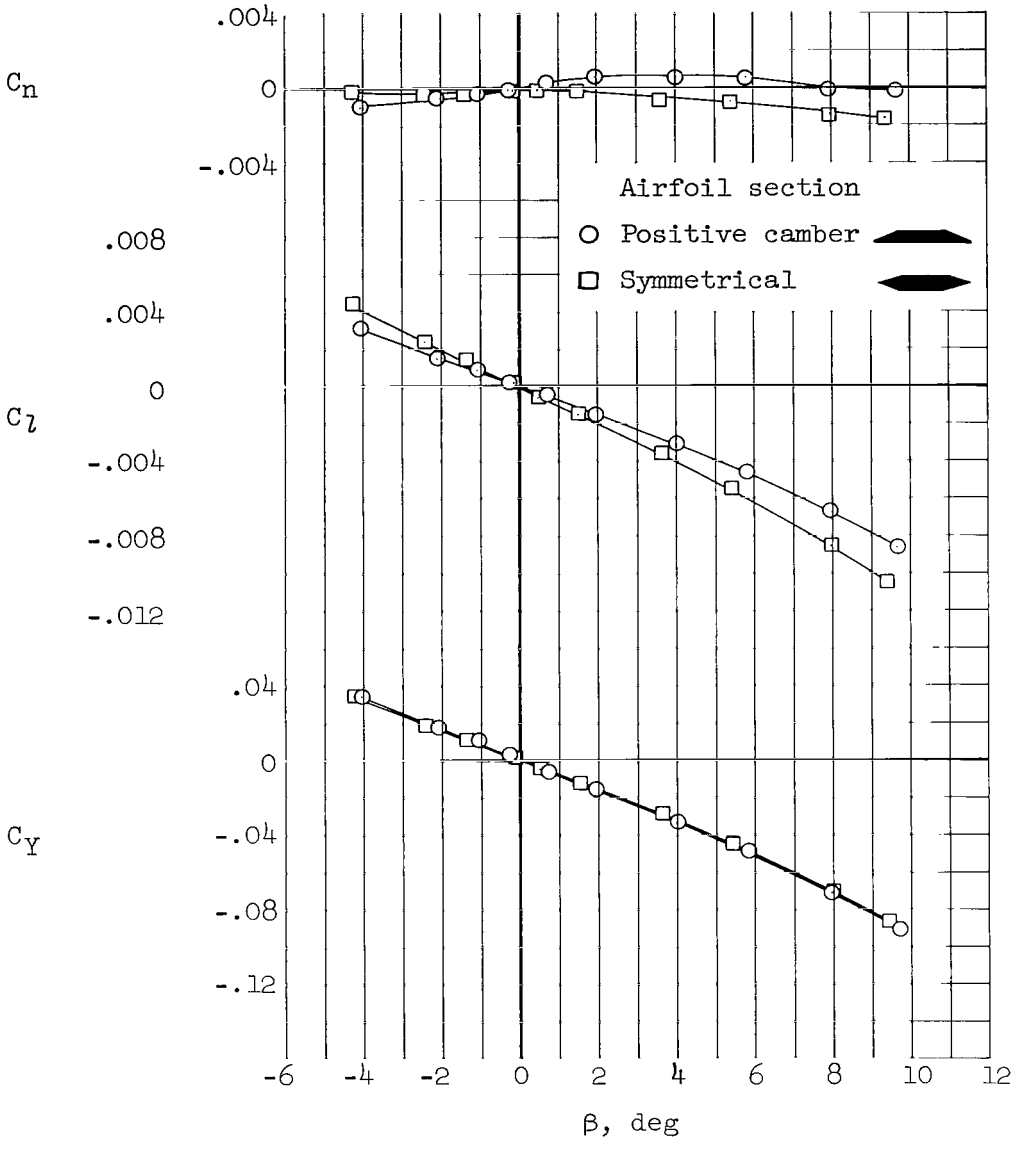

(b) M = 7.42

Figure 12.- Concluded.

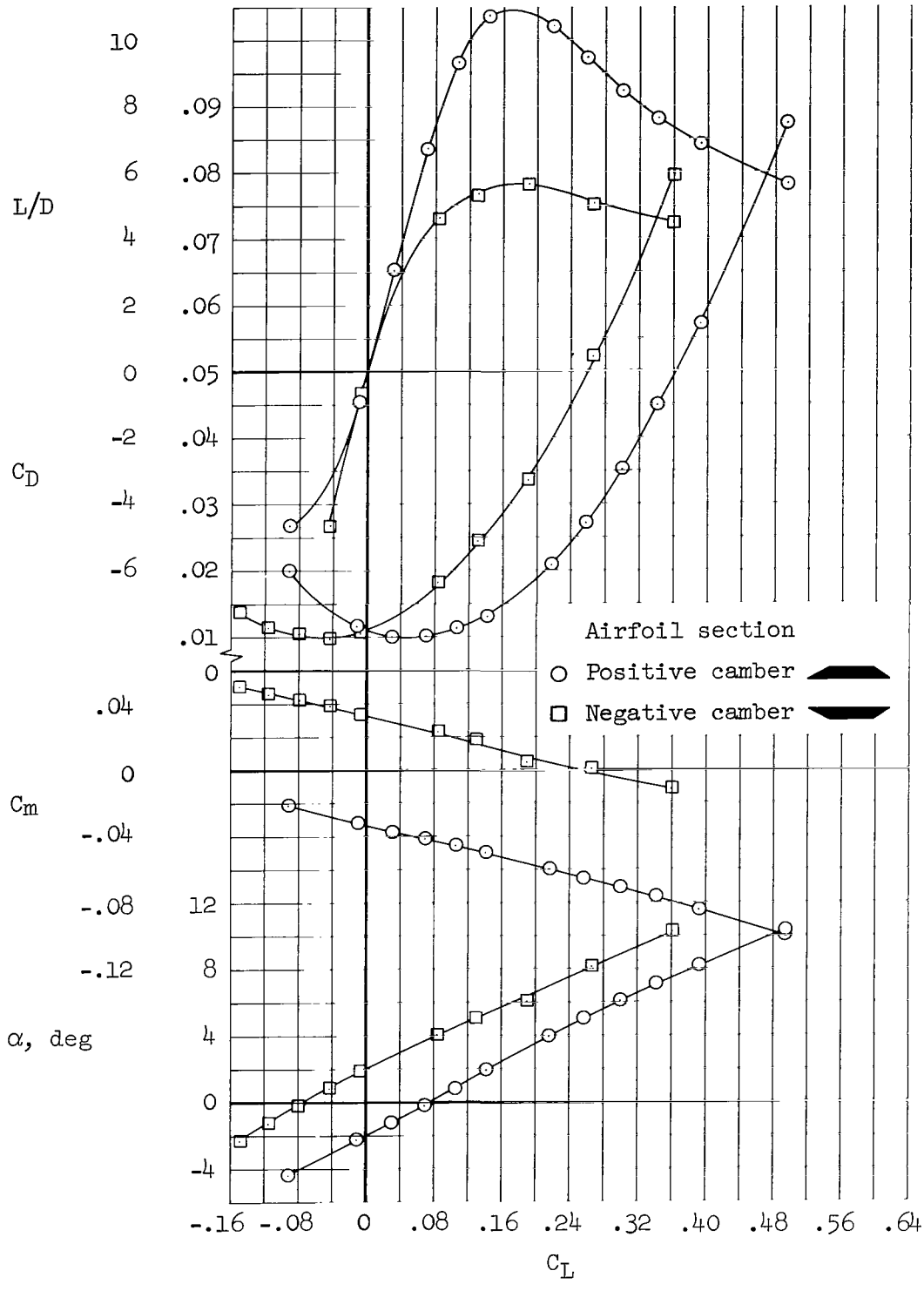

(a) M = 0.65

Figure 13.- Effect of wing camber on the longitudinal aerodynamic characteristics; positive and negative cambered airfoil sections WB configuration, mid-wing elevation, $i_w = 0°$.

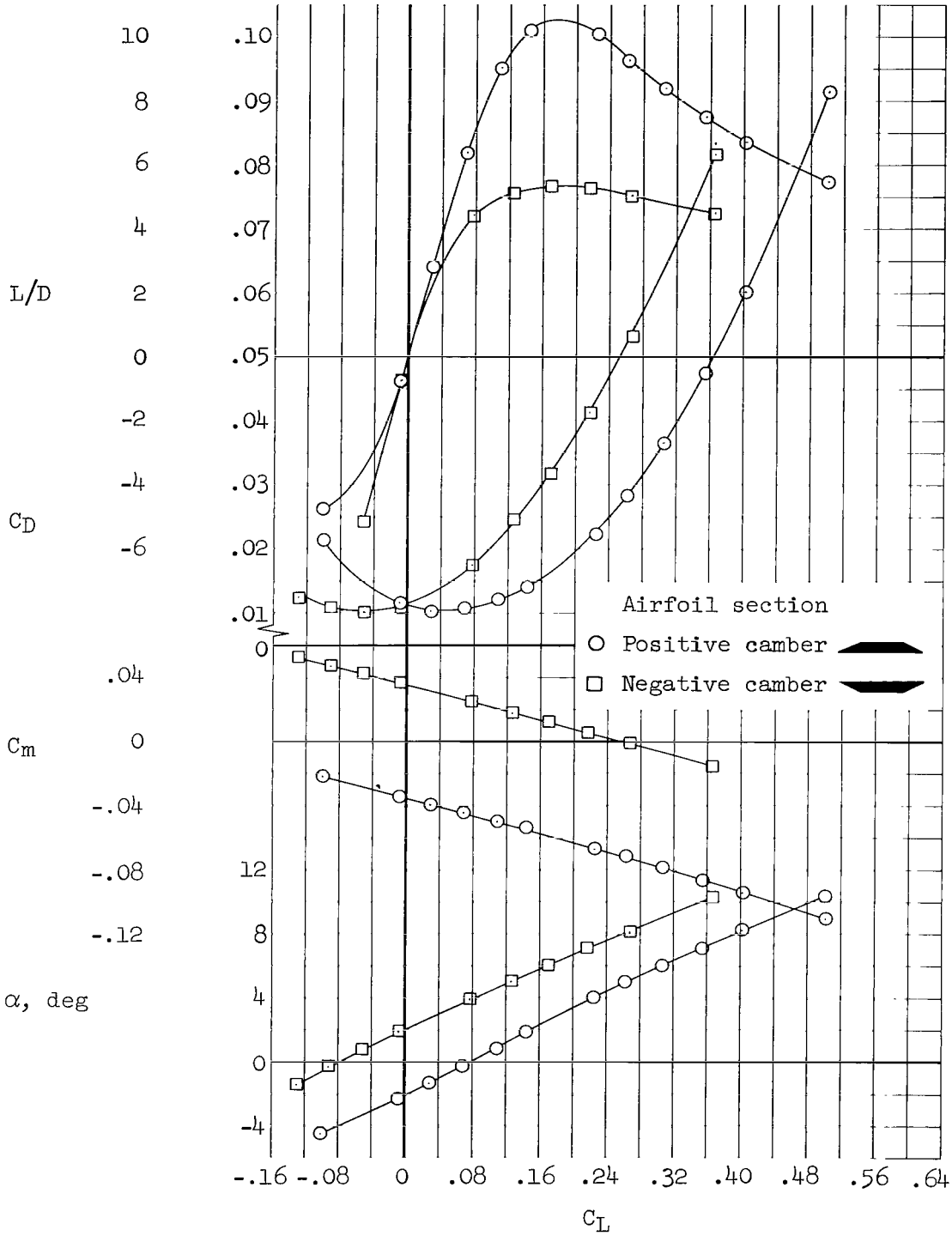

(b) M = 0.80

Figure 13.- Continued.

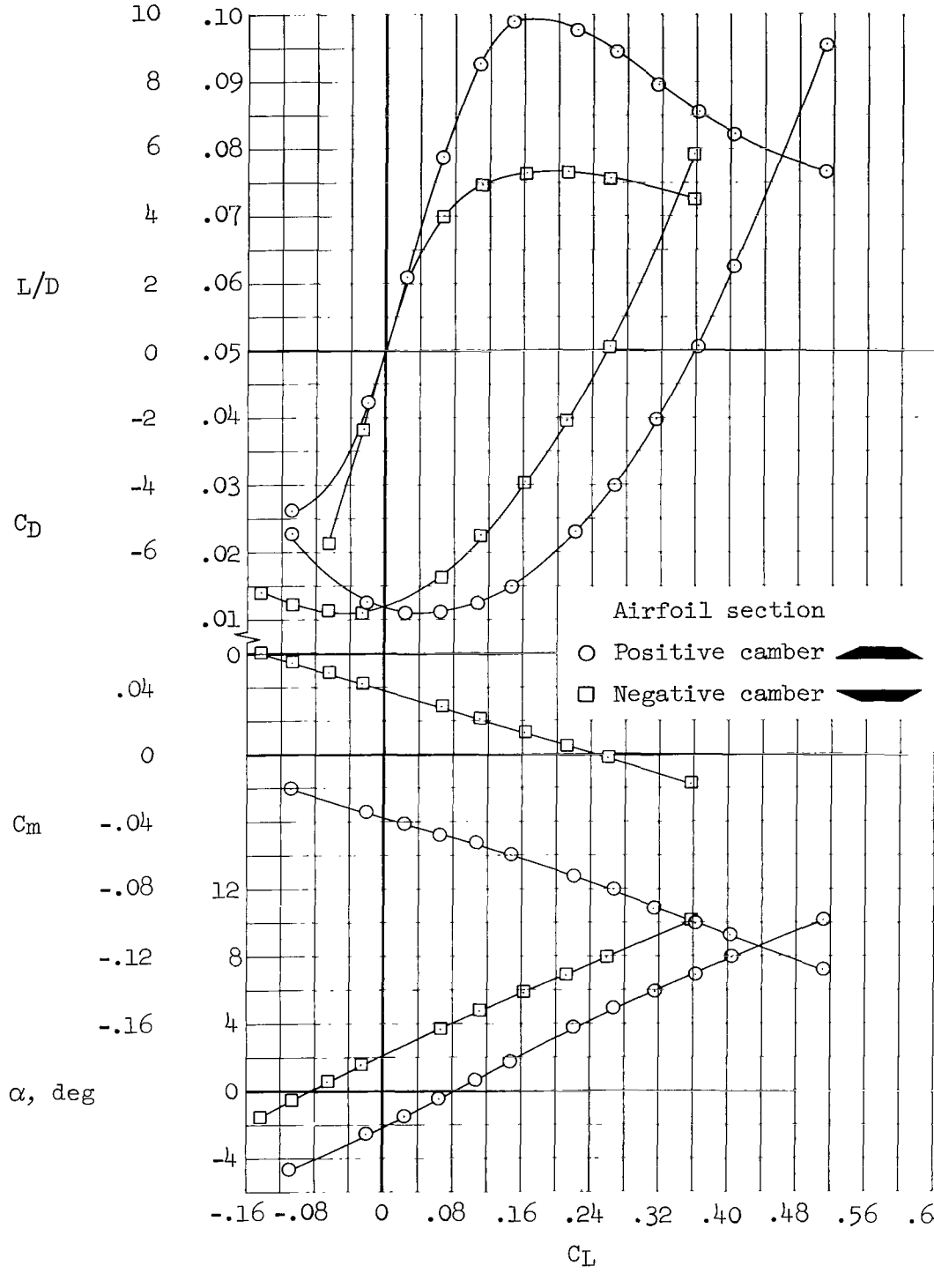

(c) M = 0.90

Figure 13.- Continued.

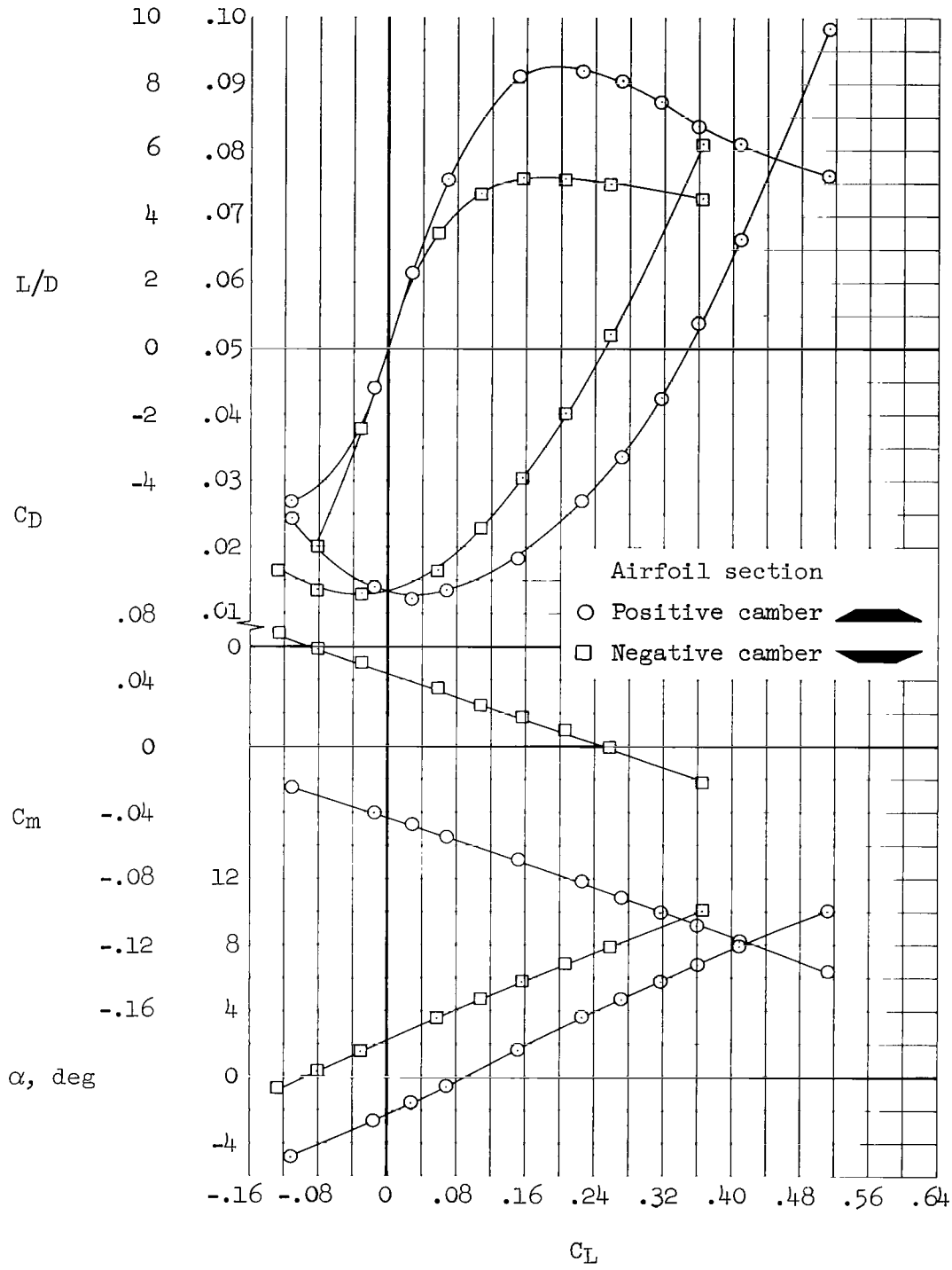

(d) M = 0.95

Figure 13.- Continued.

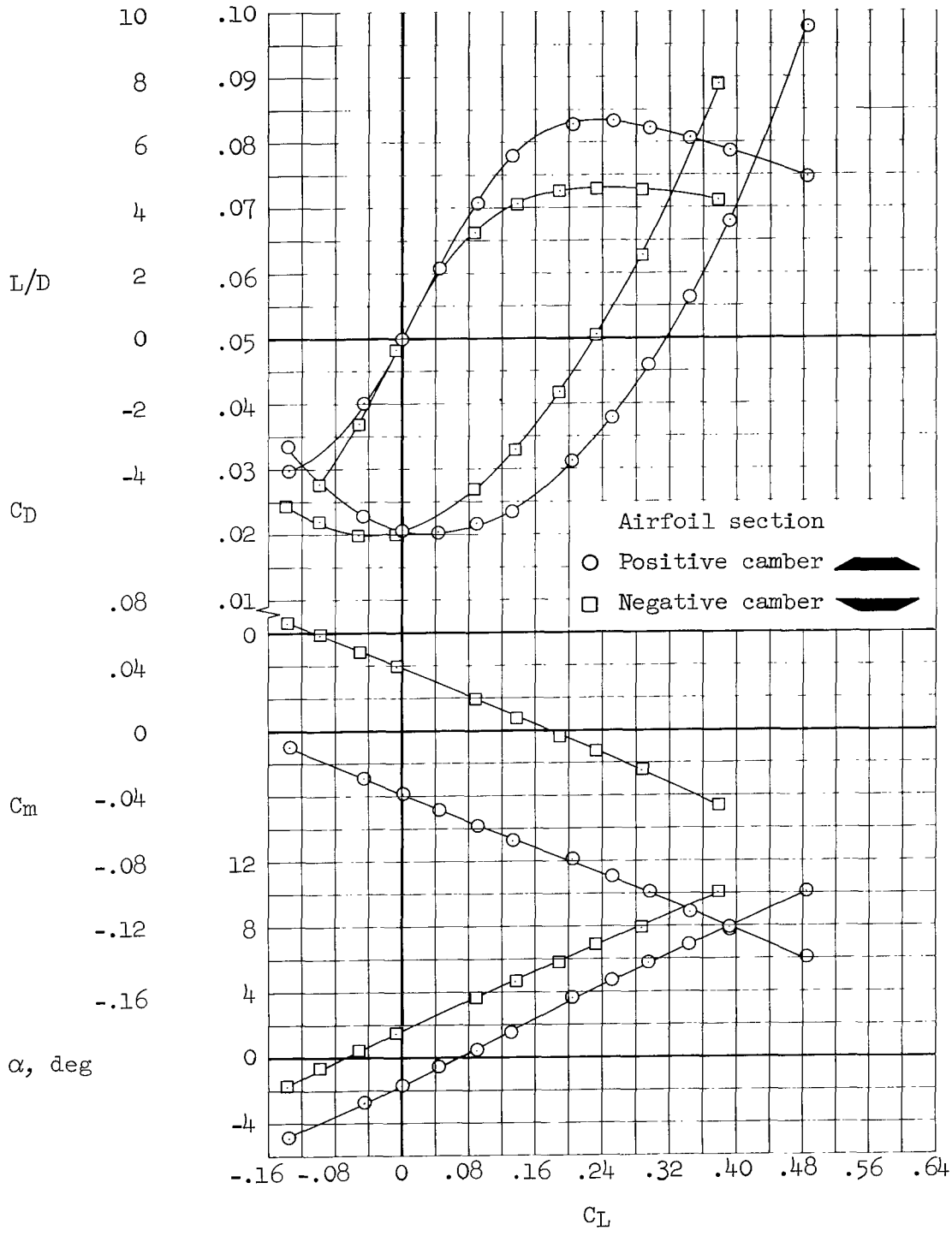

(e) M = 1.10

Figure 13.- Continued.

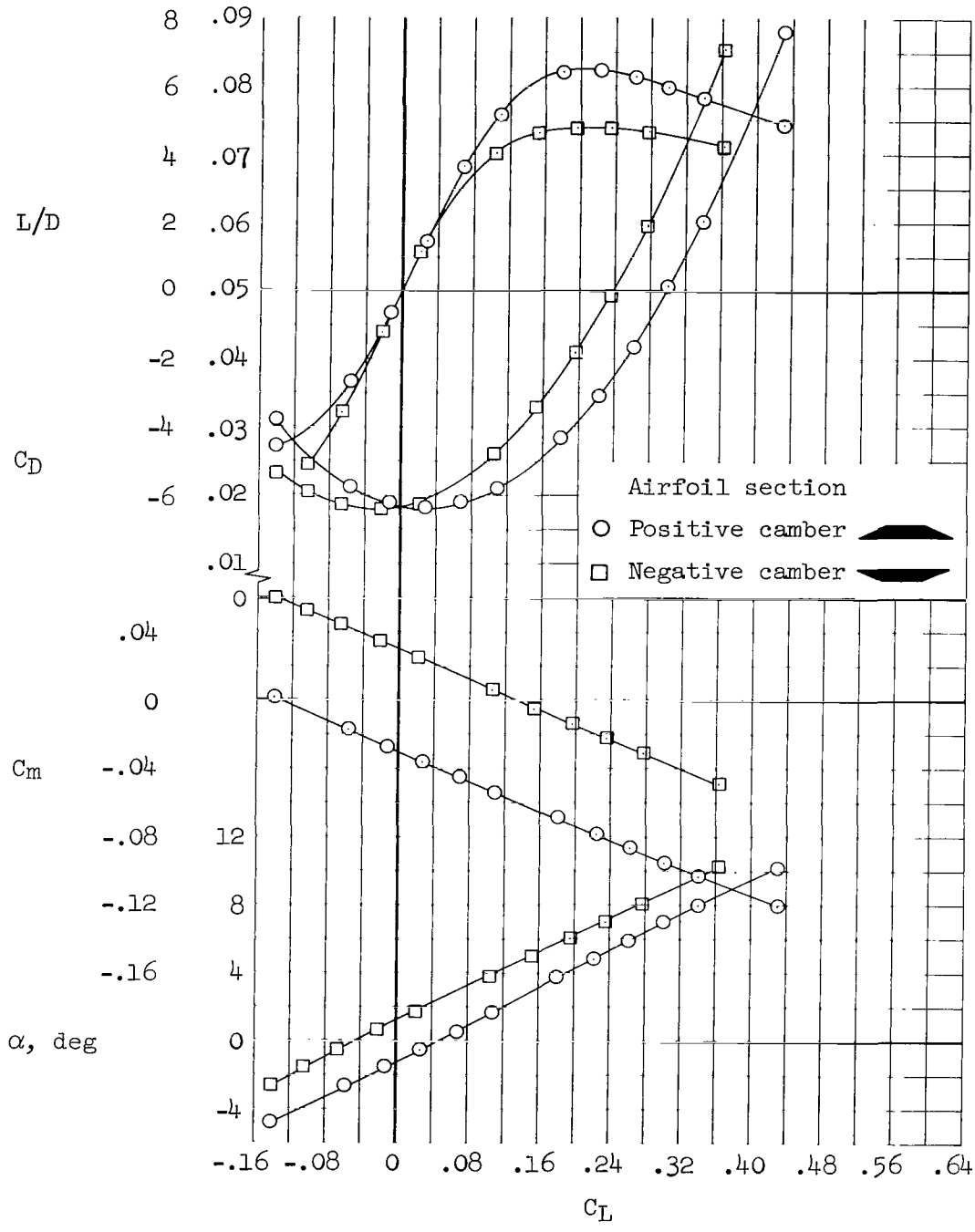

(f) M = 1.30

Figure 13.- Continued.

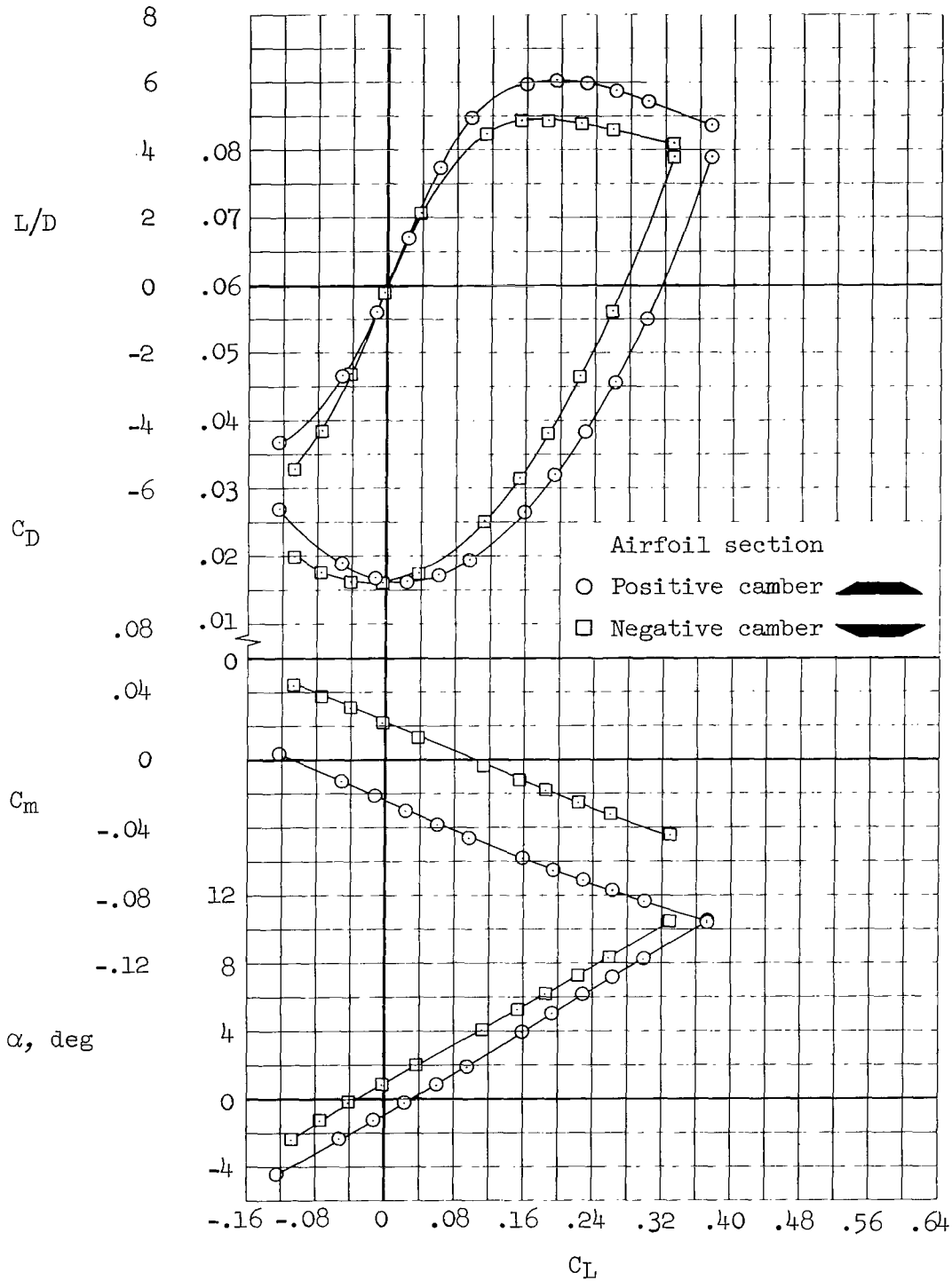

(g) M = 1.59

Figure 13.- Continued.

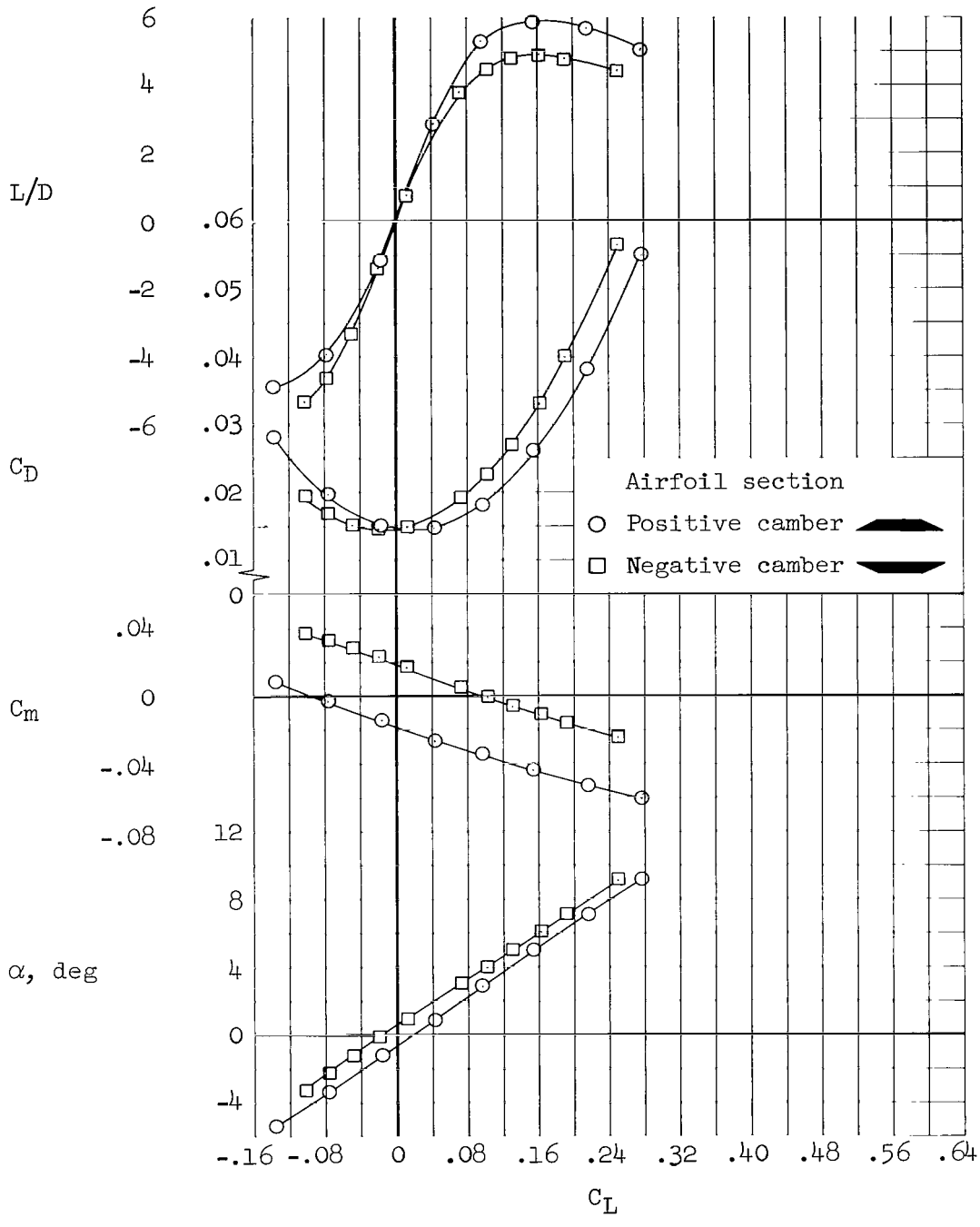

(h) M = 1.99

Figure 13.- Continued.

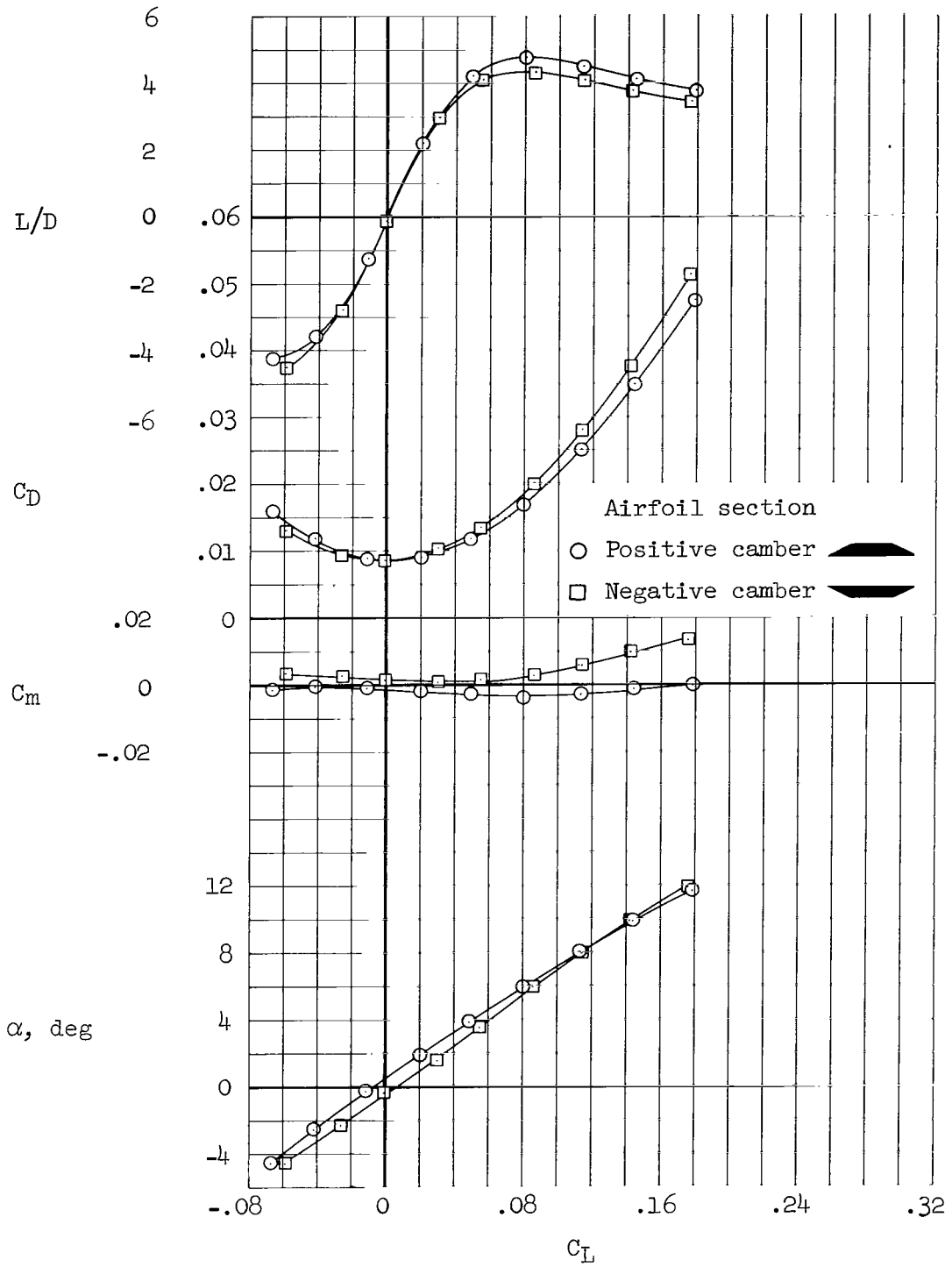

(i) M = 5.31

Figure 13.- Continued.

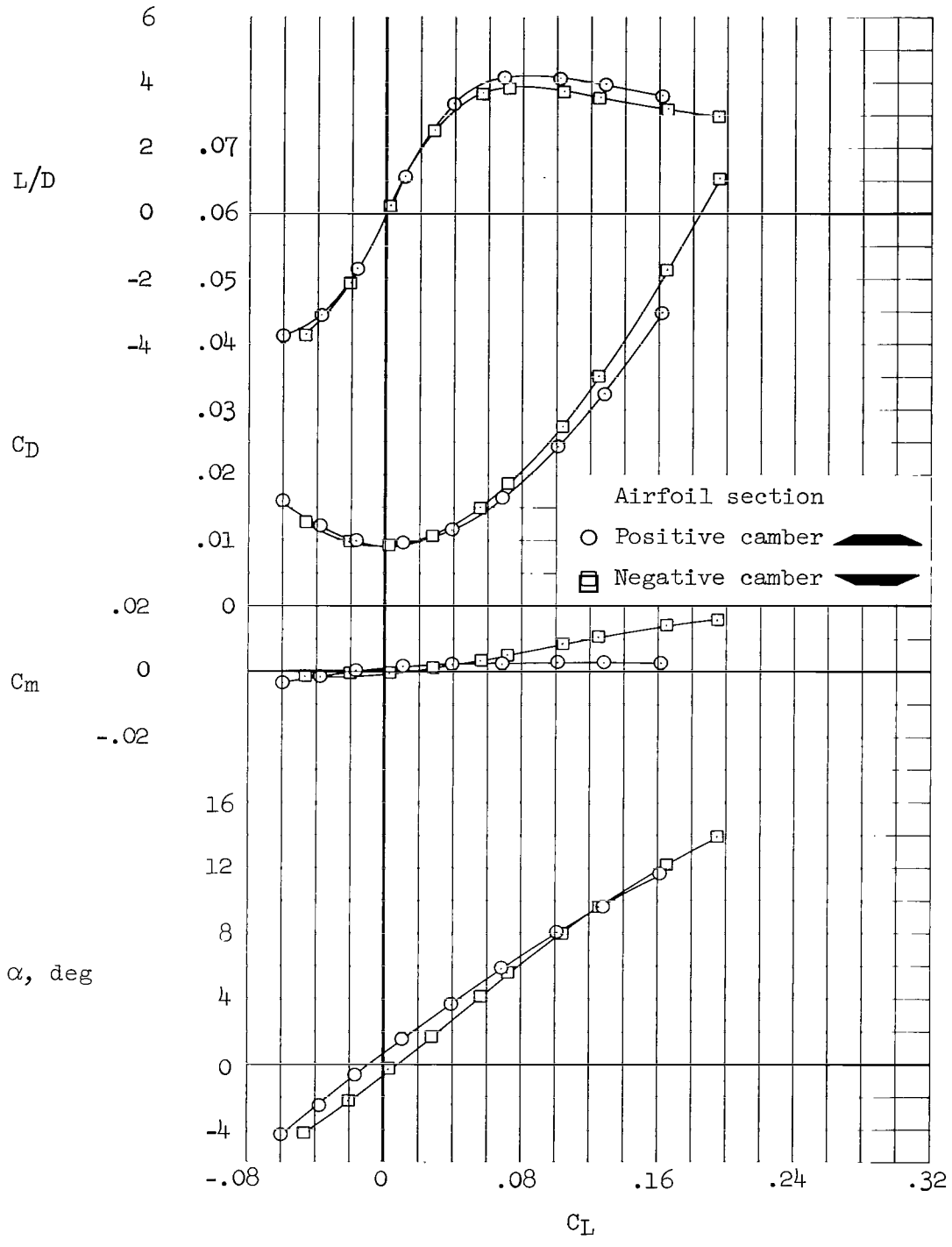

(j) M = 7.42

Figure 13.- Continued.

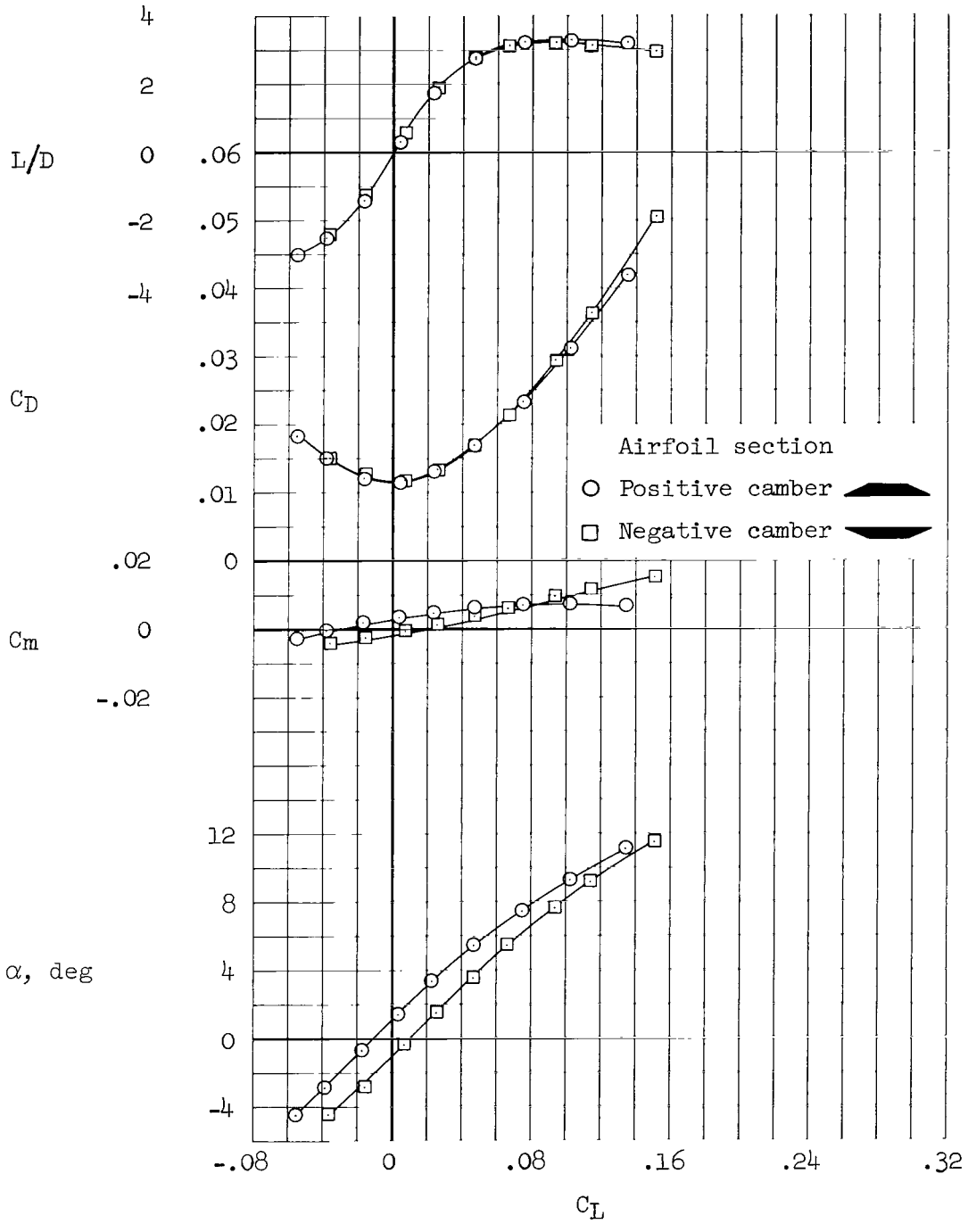

(k) M = 10.70

Figure 13.- Concluded.

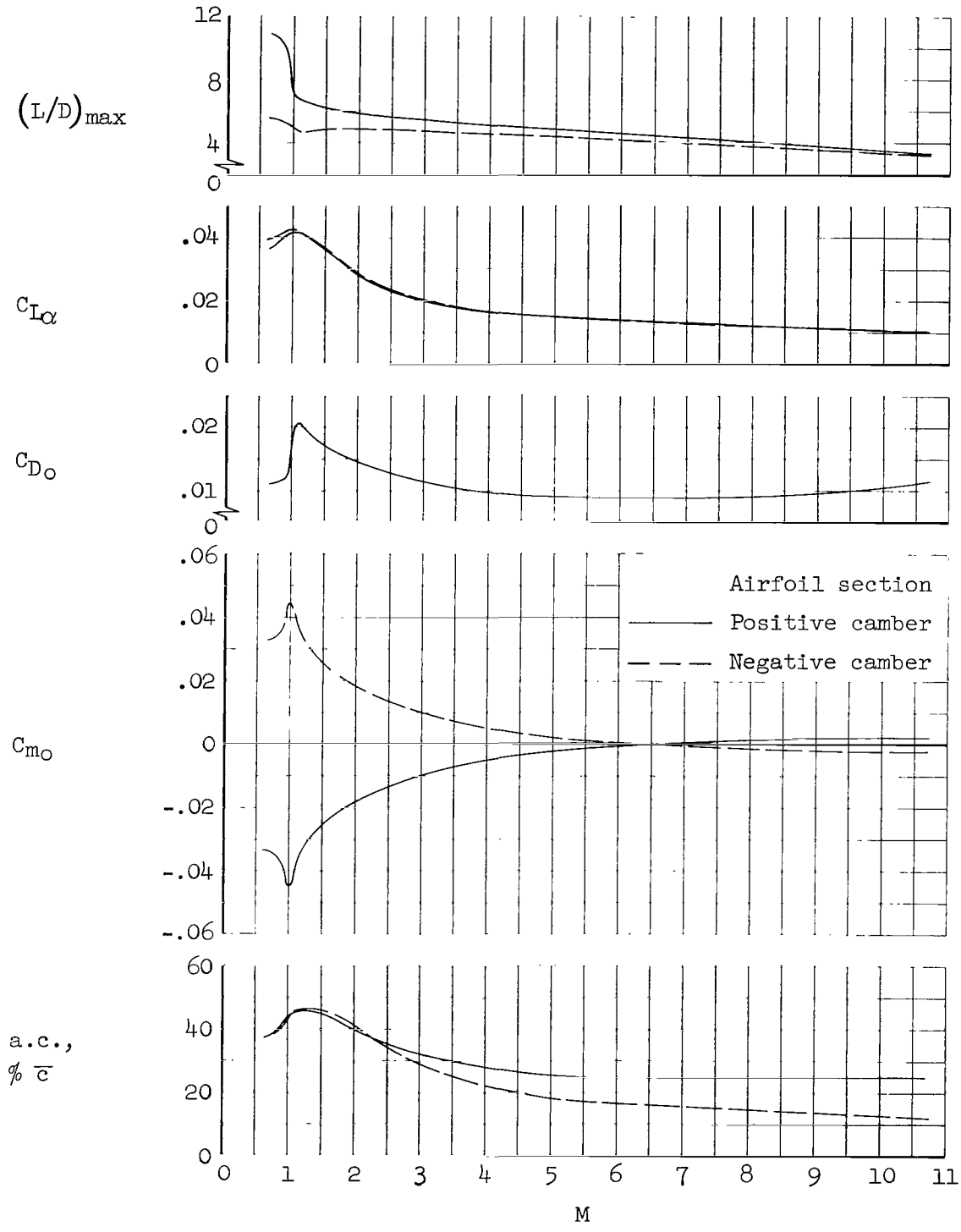

Figure 14.- Variation with Mach number of the effect of wing camber on the longitudinal aerodynamic characteristics; positive and negative cambered airfoil sections, WB configuration, mid-wing elevation, $i_W = 0°$.

"The aeronautical and space activities of the United States shall be conducted so as to contribute . . . to the expansion of human knowledge of phenomena in the atmosphere and space. The Administration shall provide for the widest practicable and appropriate dissemination of information concerning its activities and the results thereof."

—NATIONAL AERONAUTICS AND SPACE ACT OF 1958

NASA SCIENTIFIC AND TECHNICAL PUBLICATIONS

TECHNICAL REPORTS: Scientific and technical information considered important, complete, and a lasting contribution to existing knowledge.

TECHNICAL NOTES: Information less broad in scope but nevertheless of importance as a contribution to existing knowledge.

TECHNICAL MEMORANDUMS: Information receiving limited distribution because of preliminary data, security classification, or other reasons.

CONTRACTOR REPORTS: Scientific and technical information generated under a NASA contract or grant and considered an important contribution to existing knowledge.

TECHNICAL TRANSLATIONS: Information published in a foreign language considered to merit NASA distribution in English.

SPECIAL PUBLICATIONS: Information derived from or of value to NASA activities. Publications include conference proceedings, monographs, data compilations, handbooks, sourcebooks, and special bibliographies.

TECHNOLOGY UTILIZATION PUBLICATIONS: Information on technology used by NASA that may be of particular interest in commercial and other non-aerospace applications. Publications include Tech Briefs, Technology Utilization Reports and Notes, and Technology Surveys.

Details on the availability of these publications may be obtained from:

SCIENTIFIC AND TECHNICAL INFORMATION DIVISION

NATIONAL AERONAUTICS AND SPACE ADMINISTRATION

Washington, D.C. 20546